

A SOFTWARE FOR ANALYSIS OF PERMANENT MAGNET AC MOTORS

A THESIS SUBMITTED TO
THE GRADUATE SCHOOL OF NATURAL AND APPLIED SCIENCES
OF
MIDDLE EAST TECHNICAL UNIVERSITY

BY

DENİZ BULGAN

IN PARTIAL FULFILLMENT OF THE REQUIREMENTS
FOR
THE DEGREE OF MASTER OF SCIENCE
IN
ELECTRICAL AND ELECTRONICS ENGINEERING

FEBRUARY 2014

Approval of the thesis:

A SOFTWARE FOR ANALYSIS OF PERMANENT MAGNET AC MOTORS

submitted by **DENİZ BULGAN** in partial fulfilment of the requirements for the degree of **Master of Science in Electrical and Electronics Engineering Department, Middle East Technical University** by,

Prof. Dr. Canan ÖZGEN
Dean, Graduate School of **Natural and Applied Sciences** _____

Prof. Dr. Gönül TURHAN SAYAN
Head of Department, **Electrical and Electronics Engineering** _____

Prof. Dr. H. Bülent ERTAN
Supervisor, **Electrical and Electronics Engineering Dept, METU** _____

Examining Committee Members:

Prof. Dr. Muammer ERMIŞ
Electrical and Electronics Engineering Dept., METU _____

Prof. Dr. H. Bülent ERTAN
Electrical and Electronics Engineering Dept., METU _____

Prof. Dr. Kemal LEBLEBİCİOĞLU
Electrical and Electronics Engineering Dept., METU _____

Prof. Dr. Aydın ERSAK
Electrical and Electronics Engineering Dept., METU _____

Doç. Dr. Mehmet Timur AYDEMİR
Electrical and Electronics Engineering Dept., Gazi University _____

Date: 20.02.2014

I hereby declare that all information in this document has been obtained and presented in accordance with academic rules and ethical conduct. I also declare that, as required by these rules and conduct, I have fully cited and referenced all material and results that are not original to this work.

Name, Last Name :

Signature :

ABSTRACT

A SOFTWARE FOR ANALYSIS OF PERMANENT MAGNET AC MOTORS

Bulgan, Deniz

M.Sc., Department of Electrical and Electronics Engineering

Supervisor: Prof. Dr. H. Bülent ERTAN

February 2014, 155 pages

Nowadays permanent magnet motors became very popular in almost every area of industry such as automotive, aerospace and automation due to having higher efficiency, better torque-speed characteristics, longer life, higher dynamic response, higher torque per volume when compared to brushed DC and induction motors. These advantages made PM motors very essential and the need of design and analysis of PM motors became more important with the need of specialized applications.

In this thesis, a previously developed MATLAB based analysis approach will be improved to obtain an analysis tool for analysis of permanent magnet AC motors. The software will be tested with experimental data.

As a result of this study, a software for analyzing surface mount permanent magnet motors is developed. By using the developed software user can obtain the solution of

electrical and magnetic circuit solutions of the motor, see performance characteristics from graphics and see the lamination drawing from the machine dimensions and electrical limitations. The results of the software is compared with the experiment results of a manufactured motor and differences between results are explained.

Keywords: permanent magnet motors, brushless dc, surface-mounted magnet motors, analysis software, software development, determination of motor parameters, performance calculation

ÖZ

SABİT MİKNATISLI AC MOTORLARIN ANALİZİ İÇİN BİR YAZILIM

Bulgan, Deniz

Yüksek Lisans, Elektrik ve Elektronik Mühendisliği Bölümü

Tez Yöneticisi: Prof. Dr. H. Bülent ERTAN

Şubat 2014, 155 sayfa

Günümüzde sabit mıknatıslı motorlar, fırçalı DA motoru ve asenkron motorlarla kıyaslandığında daha yüksek verim, daha iyi tork-hız karakteristiği, daha uzun ömür, daha yüksek dinamik tepki ve birim hacime düşen torkun daha yüksek olmasından dolayı, otomotiv, uzay ve otomasyon gibi neredeyse endüstrinin her alanında popüler olmuşlardır. Bu avantajlar sabit mıknatıslı motorları daha özel yapmış ve de spesifik uygulamalar için tasarım ve analizini daha önemli kılmıştır.

Bu tezde, daha önceden geliştirilen MATLAB tabanlı bir analiz yaklaşımı, sabit mıknatıslı motorların analizini yapan bir analiz aracına dönüştürmek üzere geliştirilecektir. Yazılım sonuçları deneysel veriler ile karşılaştırılacaktır.

Bu çalışmanın sonucunda, sabit mıknatıslı motorların analizini yapan bir yazılım geliştirilmiştir. Kullanıcı geliştirilen yazılımı kullanarak, makine boyutları ve elektriksel limitlerden, motorun elektriksel ve manyetik eşdeğer devre çözümlerini elde edebilir, grafiklerden performans karakteristiklerini görebilir ve laminasyon

izimini gorebilir. Yazılım sonuları retilmiŐ bir motorun deneysel sonuları ile karŐılaŐtırılmıŐ ve aradaki farklar yorumlanmıŐtır.

Anahtar Kelimeler: sabit mıknatıslı motorlar, firasız dc, yzey mıknatıslı motorlar, analiz yazılımı, yazılım geliŐtirilmesi, motor parametrelerinin belirlenmesi, performans hesabı

ACKNOWLEDGEMENTS

I would like to thank my advisor, Prof. Dr. H. Bülent Ertan, for all his understanding, advices, guidance and courage he has given me during my graduate studies. Without his patience and help this study could not have been completed.

I also want to thank my professors in the department for their endless support and motivation they gave whenever I need. And I grateful to all my friends for being beside me and giving me encouragement throughout this work.

Finally and most importantly, I would like to owe my deepest love and gratitude to my parents Selim and Gülşen Bulgan for their faint in me. I cannot forget my grandparents. I owe all my success to their great orientation and support through my life. This thesis would not have been possible without their love and encouragement. They are the ones who motivated me at all stages of academic study. I dedicate my work to them.

TABLE OF CONTENTS

| | |
|---|-------|
| ABSTRACT | v |
| ÖZ | vii |
| ACKNOWLEDGEMENTS | ix |
| TABLE OF CONTENTS | x |
| LIST OF TABLES | xiii |
| LIST OF FIGURES | xv |
| LIST OF ABBREVIATIONS | xviii |
| CHAPTERS | |
| 1. INTRODUCTION | 1 |
| 1.1 Classification of PM Motors | 3 |
| 1.2 Typical PMAC Applications..... | 5 |
| 1.3 Literature Review..... | 6 |
| 1.4 Conclusion | 9 |
| 2. PMAC MOTOR PARAMETERS AND PERFORMANCE CALCULATIONS.. | 11 |
| 2.1 Calculation of Magnetic Circuit Parameters | 12 |
| 2.1.1 Air Gap Reluctance | 14 |
| 2.1.1.1 Air Gap Area..... | 15 |
| 2.1.1.2 Equivalent Air Gap Length..... | 16 |
| 2.1.2 Magnet Reluctance..... | 17 |
| 2.1.2.1 Magnet Area | 18 |
| 2.1.2.2 Magnet Height | 18 |
| 2.1.3 Stator Tooth and Back-core Reluctance..... | 21 |
| 2.1.4 Solution of the Magnetic Circuit..... | 22 |
| 2.2 Electrical Parameters..... | 25 |
| 2.2.1 Calculation of Phase Resistance | 26 |

| | | |
|---------|--|----|
| 2.2.1.1 | Wire Cross Section Area..... | 27 |
| 2.2.1.2 | Conductor Length | 28 |
| 2.2.2 | Calculation of Phase Inductance | 30 |
| 2.2.2.1 | Slot Leakage | 30 |
| 2.2.2.2 | End Winding Inductance | 32 |
| 2.2.2.3 | Magnetizing Inductance..... | 33 |
| 2.2.3 | Emf and Torque Constants..... | 35 |
| 2.2.4 | Losses..... | 36 |
| 2.2.4.1 | Copper Loss | 36 |
| 2.2.4.2 | Core Loss | 36 |
| 2.2.4.3 | Magnet Losses, Friction and Windage Losses..... | 38 |
| 2.3 | Calculation of Torque | 38 |
| 2.4 | Conclusion | 42 |
| 3. | FLOW CHART OF PM ANALYSIS SOFTWARE..... | 45 |
| 3.1 | Calculation of Outputs | 48 |
| 3.1.2 | Calculation of Dimensions..... | 51 |
| 3.1.2 | Calculation of Electrical Parameters | 53 |
| 3.1.3 | Calculation of Magnetic Parameters | 59 |
| 3.1.4 | Calculation of Performance..... | 61 |
| 3.2 | Showing Outputs..... | 65 |
| 3.3 | Conclusion | 67 |
| 4. | IMPLEMENTATION OF THE PMAC ANALYSIS SOFTWARE | 69 |
| 4.1 | Introduction | 69 |
| 4.2 | Technical Features | 70 |
| 4.3 | Creating a Form in Visual Studio | 72 |
| 4.4 | Analysis Menu | 74 |
| 4.4.1 | Torque-Speed Graph | 76 |
| 4.4.2 | Current-Speed Graph | 79 |
| 4.4.3 | Output Power-Speed Graph | 80 |
| 4.5 | Lamination Menu | 80 |
| 4.6.1 | Creation of Repeating Stator Portion | 81 |
| 4.6.2 | Creation of Repeating Rotor Portion | 90 |

| | | |
|-------|--|-----|
| 4.6 | Conclusion | 94 |
| 5. | USER GUIDE FOR ANALYSIS SOFTWARE | 95 |
| 5.1 | File Menu | 96 |
| 5.1.1 | New | 97 |
| 5.1.2 | Open | 98 |
| 5.1.3 | Save | 99 |
| 5.1.4 | Print | 100 |
| 5.2 | Analysis Menu | 100 |
| 5.2.1 | Torque vs Speed Graphic | 103 |
| 5.2.2 | Input Current vs Speed Graphic | 103 |
| 5.2.3 | Output Power vs Speed Graphic | 104 |
| 5.3 | Lamination Menu | 105 |
| 6. | RESULTS | 109 |
| 6.1 | Motor A | 111 |
| 6.1.1 | Comparison of Results | 111 |
| 6.2 | Motor B | 118 |
| 6.2.1 | Calculation of Parameters and Terminal Voltage | 123 |
| 6.2.2 | Method of Calculation of Torque Curve | 125 |
| 6.2.3 | Comparison of Test Results and Software Results | 126 |
| 6.2.4 | Calculation of Core Loss, Copper Loss and Efficiency | 129 |
| 6.3 | Conclusion | 134 |
| 7. | CONCLUSION AND FUTURE WORK | 135 |
| | REFERERENCES | 139 |
| | AAPENDICES | |
| A. | MANUFACTURER DATA FOR MOTOR A | 143 |
| B. | ANALYSIS REPORT OF MOTOR A | 145 |
| C. | ANALYSIS REPORT OF MOTOR B | 149 |
| D. | MODIFICATIONS ON EQUATIONS | 153 |

LIST OF TABLES

TABLES

| | |
|--|-----|
| Table 1.1: Classification of PM motors based on their excitation and back EMF waveforms[7] | 3 |
| Table 1.2: Basic comparison of surface magnet and buried magnet motors [7]..... | 5 |
| Table 2.1: Description of Symbols in the Magnetic Equivalent Circuit | 13 |
| Table 2.2: Number of Rows and Columns of Matrices | 40 |
| Table 3.1: Inputs of the Design Program. | 50 |
| Table 3.2: Outputs of the Design Program | 66 |
| Table 4. 1: List of the Toolboxes Used in the Software..... | 73 |
| Table 6.1: List of Inputs of Motor A..... | 110 |
| Table 6. 2: Electrical Parameters of Motor A | 112 |
| Table 6.3: Magnetic Parameters of Motor A | 114 |
| Table 6. 4: Comparison of Results and Manufacturer Data..... | 114 |
| Table 6.5: Performance Outputs of Motor A | 115 |
| Table 6.6: Comparison of Torque and Current Values | 116 |
| Table 6.7: Dimensions of Stator Lamination | 119 |
| Table 6. 8: List of Inputs of Motor B | 122 |
| Table 6.9: Armature Reactance, Induced EMF and Terminal Voltage Values for Different Speeds..... | 125 |
| Table 6.10: Test Results of Motor B | 127 |
| Table 6. 11: Output Power Results | 129 |
| Table 6.12: List of Input and Output Power, Losses and Efficiency | 132 |

Table B.1: Analysis Report of Motor A..... 145
Table B.1: Analysis Report of Motor A (continued) 146
Table B.1: Analysis Report of Motor A (continued) 147
Table C.1: Analysis Report of Motor B 149
Table C.1: Analysis Report of Motor B (continued)..... 150
Table C.1: Analysis Report of Motor B (continued)..... 151
Table D.1: Comparison of Equations..... 153
Table D.1: Comparison of Equations (continued) 154
Table D.1: Comparison of Equations (continued) 155

LIST OF FIGURES

FIGURES

| | |
|--|----|
| Figure 1.1: Sinusoidal (a) and trapezoidal (b) back EMF waveforms of a PM motor [7] | 3 |
| Figure 1.2: Surface mounted PM (a), buried PM (b) and interior (spoke) type PM (c) motor types [7] | 4 |
| Figure 1.3: RMxpert Screen View | 8 |
| Figure 1.4: SPEED Screen View | 9 |
| Figure 2.1: Main dimensions of the motor | 12 |
| Figure 2.2: Magnetic equivalent circuit | 13 |
| Figure 2.3: Fringing flux in the air gap[5] | 15 |
| Figure 2.4: Magnet heights | 19 |
| Figure 2.5: Illustration of magnet heights for regions..... | 20 |
| Figure 2.6: Abbreviations for stator steel dimensions | 21 |
| Figure 2.7: Air gap flux density waveform..... | 24 |
| Figure 2.8: Equivalent electrical circuit | 26 |
| Figure 2.9: Stator Slot Dimensions | 28 |
| Figure 2.10: Illustration of conductor parts | 29 |
| Figure 2.11: Contours showing slot leakage paths[5]..... | 31 |
| Figure 2.12: The representation of d and q axis..... | 34 |
| Figure 2.13: Torque-Speed Characteristics of a BLDC Motor[7] | 38 |
| Figure 2.14: Electrical Phase Diagram of PM Machine in Vector Control | 39 |

| | |
|---|-----|
| Figure 3.1 : Main Flow Chart of the Software | 46 |
| Figure 3.2 : Calculation of the Outputs | 49 |
| Figure 3.3 : Flow Chart of calc_dim | 52 |
| Figure 3.4 : Flow Chart of calc_elcp..... | 54 |
| Figure 3.5 : Flow Chart of calc_magp | 59 |
| Figure 3.6 : Flow Chart of Performance Calculations | 62 |
| Figure 4.1 : The Screen Shot of Microsof Visual Studio | 71 |
| Figure 4.2 : Sample Form and Toolbox Window | 72 |
| Figure 4.3 : Torque vs Speed Graph | 76 |
| Figure 4.4 : Torque-Speed Graph from Machine Parameters | 77 |
| Figure 4.5 : Sample Lamination Drawing..... | 81 |
| Figure 4.6 : Stator Slot Types | 82 |
| Figure 4.7 : Symmetricaal Element of Stator Lamination | 82 |
| Figure 4.8 : Sample Lamination Drawing Form | 83 |
| Figure 4.9 : Coordinates of Points C and D | 85 |
| Figure 4.10 : Coordinates of Point E..... | 86 |
| Figure 4.11 : Coordinates of Points G and H..... | 88 |
| Figure 4.12 : Coordinates of Point I..... | 89 |
| Figure 4.13 : Sample Rotor Drawing | 91 |
| Figure 5.1 : Menu Stucture of Program | 95 |
| Figure 5.2 : Main Screen of the Program | 96 |
| Figure 5.3 : First Tab of the New Analysis Form | 97 |
| Figure 5.4 : First Tab of Openned Analysis Form | 98 |
| Figure 5.5 : Save File Dialog | 99 |
| Figure 5.6 : Print File Dialog | 100 |
| Figure 5.7 : Torque vs Speed Graph | 101 |
| Figure 5.8 : Torque-Speed Graph from Machine Parameter..... | 102 |
| Figure 5.9 : Input Current vs Speed Graph | 104 |
| Figure 5.10 : Output Power vs Speed Graph | 105 |
| Figure 5.11 : Sample Lamination Drawing Form | 106 |

| | |
|---|-----|
| Figure 6.1 : Maximum Toque vs Speed Graph | 117 |
| Figure 6.2 : Maximum Current vs Speed Graph | 117 |
| Figure 6.3 : Stator Lamination of Motor B | 118 |
| Figure 6.4 : Stator Lamination Dimensions | 119 |
| Figure 6.5 : Rotor Drawing | 120 |
| Figure 6.6 : Equivalent Electrical Circuit of Motor B | 123 |
| Figure 6.7 : Torque vs Input Current | 126 |
| Figure 6.8 : Test Results of Motor B | 128 |
| Figure 6.9 : Copper and Core Loss versus Speed | 132 |
| Figure 6.10 : Phasor Diagram of Motor B | 133 |
| Figure 6.11 : Efficiency versus Speed..... | 134 |
| Figure A.1: Electrical and Mechanical Specifications | 143 |
| Figure A.2: Torque Speed(top) and Output Power-Speed (bottom) Characteristics | 144 |
| Figure B.1: Torque-Speed (a), Input Current-Speed (b), Output Power-Speed (c) Graphics | 148 |

LIST OF ABBREVIATIONS

| | |
|-----------|---|
| Amag | Magnet Crosssectional Area At Magnetization Direction (m ²) |
| Ag | Air gap Area Including Fringing Flux (m ²) |
| alfa | Magnet Pitch / Pole Pitch |
| Aslot | Total Slot Area (m ²) |
| Awire | Winding Wire Crosssectional Ares |
| Bbc | Peak Back Core Flux Density |
| Br | Magnet Remanent Flux Density |
| Bth | Max Peak Tooth Flux Density |
| kc | Carter Coefficient |
| Coilpitch | Coil Pitch Of The Winding |
| Dms | Diameter At Magnet Surface (m) |
| Dsi | Diameter At Stator Inner Surface (m) |
| Dso | Stator Outer Diameter (m) |
| g | Air gap (mm) |
| g3 | Air gap At Magnet Side |
| ged | Total Air gap At D-Axis |
| geq | Total Air gap At Q-Axis |
| h0 | Slot Opening Depth (m) |
| h1 | Slot Depth |
| h2 | Tooth Height (m) |
| hbc | Back Core Heigth |
| hm2 | Mean Magnet Height At Region 2 |
| hm3 | Mean Magnet Height At Region 3 |
| hmag | Magnet Maximum Height In The Middle |

| | |
|--------|--|
| hslot | Total Slot Height (M) |
| kemf | Back Emf Constant Per Phase (Vrms) |
| kfill | Slot Fill Factor |
| Kstack | Stacking Factor |
| ktorq | Torque Constant (Nm/Arms) |
| kw | Winding Factor |
| Lcon | Total Length Of Connection Between Coils |
| Ld | Total D-Axis Inductance |
| Lew | End Windind Inductance |
| Lext | External Length Of Coil |
| Llm | |
| Lmsd | D-Axis Magnetizing Inductance |
| Lmsq | Q-Axis Magnetizing Inductance |
| Lq | Total Q Axis Inductance |
| Lslm | Mutual Component Of Slot Leakage |
| Lslot | Calculated Slot Leakage Inductances |
| Lsls | Self-Component Of Slot Leakage |
| Lsta | Axial Length Of Magnetic Circuit |
| Lwire | Total Wire Length |
| mu0 | Space Air Permeability (Henry/M) |
| Ncoil | Coils Per Phase |
| Nslot | Slot Number Of Stator |
| Nturn | Turns Per Coil |
| pB | Leakage Permeance Of Bottom Part |
| p_end | Permeance coefficient of End-Winding |
| Pm | Magnet Internal Leakage Permeance Leakage Included |
| Pm0 | Magnet Internal Leakage Permeance |
| pole | Motor Pole Number |
| Pr1 | Rotor Leakage Permeance (Magnetic) |
| pT | Total Leakage Permeance Of Top Part |
| pT1 | Leakage Permeance Of First Top Part |

| | |
|--------|--|
| pT2 | Leakage Permeance Of Second Top Part |
| pTB | Leakage Permeance Of Top-Bottom Mutual Part |
| Rbc | Back Core Reluktance |
| Rg | Air gap Reluctance |
| Rg | Air gap Reluctance |
| Rm | Magnet Reluctance |
| Rrl | Rotor Leakage Reluktance |
| Rs | Total Phase Resistance |
| Rth | Tooth Reluctance |
| Spitch | Selected Slot Pitch |
| teta | Angle Span Of Magnet At Magnet Surface=Alfamag |
| w0 | Slot Opening Width (m) |
| w1 | Slot Width Near To Slot Opening (m) |
| w2 | Slot Width At Slot Dip (m) |
| Wmag | Width Of Magnet Tip (m) |
| Wth | Tooth Width |

CHAPTER 1

INTRODUCTION

Nowadays, electric motors are used to drive a variety of loads in almost every industrial process. There exist billions electric motors all over the world used in various applications which requires power at different ratings. While large powered ones are being used for heavier applications, small fractional HP motors are used in household appliances.

In this thesis, permanent magnet AC (PMAC) motors are studied because they are rapidly gaining popularity with the wide area of usage in industries such as appliances, aerospace, automotive, medical, instrumental automation equipment, consumer and instrumentation. The reason why permanent magnet motors have a rising trend is the advantages they have like high efficiency, high dynamic response, long operating time, better torque-speed characteristics, noiseless operation and higher speed ranges and higher torque per volume.

Use of electric motors started with the invention of wound field DC motor in 1832 by the British scientist William Sturgeon [26]. DC motors were very popular because of their speed control capability. After the AC (induction) motors are practically invented in 1885 by Galileo Ferraris and also by Nikola Tesla in 1887 [27], DC motors loose the popularity.

PMAC motors have many advantages over AC and DC motors. When they are compared to brushed DC motors, since lack of brushed commutation maintenance is less required, life is longer and efficiency is higher because there is no voltage drop

across the brushes. Since there is no mechanical limitations due to brushes and commutators, speed range is higher. Torque speed characteristic is flat which allows operation at all speeds with rated load. Same output power can be obtained from a smaller PM motor compared to brushed dc motors due to higher thermal characteristics. Rotor inertia is lower which gives better dynamic response.

PM motors are advantageous when they are compared to AC motor in terms of lower rotor inertia, higher output power per frame and better torque-speed characteristics. Also PM motors are advantageous since they have no slip and lower starting current.

There are two main disadvantage of PM motors. First one is the need of a control which required a controller which increase the price and second one is due to the magnets which also increase the price. But these disadvantages may be overcome with the requirements of the application [25].

The types of PM motors are discussed in the following section. Basically they are trapezoidal and sinusoidal flux motors. In sinusoidal flux motors, back EMF and input current and so the output torque have sinusoidal waveforms. To obtain a waveform which is much closed to sinusoidal, a distributed winding is needed which requires extra winding interconnections. This increase the use of copper which is a disadvantage in term of weight, price and efficiency. In trapezoidal flux motors, back-emf and input current have square waveforms.

In rotor, magnets are used to create magnetic field. Number of poles is determined by number of magnets and the number is generally between two and eight. Proper magnetic material is chosen according to the required magnetic field density.

Generally ferrite magnets are used but as the technology advances alloys of rare earth magnets are gaining popularity like Neodymium (Nd), Samarium Cobalt (SmCo) and Neodymium-Ferrite-Boron (NdFeB). The ferrite magnets are cheaper but they have lower flux density whereas alloy magnets have higher magnetic density per volume with higher price. But the most important advantage of alloy magnets are that they can give higher torque for same size motor using ferrite magnets.

1.1 Classification of PM Motors

PM motors can be classified into two groups according to flux density distribution and the shape of the current excitation. The first group is permanent magnet synchronous motors (PMSM) with sinusoidal flux density and other group is permanent magnet brushless motors (BLDC) with rectangular shaped flux density. The properties of these types of PM motors are given in Table 1.1 below.

Table 1.1: Classification of PM motors based on their excitation and back EMF waveforms [7]

| | PMSM | BLDC |
|--------------------------|------------|-------------|
| Phase current excitation | Sinusoidal | Square |
| Flux density | Sinusoidal | Trapezoidal |
| Phase back EMF | Sinusoidal | Square |
| Power and torque | Constant | Constant |

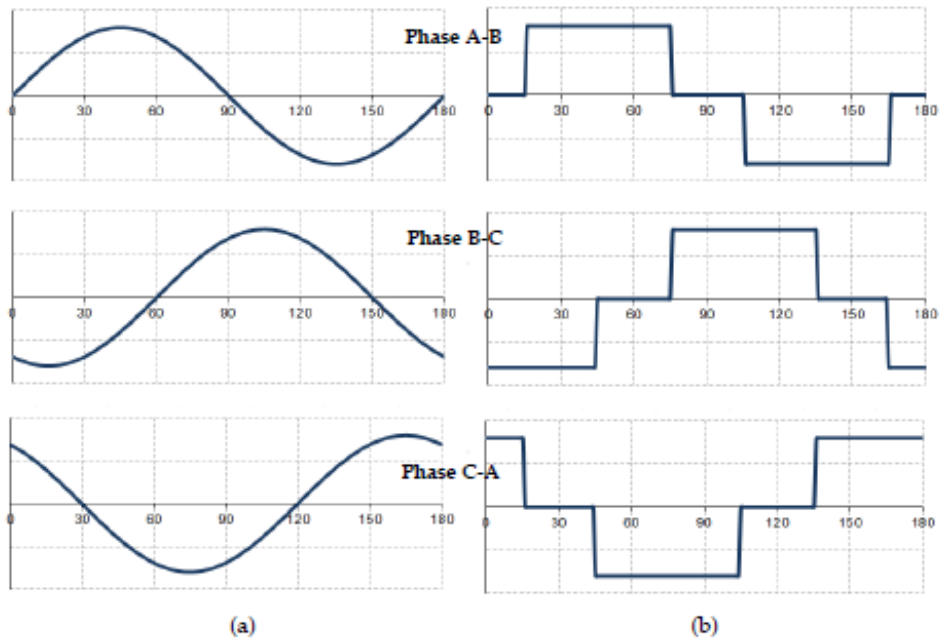


Figure 1.1: Sinusoidal (a) and square wave (b) supply voltages of a PM motor [7]

The supply voltage waveforms for three phases of a motor can be seen in Figure 1.1 in detail for two different excitations mentioned above. The back EMF waveforms are sinusoidal and trapezoidal for these motors respectively. The supply current has the same waveform shape for these two type of motors.

The stator of conventional PM motor has the same construction with an AC motor. The core is laminated and slotted. Poly phase windings are placed into the slots. The rotor consists of magnets and rotor steel which is usually laminated. PM motors can also be classified into groups according to the position of magnets in the rotor; surface mounted PM motors and buried PM motors. The cross sections of PM motors for different magnet structure is given in Figure 1.2.

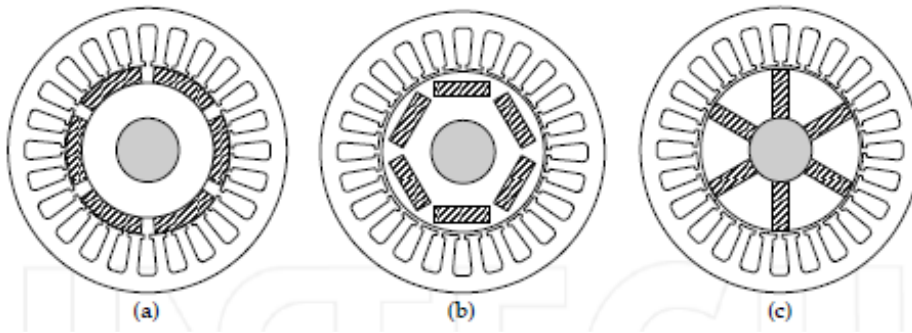


Figure 1.2: Surface mounted PM (a), buried PM (b) and interior (spoke) type PM (c) motor types [7]

In surface mounted PM motors, magnets are glued on the rotor surface. More PM material per pole is used in this type of motors and while torque production of motor increases the volume and the cost of the motor increases too. In buried PM motors, flux concentration principle is used where magnet flux concentrated in rotor core before passing the air gap. This causes reluctance torque due to the position dependent inductance which is a result of flux concentration in the rotor core. The comparison of surface mounted PM motors and buried PM motors are simply given in Table 1.2 where w_R is the rated speed of the motor.

Table 1.2: Basic comparison of surface magnet and buried magnet motors [7]

| | Surface Mounted PM Motors | Buried/Interior PM Motors |
|-----------------------|----------------------------|---------------------------|
| Flux distribution | Trapezoidal or Sinusoidal | Usually Sinusoidal |
| Complexity of rotor | Simple | Complex |
| Speed limit | $\sim 1.2 \times \omega_R$ | $\sim 3 \times \omega_R$ |
| High speed capability | Difficult | Possible |
| Control | Relatively easy | More complex |

The surface mounted PM motors have simpler rotor construction with fairly small speed limits. On the other hand, buried or interior PM motors have wider speed ranges with more complex rotor structure. The buried PM motors can reach very high speeds although they are more complex to control unlike surface mount PM motors.

1.2 Typical PMAC Applications

PMAC motors have a wide range of usage in the market due the advantages discussed above. These applications can be classified into three main categories according to the required control;

- Constant loads
- Varying loads
- Positioning applications

For constant loads, keeping the speed at a constant level is less important than variable speed. Also there is no dynamics changes in acceleration and deceleration rates. Load is directly coupled to rotor (shaft). Fans, pumps, blowers are the examples of constant load applications. These type of loads generally operates in open-loop which makes the cost of controller cheap.

In this type of applications, motor load varies within a speed range. Since speed is changing, an accurate high-speed control and good dynamic responses may be required. The speed control can be done by speed feedback devices running in semi-

closed loop or total closed loop. There may be used advanced control algorithms which complicates the controller and increases the price of the complete system.

Most of the industrial and automation application are under this category. Dynamic response of speed and reversal of rotation direction may be required for these applications. Also load may vary during operation which makes the control more complex which are usually operates in closed loop. Torque, speed and control can be controlled in different closed loops, which means there could be three different closed loop control at the same time [25].

1.3 Literature Review

In literature there many analysis approaches for different type of motors. In our department, a tool for single phase induction motor design [8] and a software for analysis and design optimization of switched reluctance motor [9] was studied. Analysis of conventional type of permanent magnet synchronous motors are mostly studied in 1990s, studies of A. Consoli are the most known examples for the PM motor analysis; a detailed representation of buried PMSM for steady-state operating conditions with equivalent circuit which includes the effect of saliency of rotor and core loss [10] and interior type PMSM is studied with an equivalent circuit to predict steady-state core loss for different operating conditions such as under demagnetizing or magnetizing armature reaction or saturation [11]. But recent ones are generally for new type of constructions which are not included in this study like axial flux PM motors with dual air gap such that the motor have twin stators and double-side single rotor sandwiched between these two stators and this motor is compared with an induction motor with same structure by C. Zhang [12], H.C. Jong theoretically and geometrically calculated the minimum cogging torque of an axial flux PM motor without FE analysis [13] and A. Cavagnino compared the axial flux PMSM with conventional radial flux PMSM in terms of delivered electromechanical torque for different dimensions and pole numbers and figured out that axial flux motors with short stack length and high number of poles are an alternative for conventional radial flux motors[14], a surface mounted non-slotted disc type PM motor is analyzed by a FEA software and results are compared with a slotted disc type PM motor in terms of torque quality which is obtained with minimum cogging torque and ripple torque by

T.A. Lipo [15], an interior type PM motor with two magnet layers delivering 50 kW constant power is designed and experimentally verified by W. Soong [16], C.C. Hwang presented a magnetic circuit model which gives the machine parameters of an interior PMSM [17] and Y.C. Jang investigated cogging torque, torque ripple, d and q axis inductances, THD of back-EMF for a conventional internal PM motor for different number of slots [18] or dual-rotor radial flux surface mounted PM machines studied and figured out that with this structure machine torque density and efficiency can be improved by T. A. Lipo [19].

Also there are many studies for improving the PM motors like minimizing the cogging torque, lowering the noise and smoothening the torque. In 2009, Z. Wu and D. Depernet made a design of a surface-mounted PMSM with high electromagnetic torque for hybrid heavy-duty electrical powertrain [20]. G. R. Slemon derived the expressions for maximum acceleration and torque limits of a surface-mounted PM motor and showed the range of a PM motor acceleration capability [21]. Bianchi compared the classical and innovative techniques for minimizing the cogging torque for surface-mounted PM motors [22].

Additionally design improvements are also done by optimizing the design dimensions and position of magnets. In 2013, Wang and Yuan made a design optimization of surface-mounted PM motors depending on the machine key parameters like slot-pole number combination, axial length and etc. for electric vehicle applications [23].

Apart from these studies, there are similar software which are being used commercially in the industry. One of the most widely used analysis software is RMxpert presented by ANSYS. In RMxpert, user chooses one of the defined machine models like PMSM or induction motor or etc. and enters the dimensions and electrical limits like voltage and current. User can select slot type, magnet type, winding type and whether the shaft is magnetic or non-magnetic.

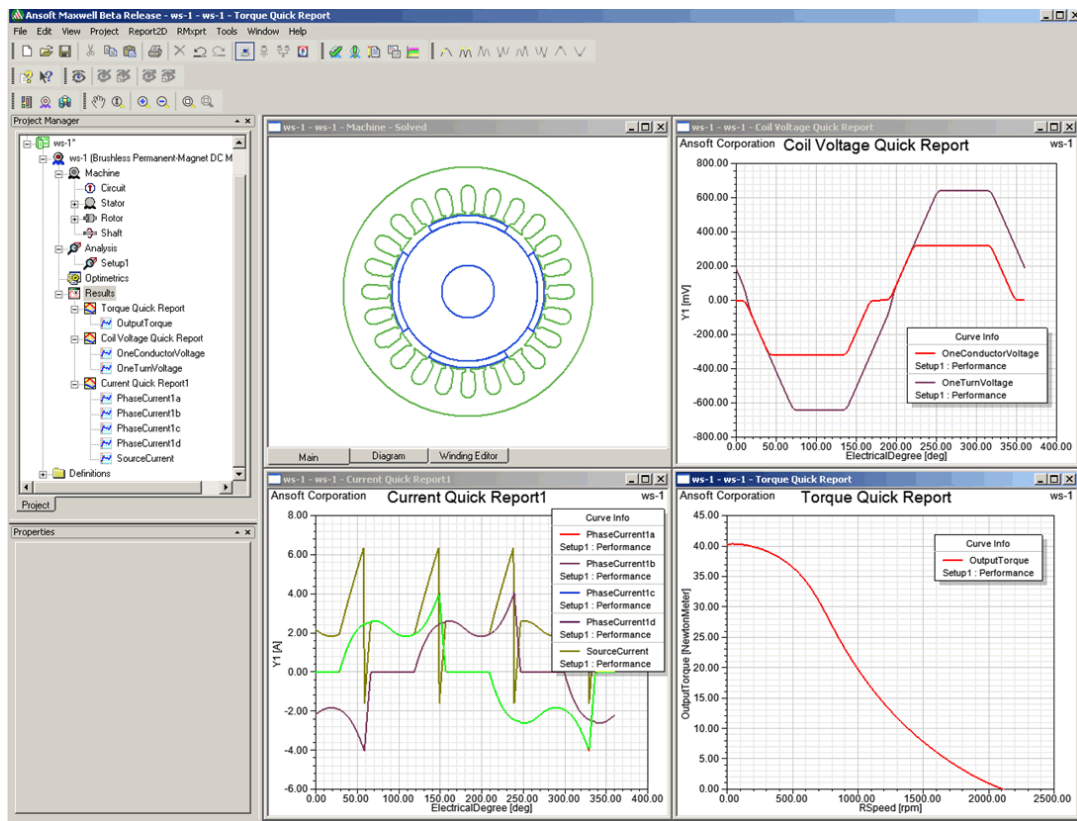


Figure 1.3: RMxprt Screen View

Then program automatically does the analysis for the given voltage, current and power values. User can see torque-speed characteristics, voltage and current waveforms and etc. A screenshot of the program is given in Figure 1.3. If required program can create 2D and 3D models for Maxwell program presented by ANSYS and these models are used in electromagnetic transient analysis [28].

SPEED is the other well known design and analysis program used in the market. The program include many machine model like RMxprt and user chooses which type of machine will be analyzed. Geometrical dimensions are entered by the user and machine is sized easily [29].

The analysis method for surface mount PM motors and the developed software is somewhat similar to the software described above.

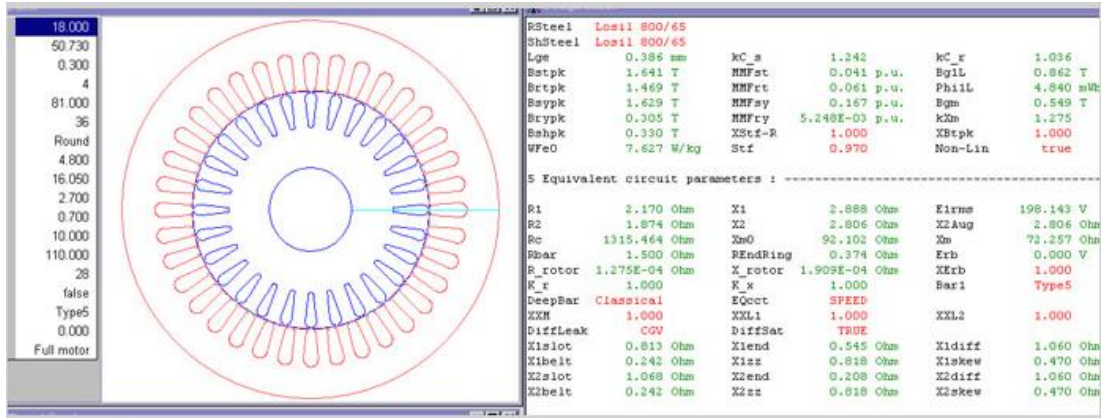


Figure 1.4: SPEED Screen View

1.4 Conclusion

The comparison of PMAC motors to other conventional motor like DC and induction are discussed above. Due to the advantages PMAC motors are used in various applications nowadays. Also the new drive and control techniques make the popularity of these motors higher.

In this thesis, a PMAC analysis software is developed. For this purpose a previously obtained MATLAB based model is used and modifications are made to have a more accurate model.

In Chapter 2, magnetic and electrical equivalent circuits of the motor is given. The parameters in these circuits are calculated. These calculations are used in the program to find the design outputs of the motor. The program is designed by following the steps given in the flow charts which are described in Chapter 3. The steps of calculations are done with the equations derived in Chapter 2. In Chapter 4, the implementation of the software in Microsoft Visual Studio program are described. In Chapter 5 a simplified user guide is given which basically explains how to run the analysis in the software. In Chapter 6, results of the software program is compared with test results of two manufactured motors data and the differences between results are explained.

CHAPTER 2

PMAC MOTOR PARAMETERS AND PERFORMANCE CALCULATIONS

In this chapter, magnetic and electric model of a surface mount PM motor are going to be discussed in detail. For this purpose mathematical equations are going to be derived to solve the magnetic and electrical equivalent circuits. Main objective is to obtain a mathematical model of a radial flux inset magnet motor which gives the chance to perform analytical performance analysis.

Inputs of the model are going to be main machine dimensions such as air gap length, slot dimensions and axial length of the motor. The outputs are going to be machine parameters such as equivalent circuit resistances and inductances. Also output power-speed, electromechanical torque-speed graphs are going to be obtained as outputs of the model.

This model is going to be used in the design program in Chapter 3 and the results are going to be compared with a manufactured motor.

In Figure 2.1, main dimensions of the motor are shown which are used in most of the equations. The dimensions of stator slot and back-core are zoomed out for being seen clearly.

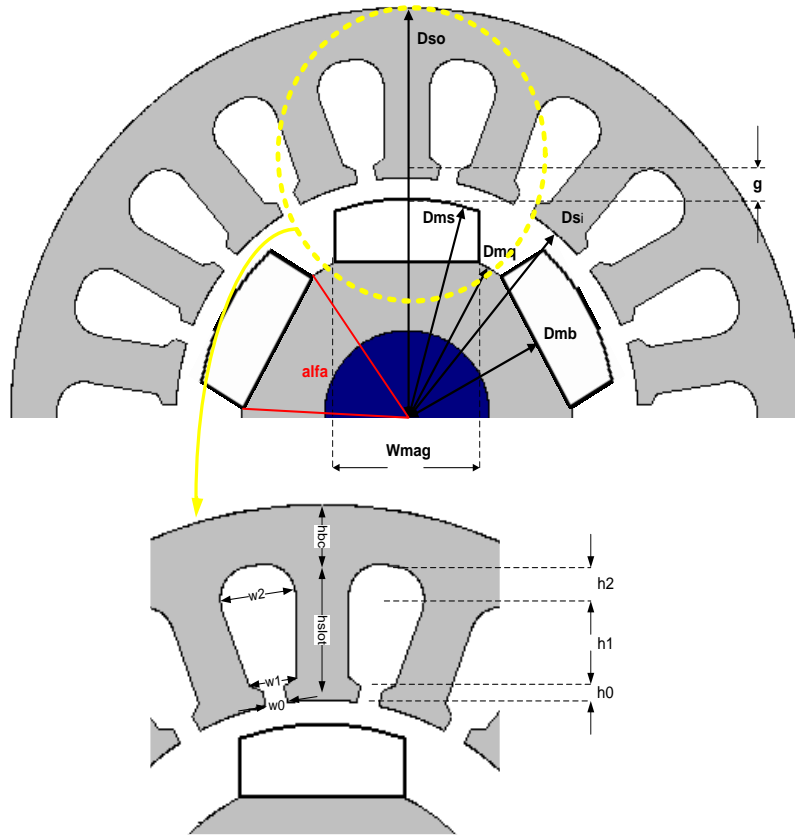


Figure 2.1: Main dimensions of the motor

2.1 Calculation of Magnetic Circuit Parameters

Magnetic model is given in Figure 2.2. Equations for calculation of air gap, magnet, stator tooth and back core reluctances and flux densities are going to be derived. Each magnet is presented by a Norton equivalent circuit where \mathcal{O}_r is flux source and R_{m0} is internal reluctance of magnet. The reluctance seen by air gap flux passing from magnets to stator side is modelled with R_g , R_{th} and R_{bc} represents equivalent reluctances of tooth and back-core path respectively. The leakage fluxes between magnets are modelled with R_{rl} and rotor side reluctance with R_r . The symbols used in the circuit is described in Table 2.1.

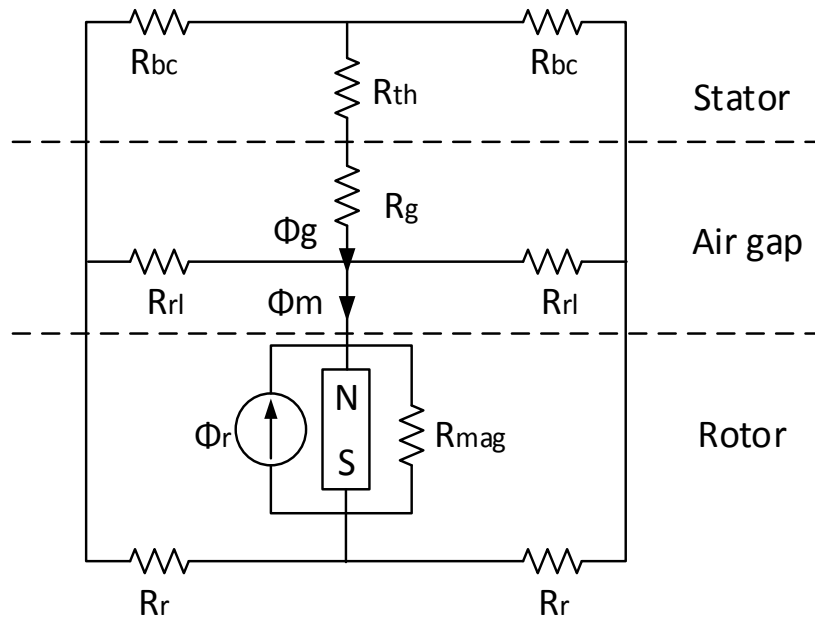


Figure 2.2: Magnetic equivalent circuit

Table 2.1: Description of Symbols in the Magnetic Equivalent Circuit

| Symbol | Description |
|-------------|---|
| Φ_g | Air gap flux (passing from air gap to stator) |
| Φ_{rl} | Rotor leakage flux between rotor poles |
| Φ_m | Magnet flux (passing from magnet to air gap) |
| Φ_r | Flux generated by the magnet |
| R_{bc} | Reluctance of stator back-core |
| R_{th} | Reluctance of stator tooth |
| R_g | Reluctance of air gap |
| R_{rl} | Reluctance of rotor leakage |
| R_{mag} | Reluctance of internal leakage of the magnet |
| R_r | Reluctance of rotor yoke |

In the circuit, a Norton model is used for magnet; flux source Φ_r in parallel with internal permeance P_{m0} called magnet leakage permeance. Φ_r is called as remanent flux which describes how much flux remains in the magnet after it has been magnetized.

A magnetic circuit is in fact analogous to an electric circuit where Flux - MMF - Reluctance that are present instead of Current - Voltage - Resistance respectively. Magnetic circuits can be solved like an electrical circuit and representations like Thevenin or Norton can be applied to both.

2.1.1 Air Gap Reluctance

In this section, air gap reluctance is going to be calculated in terms of equivalent air gap length, air gap area. Air gap reluctance is going to be used in the solution of the magnetic circuit to find the air gap flux density.

Most of the magnet flux crosses the air gap via air gap reluctance. It is known that for calculation of a reluctance, flux path length and area that flux passes has to be calculated. At calculation of air gap reluctance, flux path is the equivalent air gap length which is figured out by the Carter's coefficient k_c and the area that flux passes is the area of air gap A_{gap} .

$$R_g = \frac{g \times k_c}{\mu_0 \times A_{gap}} \quad (2.1)$$

The air gap length does not remain constant through the magnet surface. This length slightly changes, the effect of this change is very small on air gap reluctance and this effect is neglected during calculations.

The parameters required to calculate air gap reluctance are described below and the calculations are explained with the help of figures and equations.

2.1.1.1 Air Gap Area

The air gap area is the area through which the flux passes as it crosses the air gap. While air gap area A_{gap} is being calculated, the surface of magnet is considered as the width on the radial side, where axial length of the motor L is taken as the length on axial side.

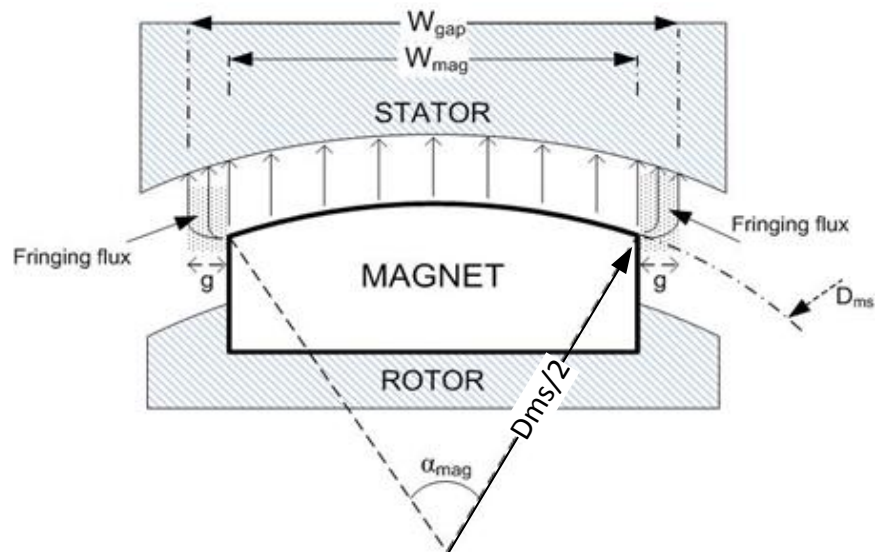


Figure 2.3: Fringing flux in the air gap[5]

Due to the existence of air gap in the flux path, fringing flux is inevitable. Fringing flux is only added for radial direction shown in Figure 2.3 because flux paths are only on the radial axis of the motor. If stator and rotor stack lengths were different, then fringing flux has to be considered in axial direction. Also it is difficult to calculate the shape of fringing flux, instead of this calculations, approximations are used. Width of the fringing flux is approximately taken as same with air gap length g . In other words, magnet surface is expanded with approximately an air gap length at both sides to include the effect of fringing flux.

$$A_{gap} = \left(\frac{1}{2} \times D_{ms} \times \alpha_{mag} + 2 \times g \right) \times L \quad (2.2)$$

Magnet surface is assumed as circular with a diameter D_{ms} . The mechanical angle span of magnet span in radians is represented as α_{mag} which can be calculated in equation 2.3 where W_{mag} is the width of the magnet.

$$\alpha_{mag} = 2 \times \sin^{-1} \left(\frac{W_{mag}}{D_{ms}} \right) \quad (2.3)$$

2.1.1.2 Equivalent Air Gap Length

In stator, semi closed slots are chosen for ease of placing stator winding. But, due to this slot openings, there exists a non-uniform air gap which causes an increase in the reluctance of the air gap. Carter has found a coefficient to model this increase in the analytical calculations.

If motor has slot opening only on stator, Carter's coefficient is calculated for stator. But motor may have slots (or saliency) both on stator and rotor, for this case Carter's coefficient must be calculated separately for stator and rotor. Total Carter's coefficient is calculated from multiplication of coefficients of stator and rotor.

Carter's coefficient depends on a ratio of slot opening to air gap length. Calculation on stator Carter's coefficient is shown in Equation 2.4 [3].

$$k_{cs} = \frac{\pi \times D_{si} / N_{slot}}{\pi \times D_{si} / N_{slot} - \frac{w_0^2}{w_0 + 5 \times g}} \quad (2.4)$$

In Equation 2.4, $\pi \times D_{si} / N_{slot}$ is the slot pitch where D_{si} inner diameter of stator and N_{slot} is the number of slots, g is the air gap length and w_0 is the opening width of stator slot.

After calculation of Carter's coefficient for stator equivalent air gap length can be found from Equation 2.5 given below.

$$g' = g \times k_{cs} \quad (2.5)$$

2.1.2 Magnet Reluctance

In this section, magnet parameters are going to be calculated such as magnet area and magnet reluctance. This parameters are going to be used in the solution of the equivalent magnetic circuit for calculating the magnet operating point.

Magnet reluctance R_{mag} is shown in magnetic equivalent circuit given in Figure 2.2. Magnet reluctance R_{mag} is modelled with R_{mag0} magnet internal reluctance and R_{rl} rotor leakage reluctance as shown in equivalent magnetic circuit.

If rectangular magnets are used in the motor the equation will be as given in equation 2.6, where h_{mag} is the magnet height in the direction of magnetization, A_{mag} is magnet area in normal direction of magnetization.

$$R_{mag} = \frac{h_{mag}}{\mu_r \times \mu_0 \times A_{mag}} \quad (2.6)$$

For getting better results magnet is divided into 5 regions which is described before. As a result, magnet reluctance is calculated as reluctance of five parallel branches (rectangular magnet regions with equal magnet width given in Figure 2.4). Flux path is the parallel branch of the magnet heights and the area that flux passes is one fifth of magnet area. The magnet internal leakage reluctance equation becomes as shown in Equation 2.7.

$$R_{mag0} = \frac{1}{\mu_r \times \mu_0 \times \frac{A_{mag}}{5}} \times \left(\frac{2}{h_{mag1}} + \frac{2}{h_{mag2}} + \frac{1}{h_{mag3}} \right)^{-1} \quad (2.7)$$

Rotor leakage reluctance represents the paths of magnet flux components that fail to cross the air gap and this leakage is difficult to estimate. Rotor leakage reluctance is assumed to be ten times magnet reluctance [1].

$$R_{rl} = 10 \times R_{mag0} \quad (2.8)$$

Overall magnet reluctance become the parallel of magnet reluctance and rotor leakage reluctance as described above.

$$R_{mag} = \left(\frac{1}{R_{mag0}} + \frac{1}{R_{rl}} \right)^{-1} \quad (2.9)$$

The parameters required to calculate magnet reluctance is magnet height and magnet area of which calculations are described below.

2.1.2.1 Magnet Area

In the equation, A_{mag} is the cross sectional area of magnet. Magnet area is assumed rectangular of which short edge is magnet width W_{mag} shown in Figure 2.1 and long edge is axial length of the motor.

$$A_{mag} = W_{mag} \times L \quad (2.10)$$

2.1.2.2 Magnet Height

The magnet used in the motor does not have same height through magnet width. That is why magnet height needed to be calculated for different regions to get better results in the calculations. The magnet is modeled as 5 rectangular pieces which are connected in parallel. These heights are going to be used in reluctance calculation to find a closer solution to the real reluctance value.

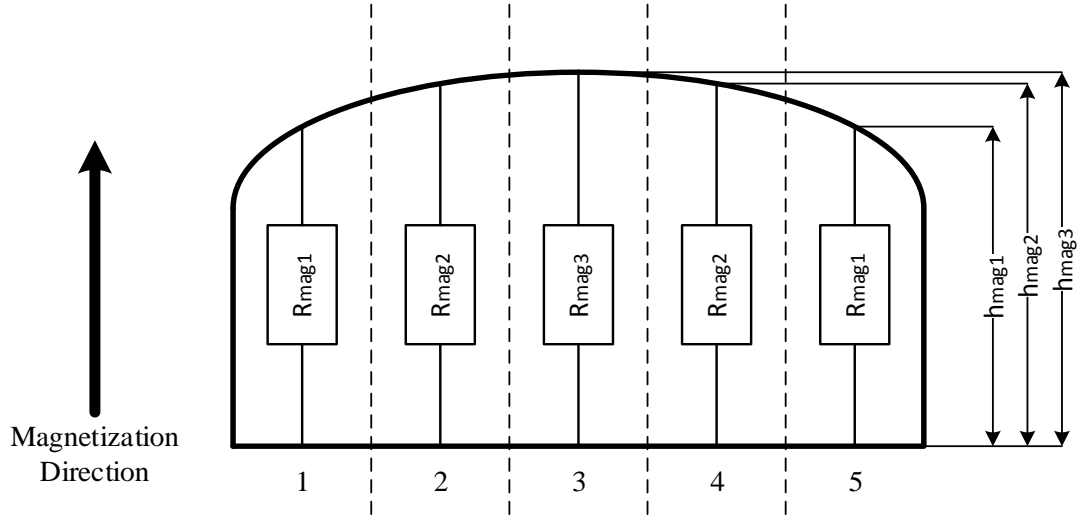


Figure 2.4: Magnet heights

Magnet region is divided by 5 with same widths, the heights of the regions are $h_{mag1} - h_{mag2} - h_{mag3} - h_{mag2} - h_{mag1}$ for regions 1-5 shown in Figure 2.4. h_{mag1} is the height of region 1 and 5, h_{mag2} is the height of region 2 and 4 and h_{mag3} is the height of region 3 and which is also the maximum magnet height as shown in Figure 2.4.

Each height is taken as the height in the middle of that corresponding rectangular region which is used for modeling the magnet. If magnet is divided into more regions this means better approximate magnet model. But for ease of calculation 5 regions are enough for the model.

Magnet height calculations are given in equations 2.11-13 where D_{ms} is the diameter of the magnet surface and D_{mb} is the diameter of magnet base and α_{mag} is the angle span of the magnet shown in Figure 2.5(α_{mag} is shown as $teta$).

$$h_{mag1} = 0.5 \times \left[D_{ms} \times \cos\left(\frac{2}{5} \alpha_{mag}\right) - D_{mb} \right] \quad (2.11)$$

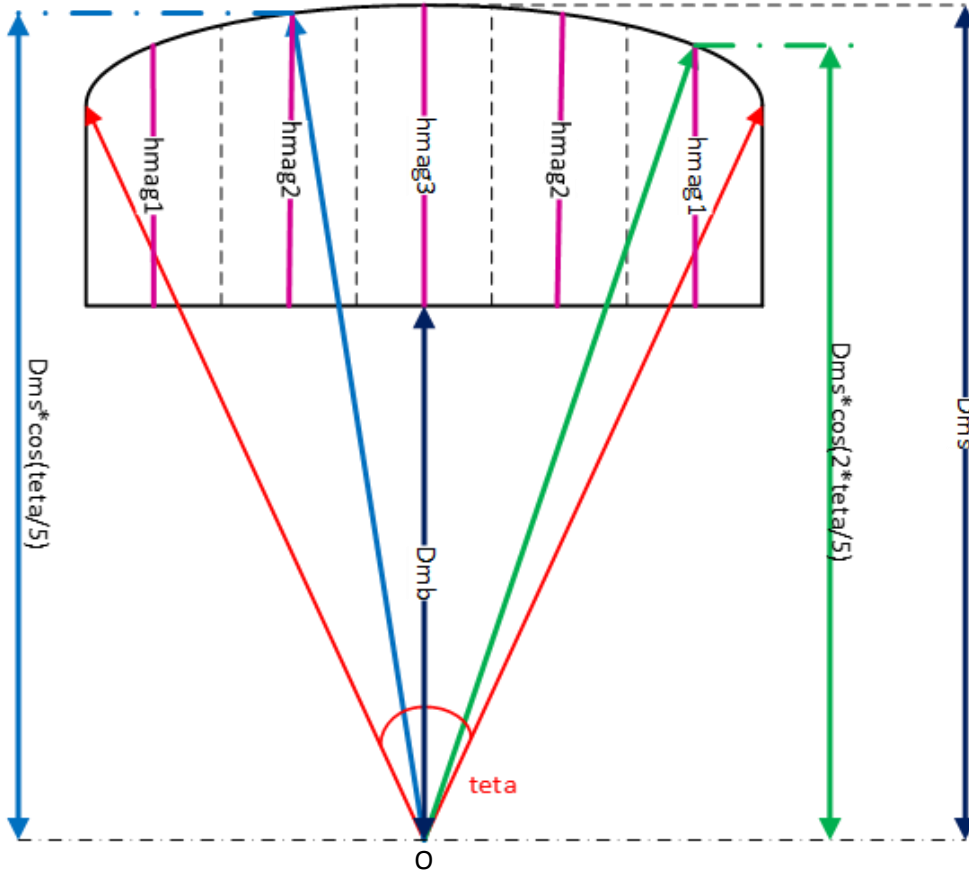


Figure 2.5: Illustration of magnet heights for regions

$$h_{mag2} = 0.5 \times \left[D_{ms} \times \cos\left(\frac{1}{5} \alpha_{mag}\right) - D_{mb} \right] \quad (2.12)$$

$$h_{mag3} = 0.5 \times \left[D_{ms} \times \cos\left(\frac{0}{5} \alpha_{mag}\right) - D_{mb} \right] = 0.5 \times (D_{ms} - D_{mb}) \quad (2.13)$$

The equations above are derived geometrically from Figure 2.5 where point O is the center of the motor.

2.1.3 Stator Tooth and Back-core Reluctance

The stator teeth and back core can be often assumed to be infinitely permeable and their reluctance may be neglected. However, for high field density motors such as servo applications, motor volume is forced to be minimized by pushing flux densities to saturation level. In such cases there can be considerable amount of MMF drop on tooth and back core path, so reluctances for these paths should be included in magnetic field calculations.

$$R_{th} = \frac{h_{slot}}{\mu_{steel} \times \mu_0 \times A_{th}} / S_{pitch} \quad (2.14)$$

$$R_{bc} = \frac{\pi \times (D_{so} - h_{bc})}{\mu_{steel} \times \mu_0 \times A_{bc}} / p \quad (2.15)$$

In Equation 2.14, h_{slot} is length of path from tooth tip to slot dip equals to slot height, A_{th} is the area of stator tooth and S_{pitch} is the slot pitch. The path for back core reluctance is assumed to be in the middle of back core depth. Therefore the diameter of the path is taken as $D_{so} - h_{bc}$ (in the middle of stator yoke), and A_{bc} is the back-core area and p is number of poles.

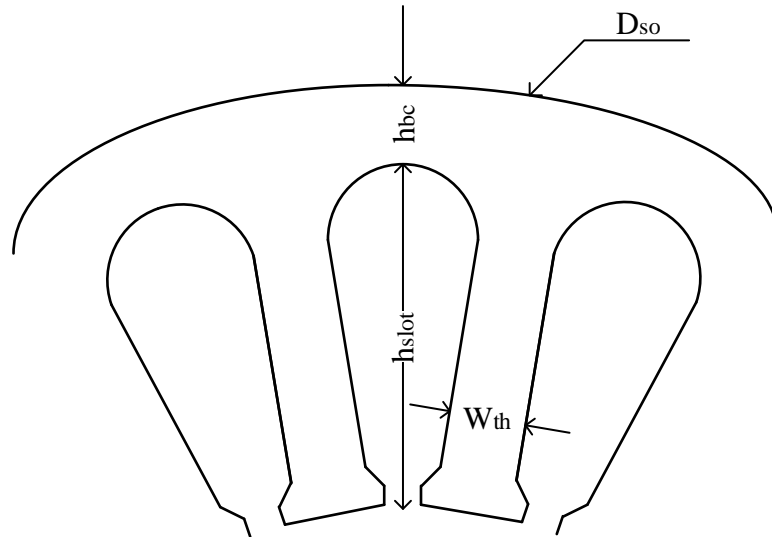


Figure 2.6: Abbreviations for stator steel dimensions

Tooth area is calculated from tooth width W_{th} as given in Equation 2.16 and back-core area is calculated from back-core height h_{bc} which is shown in Equation 2.17 where L is the stack length.

$$A_{th} = W_{th} \times L \quad (2.16)$$

$$A_{bc} = h_{bc} \times L \quad (2.17)$$

2.1.4 Solution of the Magnetic Circuit

The reluctances shown in the equivalent magnetic circuit given in Figure 2.2 are derived in previous sections. In this section flux densities are going to be calculated.

It is said before that the magnetic circuits can be solved like electric circuits. The magnetic circuit is solved from the information that the MMF drop in the magnetic circuit is equal to the MMF created by the magnet. The MMF drop on stator tooth and back core reluctances are too small according to drop on air gap reluctance, so that the effect of back core and tooth reluctance is omitted. The MMF equation becomes as shown in Equation 2.18.

$$\Phi_g \times R_g = (\Phi_r - \Phi_g) \times (R_{mag} + R_{rl}) \quad (2.18)$$

Air gap flux density is calculated from the Equation 2.19, where B_r is remanent flux density which is given by the magnet manufacturer and it changes with temperature.

$$B_g = \frac{A_{mag}/A_g}{1 + R_g/R_{mag}} \times B_r \quad (2.19)$$

Mean and peak values of air gap flux density is presented in Figure 2.6. Mean value is calculated from the ratio of air gap area to pole area.

$$\overline{B}_g = \frac{A_{gap}}{A_{pole}} \times B_g \quad (2.20)$$

Where A_{pole} is the pole area of which calculation is given below.

$$A_{pole} = \pi \times (D_{si} - g) \times L/p \quad (2.21)$$

Equation 2.22 is the simplified version of equation 2.20.

$$\overline{B}_g = \frac{0.5 \times D_{ms} \times \alpha_{mag} + 2 \times g}{\pi \times (D_{si} - g)/p} \times B_g \quad (2.22)$$

Peak value of air gap flux density is given in equation 2.23.;

$$\widehat{B}_g = \frac{h_{mag}}{h_{mag} + g \times \mu_r} \times B_r \quad (2.23)$$

This value can also be found via Fourier transformation of the rectangular waveform of air gap flux density where $f(\theta)$ is the function of air gap flux density waveform which is given in Figure 2.7 with blue color. It is known that since the waveform is symmetric, the integral is multiplied by two and since the waveform is accepted as rectangular (the distortion due to fringing flux is omitted) only bandwidth of the waveform is considered in integral. In other words, $f(\theta)$ is zero in the region out of the magnet angle span and in integral region $f(\theta)$ is constant at B_g which can be seen from Figure 2.7.

$$\begin{aligned} \frac{1}{\pi} \int_0^{360} f(\theta) \times \sin \theta \times d\theta &= \frac{2}{\pi} \int_0^{180} f(\theta) \times \sin \theta \times d\theta \\ &= \frac{2}{\pi} \int_{\frac{180-\alpha_{mag}}{2}}^{\frac{180+\alpha_{mag}}{2}} f(\theta) \times \sin \theta \times d\theta \end{aligned} \quad (2.24)$$

Magnet operating flux density is calculated from Equation 2.25 given below. The reluctance of rotor leakage, airgap and magnet is given in the previous section.

$$B_m = \frac{1 + \frac{R_g}{R_{rl}}}{1 + \frac{R_g}{R_{mag}}} \times B_r \quad (2.25)$$

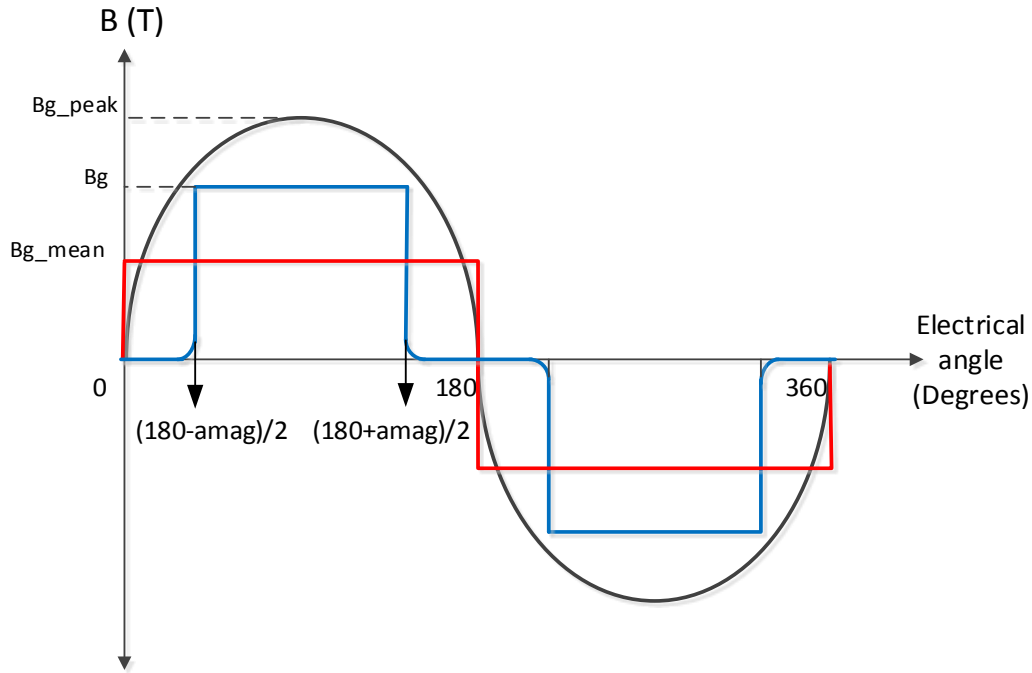


Figure 2.7: Air gap flux density waveform

The back core and tooth flux densities are very important for the designer because it shows whether the magnetic material saturated or not.

Peak value of stator tooth flux density:

$$B_{th} = \frac{h_{mag}}{h_{mag} + g \times \mu_r} \times \frac{\pi \times (D_{si})/N_{slot}}{W_{th}} \times B_r \quad (2.26)$$

It is known that the flux of back core is half of the air gap flux. So:

$$\Phi_{bc} = \frac{1}{2} \times \Phi_g \quad (2.27)$$

$$B_{bc} \times A_{bc} = \frac{1}{2} \times B_g \times A_g \quad (2.38)$$

Peak value of back-core flux density is derived by the simplification of equation 2.29.

$$B_{bc} = \frac{\frac{1}{2} \times \widehat{B}_g \times A_g}{h_{bc} \times L} \quad (2.29)$$

2.2 Electrical Parameters

The permanent magnet motors operates similar to synchronous motors. Both have three phase windings on stator. Instead of field winding on rotor of synchronous motors, magnets creates the field in the rotor of pm motors. Due to placement of magnets two different axis occurs, d and q, like salient pole rotors. The pm motors can be modelled with two electrical circuits due to these d and q axis. The circuits consist of resistances to model copper and core loss, an inductance and a voltage source to model back EMF. This model is sufficient for a pm motor working in linear operation region as in synchronous motors case.

In this two-axis model, following assumptions are accepted which are given below:

- Rotor and stator winding only excite spatial sinusoidal voltage and current.
- Magnetic materials are isotropic.
- There is no saturation (linear magnetic equations).

First assumptions declares that there are no winding factors of harmonic and only fundamental component of current and voltage linkages are considered. In second assumption, it is meant that permeability “ μ ” and the permittivity “ ϵ ” of the motor core are uniform in all directions. The third assumption says that the magnetic saturation of the core is neglected.

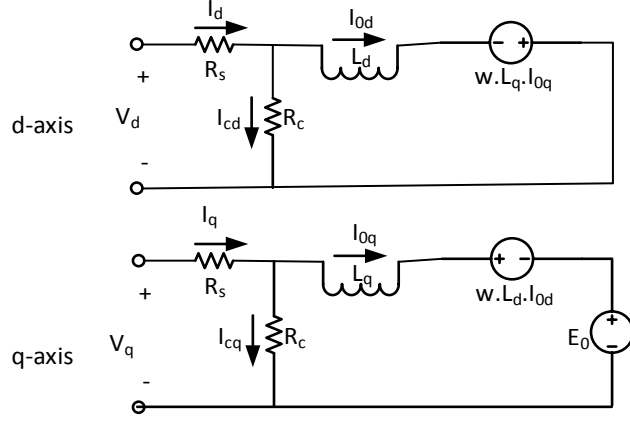


Figure 2.8: Equivalent electrical circuit

To solve the equivalent electrical circuits in Figure in 2.8, Equations 2.30-31 must be solved.

$$V_d = R_s \times i_d + L_d \times \frac{dI_{0d}}{dt} - \omega \times L_q \times i_q \quad (2.30)$$

$$V_q = R_s \times i_q + L_q \times \frac{dI_{0q}}{dt} + \omega \times L_d \times i_d + \omega \times \Psi_M \quad (2.31)$$

The phase resistance is shown with R_s , the current flowing on this resistance is given with symbols i_d and i_q , the inductances are L_d and L_q , the current flowing on these inductances are I_{0d} and I_{0q} for d and q axis respectively. Ψ_M is the magnet flux and ω is the electrical speed of shaft in rad/sec .

2.2.1 Calculation of Phase Resistance

Phase resistance calculation is very important because it affects the current flowing through the winding and also the copper loss on that winding which cause heating in the stator. The calculation is done from the resistivity of copper, total wire length and wire area. But the known calculation given in Equation 2.32 is valid for room temperature value which is $25^\circ C$.

$$R = \rho_{cu} \times \frac{(N_{coil} \times L_{wire} + L_{con})}{A_{wire}} \quad (2.32)$$

In Equation 2.32, ρ_{cu} is resistivity of copper, N_{coil} is number of coils per phase and L_{wire} is conductor length in one coil, L_{con} is conductor used for connection of coils and A_{wire} is the area of the conductor.

Resistance value changes with the change of temperature. For steady state operation, resistance should be calculated at working temperature of the motor. This working condition temperature is obtained where motor no longer heats up at rated conditions around 150°C.

$$R' = R \times \frac{234.5 + T}{234.5 + 25} \Big|_{T=150^\circ\text{C}} \quad (2.33)$$

This resistance value calculated from Equation 2.33 is more important for the designer, because it affects the nominal values of the motor.

For calculating phase resistance, equations of slot area, wire diameter, total wire length have to be derived. These derivations are explained below in detail.

2.2.1.1 Wire Cross Section Area

While calculating the wire area fill factor k_{fill} is very important. This factor gives the ratio of total wire (copper) area to slot area. Fill factor is given by the manufacturer. Then with wire diameter can easily be calculated which is critical for choosing the copper from manufacturer sheets. N_{turn} is the number of turns per coil.

$$A_{wire} = \frac{1}{2} \times \frac{A_{slot} \times k_{fill}}{N_{turn}} \quad (2.34)$$

Stator slot dimensions are shown in Figure 2.9. Top part is a half circle and the lower part is a trapezoidal. Slot type used in the motor is a semi-closed slot which is connected to air gap with slot opening. Slot area is calculated geometrically.

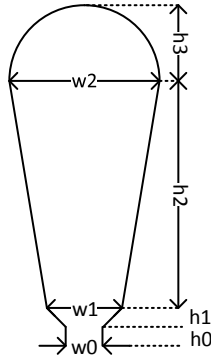


Figure 2.9: Stator Slot Dimensions

Slot area is calculated for to be used in wire cross sectional area and then in phase resistance.

$$A_{slot} = \frac{1}{2} \times (w_1 + w_2) \times h_2 + \frac{1}{2} \times \pi \times \left(\frac{h_3}{2}\right)^2 \quad (2.35)$$

2.2.1.2 Conductor Length

For calculation of total conductor length, winding is divided into two parts. First one is the length of conductor in one coil and the second one is the conductor used for connection of coils.

- **Conductor Length in One Coil**

Conductor length in one coil is needed for calculating total conductor length so the phase resistance. During this calculation, conductors are assumed to be placed in the middle of the slot.

$$L_{wire} = 2 \times N_{turn} \times \left[L + L_{ext} + \left(\frac{S_{pitch}}{N_{slot}} \times (D_{si} + h_{slot}) \times \pi \right) \right] \quad (2.36)$$

where N_{turn} is the number of turns per coil and N_{slot} is the number of slots, L is the stack length and L_{ext} is the external length in the radial axis of the motor. S_{pitch} is the stator slot pitch.

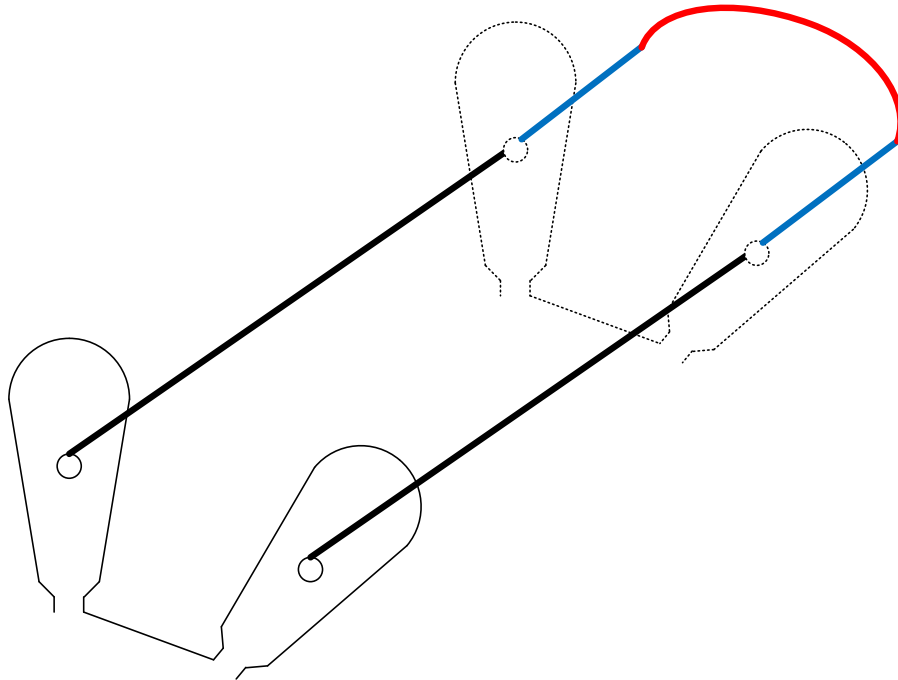


Figure 2.10: Illustration of conductor parts

The black part shows the conductor in stator core of which length is equal to stack length, the blue part is the external conductor of which value is taken as approximation and the red part is the conductor between two sides of a coil.

- **Conductor Length for Series Connection of Coils**

Conductor length for series connection of coils is calculated similar to the calculations done above. The lengths are calculated with the help of stator steel dimensions.

The conductor is assumed to be going from one slot to other slot (according to winding scheme) at a diameter $D_{so} - h_{slot}$.

$$L_{con} = \frac{N_{coil} \times S_{pitch}}{N_{slot}} \times (D_{so} - h_{slot}) \times \pi + 2 \times N_{coil} \times L_{ext} \quad (2.37)$$

2.2.2 Calculation of Phase Inductance

In the calculation of phase inductance, three components of inductance is considered which are slot leakage inductance, end winding leakage inductance and magnetizing inductance.

Total inductance is the sum of slot, end winding and magnetizing inductance as shown in Equations 2.39-40. Due to the difference in d and q-axis magnetizing inductances, total inductances are not equal in d and q-axis.

$$L_d = L_{slot} + L_{end} + L_{md} \quad (2.38)$$

$$L_q = L_{slot} + L_{end} + L_{mq} \quad (2.39)$$

2.2.2.1 Slot Leakage

Specific slot permeances are related to magnetic structure on leakage flux paths. These flux paths differs in single and double layer winding.

For single layer windings, slot leakage permeance coefficient p_{slot} is calculated from the Equation 2.40 given below [2].

$$p_{slot} = \mu_0 \times \left(\frac{h_0}{w_0} + 2 \times \frac{h_1}{w_1 + w_2} + k_t \times \frac{h_2}{3 \times w_1} \right) \quad (2.40)$$

Where k_t is a constant coming from slot geometry which is found from Equation 2.41.

$$k_t = 3 \times \frac{(4t^2 - t^4 \times (3 - 4 \times \ln(t) - 1))}{(t^2 - 1)^2 \times (t - 1)} \quad (2.41)$$

In Equation 2.41, t is the ratio of width of slot top to width of slot bottom (w_2/w_1). After calculation of slot leakage permeance, the leakage inductance can be obtained with Equation 2.42.

$$L_{slot} = \frac{3 \times N^2 \times L}{N_{slot}} \times p_{slot} \quad (2.42)$$

For double layer windings, the leakage flux due to top layer conductor travels a different path than leakage flux due to bottom layer conductor. Also there is a mutual flux path due to interaction of top and bottom layer winding

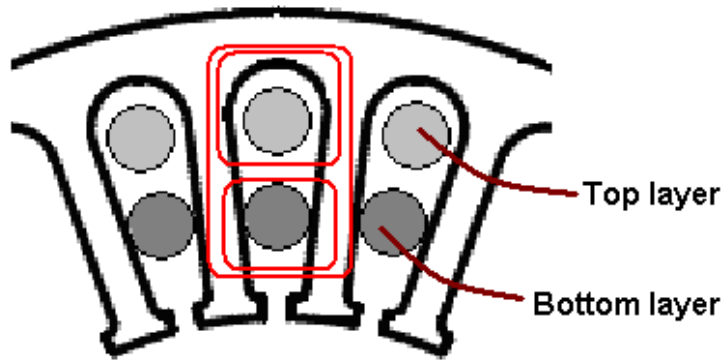


Figure 2.11: Contours showing slot leakage paths[5]

Leakage permeances are calculated as pT for top conductor, pB for bottom conductor and pTB for the interaction of coils [4].

$$pT = \frac{1}{2} \times \mu_0 \times \left(0.623 + \frac{h_0}{w_0}\right) + \frac{1}{3} \times \mu_0 \times \frac{h_3}{w_2} \quad (2.43)$$

$$pB = \mu_0 \times \left(\frac{h_0}{w_0} + 2 \times \frac{h_2 - h_3}{w_1 + w_2}\right) \quad (2.44)$$

$$pTB = \mu_0 \times \left(\frac{h_0}{w_0} + \frac{h_1 - h_3}{w_1 + w_2} \right) \quad (2.45)$$

Self-component of slot leakage for all three phase is calculated as given in Equation 2.46. This component will be maximum when coil pitch is unity.

$$L_{sls} = \frac{3 \times N^2 \times L}{N_{slot}} \times (pT + pB + 2 \times pTB \times (3 \times C_{pitch} - 2)) \quad (2.46)$$

Mutual-coupling between three phases due to slot flux is found with the equation given below. This term will be zero when coil pitch is unity.

$$L_{slm} = \frac{3 \times N^2 \times L}{N_{slot}} \times pTB \times 3 \times (1 - C_{pitch}) \quad (2.47)$$

Slot leakage inductance of a single slot is sum of self-component and mutual components calculated above.

$$L_{slot} = L_{sls} + L_{slm} \quad (2.48)$$

2.2.2.2 End Winding Inductance

There exists a leakage on end-winding which is the part out motor lamination. To calculate the end winding leakage inductance, total length of end-winding has to be calculated. Here w_{c1} is the length of the distance that end winding is located on the radial axis out of the motor's axial axis. L_{1e} is the total end winding length [2].

$$w_{c1} = \pi \times (D_{si} + h_{slot}) \times \frac{S_{pitch}}{N_{slot}} \quad (2.49)$$

In the Equation 2.49, it is assumed that the end winding turns out from a diameter which is $D_{si} + h_{slot}$. Total end winding length is given in Equation 2.50.

$$L_{1e} = 2 \times L_{ext} + w_{c1} \quad (2.50)$$

End winding leakage permeance equation is estimated on the basis of experiments. Equation 2.51 is used for double-layer, low voltage, small and medium power motors. After calculation end winding leakage permeance, the leakage inductance due to end-winding is calculated as given in Equation 2.52.

$$p_{end} = 0.34 \times \mu_0 \times \frac{N_{slot}}{phase \times pole} \times \left(1 - \frac{2}{\pi} \times \frac{w_{c1}}{L_{1e}}\right) \quad (2.51)$$

$$L_{ew} = 2 \times \frac{(N_{coil} \times N_{turn} \times k_w)^2}{pole / 2 \times \frac{N_{slot}}{phase \times pole}} \times p_{end} \times (2 \times L_{ext} + w_{c1}) \quad (2.52)$$

2.2.2.3 Magnetizing Inductance

Magnetizing inductance is calculated as given in Equation 2.53 where A_{pole} is pole area given in Equation 2.17.

$$L_m = \frac{3}{2} \times \frac{4}{\pi} \times \frac{1}{pole} \times (N_s \times k_w)^2 \times \frac{\mu_0 \times A_{pole}}{g'} \quad (2.53)$$

Due to the saliency of rotor (placement of magnets), two different axes occur. First one is the direct axis which passes through the magnet directly. The other one is the quadratic axis which flux passes through the rotor steel. The representation of d and q axis is shown in Figure 2.12.

The presence of a permanent magnet across the air gap from the slotted structure changes the computation of Carter's coefficient. In this case, the air gap length g must be replaced by $g + l_m/\mu_r$, where l_m is the magnet length and μ_r is the magnet relative recoil permeability. $g + l_m/\mu_r$ value is used for calculating the d-axis equivalent air gap in Equation 2.54 which is used for d-axis magnetizing inductance calculated from Equation 2.57. This value is only used for d-axis calculations because there is no magnet on q-axis of the motor ($l_m = 0$).

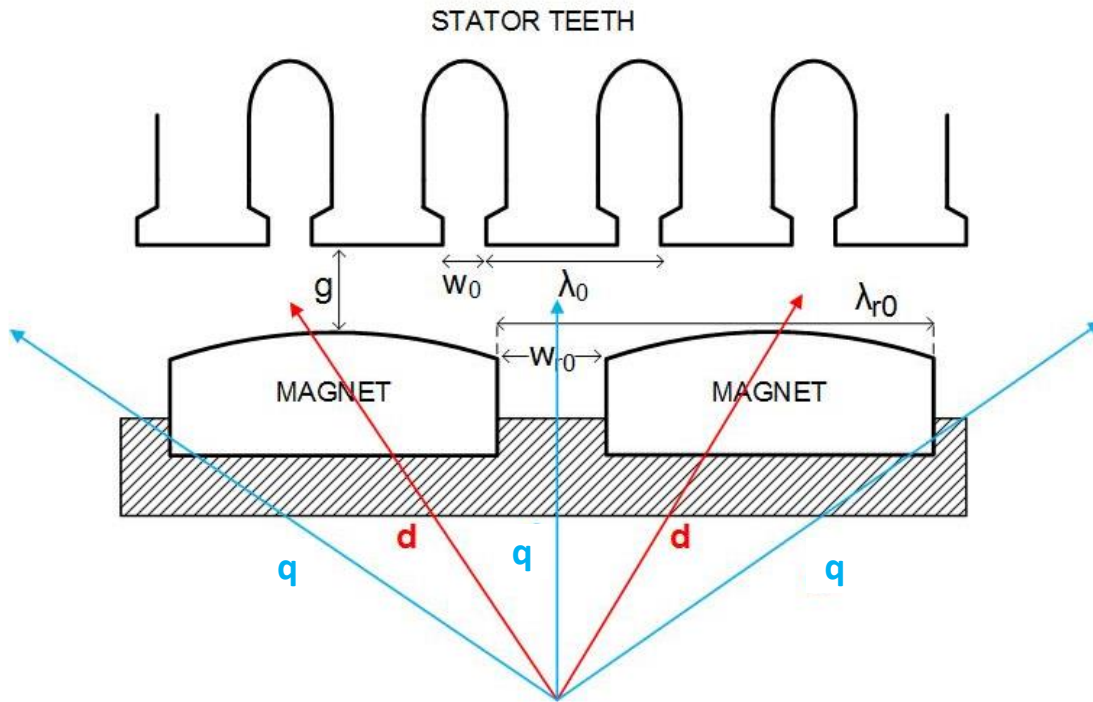


Figure 2.12: The representation of d and q axis

While calculating magnetizing inductance, equivalent air gap length g' must be calculated for d and q axis. Equivalent air gap will be different for d and q axis and this will result in difference in magnetizing inductance of d and q axis.

In the calculation of d-axis equivalent air gap, the magnet height is considered which is added to air gap length of air gap length.

$$g'_d = g \times k_{cs} + \frac{h_{mag,mean}}{\mu_r} \quad (2.54)$$

In Equation 2.54, mean magnet height is considered due to the direct axis which is passing through magnet.

The q-axis equivalent air gap is calculated by the multiplication of stator and rotor Carter's coefficients (k_{cs} is the Carter's coefficient of stator and k_{cr} is the Carter's

coefficient of rotor). Calculation of stator Carter's coefficient is explained in previous chapter. In the calculation of rotors Carter's coefficient, the rotor slot pitch needs to be calculated. In PM motors, there is no slot on rotor, so instead of slots the area where magnets are placed is used. D_{mb} is the diameter of magnet base used as the base of the area mentioned before.

$$k_{cr} = \frac{\pi \times D_{mb}/pole}{\pi \times D_{mb}/pole - \frac{W_{mag}^2}{W_{mag} + 5 \times \left(g + \frac{D_{mq} - D_{mb}}{2}\right)}} \quad (2.55)$$

$$g'_q = \frac{(D_{si} - D_{mq})}{2} \times k_{cs} \times k_{cr} \quad (2.56)$$

After finding the equivalent air gap lengths for d and q axis, magnetizing inductance can be found by modifying Equation 2.53 with related axis equivalent air gap lengths.

$$L_{md} = \frac{3}{2} \times \frac{4}{\pi} \times \frac{1}{8} \times (N_s \times k_w)^2 \times \frac{\mu_0 \times A_{pole}}{g'_d} \quad (2.57)$$

$$L_{mq} = \frac{3}{2} \times \frac{4}{\pi} \times \frac{1}{8} \times (N_s \times k_w)^2 \times \frac{\mu_0 \times A_{pole}}{g'_q} \quad (2.58)$$

2.2.3 Emf and Torque Constants

The emf constant k_e , is the gain which tells the amount of voltage which will be induced per unit speed as calculated in Equation 2.60. And similarly, torque constant k_t is the gain of the motor showing the amount of torque which is produced per unit current which is shown in Equation 2.59.

$$k_e = \sqrt{3} \times \frac{pole}{2} \times N_s \times B_g \times A_{pole} \times k_w \times k_{st} \quad (2.59)$$

$$k_t = 3 \times \frac{\text{pole}}{\sqrt{2}} \times N_s \times B_g \times A_{\text{pole}} \times k_w \times k_{st} \quad (2.60)$$

These constants are very important for the user, because these values are directly related to the system requirements. The user chooses which motor is appropriate for the application that the motor will be used in, by looking these coefficients.

2.2.4 Losses

Calculation of losses is one of the key issues that must be involved in a design process. If optimization is going to be carried out this prediction or calculation becomes more important. For PM machines, it is known that the higher torque density for smaller design means lower the efficiency due to the increasing loss. It is difficult to find an optimum design without modelling the losses. The losses are classified into four groups which are copper, core, magnet and mechanical loss.

2.2.4.1 Copper Loss

The copper loss calculated from the phase resistance R which is calculated in Section 2.2.1.5 and from the rms armature current I . The total winding loss is calculated according to the equation 2.61.

$$P_{cu} = 3 \times I^2 \times R \quad (2.61)$$

It must be noted that per phase resistance value has to be modified by Equation 2.34 if copper loss is to be calculated at high or low temperatures different than room temperature.

2.2.4.2 Core Loss

Best estimations can be obtained by using FE numerical computations. But an approximate equation is given below for analytical calculations. This equation separates core loss in two parts which are eddy and hysteresis losses with the help of

constants k_h and k_e respectively. f is operating electrical frequency, \widehat{B} is peak of flux density and M is total weight of the medium where loss is calculated.

$$P_{loss} = (k_h \times f \times \widehat{B}^2 + k_e \times f^2 \times \widehat{B}^2) \times M \quad (2.62)$$

Friction and windage losses are assumed to be very small and do not effect total loss result. And since magnets creates a constant magnetic field, the loss in rotor core assumed to be negligible. Equation 2.62 needs to be solved for tooth and back-core regions separately as follows.

$$P_{loss} = P_{teeth} + P_{back-core} \quad (2.63)$$

The total mass of teeth and back-core can be calculated from Equations 2.64-65 respectively.

$$W_{th} = N_s \times h_{slot} \times w_{th} \times L \times m_0 \quad (2.64)$$

$$W_{bc} = (D_{so} - h_{bc}) \times \pi \times h_{bc} \times L \times m_0 \quad (2.65)$$

In the equations above, w_{th} is tooth width, D_{so} is stator outer diameter, h_{bc} is stator back core depth behind slot dip, L is axial length, p is pole number and m_0 is weight density of steel core which is read from catalogues. Calculation of total core loss can be derived as in Equation 2.66 which is obtained by rewriting Equation 2.63 which the sum of losses in teeth and back core of stator.

$$P_{core} = (k_h \times f \times \widehat{B}_{th}^2) \times W_{th} + (k_h \times f \times \widehat{B}_{bc}^2) \times W_{bc} \quad (2.66)$$

In the above equation B_{th} and B_{bc} are peak values of tooth and back core flux densities, W_{th} and W_{bc} are total mass of teeth and back core material respectively.

After calculation of core loss, the core loss resistance can be found from the resistance calculation given in Equation 2.67.

$$R_{core} = \frac{(V_q - I_q \times R_s)^2}{P_{core}} \quad (2.67)$$

2.2.4.3 Magnet Losses, Friction and Windage Losses

In this thesis models of magnet, windage and friction losses are not studied. Since magnets coercivity and resistivity is very high, it is assumed that no eddy current induced in the magnets. Friction and windage losses known to be slightly smaller than output power and since the output power is small, friction and windage loss is small which can be neglected. There are available equations to model these friction and windage losses which can be included in future studies.

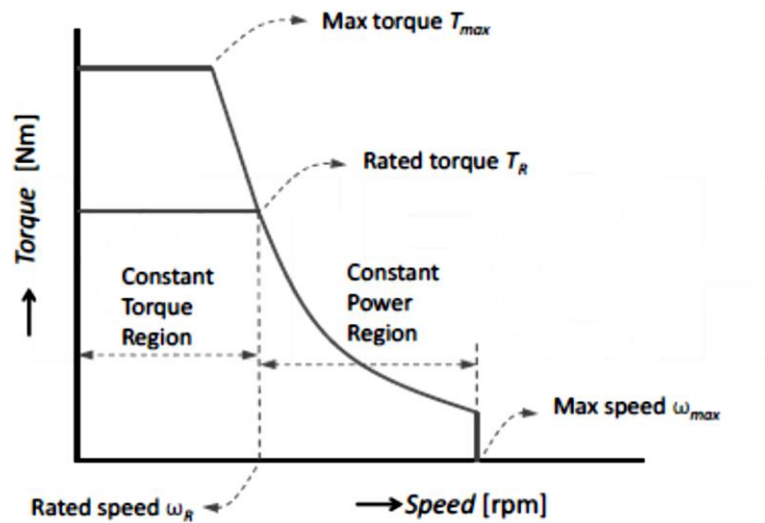


Figure 2.13: Torque-Speed Characteristics of a PM Motor[7]

2.3 Calculation of Torque

Typical torque-speed characteristics of a PM motor is given in Figure 2.13. There are two regions in the graph which are determined by maximum torque T_{max} rated torque T_r and two speed points rated speed w_r and maximum speed w_{max} . The region up to w_r is called as “constant torque region” and the region between w_r and w_{max} is called as “constant power region.”

The calculation of developed electromechanical torque is done under vector control operation where d-axis current $I_d = 0$. Electrical equivalent circuits of a permanent

magnet motor is given in Figure 2.7. When $I_d = 0$, the phase diagram becomes simplified which is given in Figure 2.14 below.

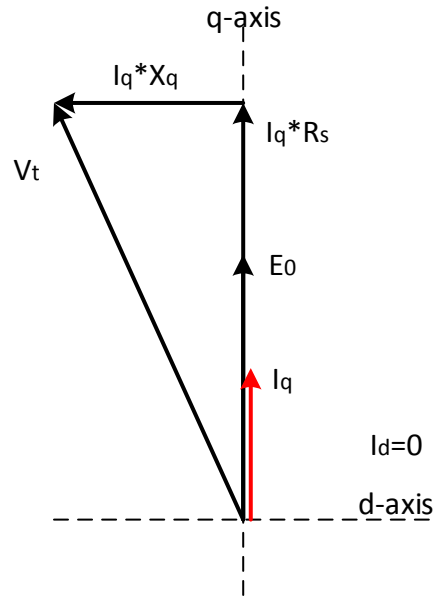


Figure 2.14: Electrical Phase Diagram of PM Machine in Vector Control

The equation of terminal voltage V_t is given in Equation 2.68. In this equation E_0 is the induced emf calculated from frequency and emf constant, R_s is phase resistance calculated from geometry of the stator, X_q is q-axis reactance calculated from inductance and frequency, I_q and I_d are q and d-axis currents respectively.

$$V_t = \sqrt{(I_q \times R_s + E_0)^2 + (I_q \times X_q)^2} \quad (2.68)$$

The only unknown value is I_q . After the I_q is found, then multiplied by torque constant and developed torque is calculated. The calculation process is described in detail below.

Since the speed changes from zero to maximum value, induced emf and q-axis reactance values are changing. Also it is known that current value is between zero

and maximum input current which is limited by the inverter ratings. To carry out the calculations, matrix operations are used. In this matrices, rows represent the current values which does not change in same row and increase 0.05A in each row; columns represent the speed values. The number of rows and columns of the matrices used in the following equations are given in Table 2.2.

Table 2.2: Number of Rows and Columns of Matrices

| Description | Symbol | Number of Rows | Number of Columns |
|-----------------------|-------------|----------------|-------------------|
| Terminal Voltage | V_t | n | m |
| Input Current | I_q | n | m |
| Maximum Input Current | I_{max} | 1 | m |
| Rated Input Current | I_{rated} | 1 | m |
| Speed in rpm | w | 1 | n |
| Electrical Frequency | f_e | 1 | n |
| q-Axis Reactance | X_q | 1 | n |
| Phase Resistance | R_s | 1 | 1 |
| Induced Emf | E_0 | n | m |

In Table 2.2, n is number of rows which is equal to $I_{max} \times 20$, as mentioned above current is increasing 0.05A in each row. In columns, m represents the speed, but it is known that the speed value is higher than thousands so it is preferred to increase speed 100 rpm in each column for shortening the calculation time.

First speed matrix, w should be defined which is shown in Equation 2.69.

$$w = [0 \quad 100 \quad 200 \quad \dots \quad w_{max}] \quad (2.69)$$

After the speed matrix is defined, parameters like electrical frequency f_e , q-axis reactance X_q and induced emf E_0 can be calculated as given in Equations 2.70-72.

$$f_e = w \times \frac{60}{p/2} \quad (2.70)$$

$$X_q = 2 \times \pi \times f_e \times L_q \quad (2.71)$$

$$E_0 = w \times \frac{2 \times \pi}{60} \times k_{emf} \quad (2.72)$$

In the equations above, p is number of poles, L_q is q-axis inductance and k_{emf} is emf constant. Since all the unknowns in Equation 2.68 is calculated, terminal voltage V_t can be found. The terminal voltage and input current matrices are shown below.

$$V_t = \begin{bmatrix} V_{t1,1} & V_{t1,2} & \cdots & V_{t1,m} \\ V_{t2,1} & V_{t2,2} & \cdots & V_{t2,m} \\ \vdots & \vdots & \ddots & \vdots \\ V_{tn,1} & V_{tn,2} & \cdots & V_{tn,m} \end{bmatrix} \quad (2.73)$$

$$I_t = \begin{bmatrix} 0 & 0 & \cdots & 0 \\ 0.05 & 0.05 & \cdots & 0.05 \\ 0.1 & 0.1 & \cdots & 0.1 \\ \vdots & \vdots & \ddots & \vdots \\ I_{max} & I_{max} & \cdots & I_{max} \end{bmatrix} \quad (2.74)$$

Then terminal voltage matrix is checked and the values which are negative and higher than bus voltage is eliminated. Then, same elements in the current matrix are became equal to zero. Maximum of each column in current matrix is assigned to a new matrix called I_{max} given below.

$$I_{max} = [I_{max} \quad \cdots \quad I_{max} \quad I_{max} - 0.05 \quad I_{max} - 0.1 \quad \cdots \quad 0.1 \quad 0.05 \quad 0] \quad (2.75)$$

A similar procedure is repeated to determine rated input current I_{rated} which has same dimensions with I_{max} . Maximum torque and rated torque are found from multiplication of maximum input current matrix and torque constant k_t .

$$T_{max} = I_{max} \times k_t \quad (2.76)$$

$$T_{rated} = I_{rated} \times k_t \quad (2.77)$$

Mechanical output power is calculated from multiplication of torque and speed as shown in Equation 2.78.

$$P_{out} = T_{max} \times w \times \frac{2 \times \pi}{60} \quad (2.78)$$

These matrices are used for drawing graphics in analysis menu. For example, i^{th} element of the torque matrix is the torque value for i^{th} element of the speed matrix. When the points (i^{th} element) are connected to next point ($i+1^{\text{th}}$) via lines the complete torque speed graphic is drawn. The other graphics are drawn with same method.

2.4 Conclusion

In Chapter 2, a previously obtained pm motor model is improved. All equations used in the model are verified and upgraded if needed. New features are added to the new model too. All these changes are going to be explained in Chapter 3.

The main objective of this software is to develop a user friendly interface. This can be done by simplifying the inputs. Also user has to be able to change key parameters whenever a change is wanted. For this purpose slot parameters are entered by user in the software, but in the previous model slot dimensions are calculated in by the program. With this change, user has the freedom to change slot dimensions to see how output parameters are changing with these dimensions.

For the design software, new slot types are added to the model which brings variety to the software and also to the user, and slot leakage inductance and resistance calculations are derived for these new slot types. Also a new magnet type is added to the software.

While magnet reluctance is being calculated, the effect of rotor leakage reluctance was omitted. In the new model, rotor leakage reluctance is included in the calculation of the magnet reluctance.

In the calculation of inductances, number of turns used in the equations are replaced with effective number of turns. So, results got closer to the real values.

For calculation of end-winding leakage inductance, a newly derived equation is used to have better estimations on the inductance.

Also in new model stacking factor which effects the active length of the stator steel pack is considered in calculations to have better results.

New results are going to be compared with previous model results in Chapter 5. Moreover, new results are going to be compared with manufacturer data and the error in the results are going to be calculated and discussed.

CHAPTER 3

FLOW CHART OF PM ANALYSIS SOFTWARE

In this chapter, the developed software is modelled with flow charts and main flow chart of the program and sub flow charts under the main flow chart are going to be described with the help of the calculations in Chapter 2. Each flowchart step named with numbers and these steps are going to be explained one by one.

The model described in Chapter 2 is transformed into a user friendly interface with the programming language C#. Main objective of the program is to take inputs from user such as dimensions, B-H curves and core loss curves. Then the electrical and magnetic parameters are calculated and these results used in the graphical analysis which are torque-speed, input current-speed and output power-speed curves. Also user is able to see the lamination drawn from the dimension inputs. The outputs like machine parameters, graphics and lamination can be saved and printed which are described in the following sections.

The main body of the software is given in Figure 3.1. Once the program is opened, the user have to choose whether a new analysis is going to be made or a previously analyzed motor is going to be analyzed again. If the inputs are known they can be easily entered to the program. But if the inputs are not known a predesign is needed. This predesign can be done from starting from power rating [8]. After the analysis user can choose to print the results or save the results. Finally, after the results are saved or printed user can choose to close the program or start a new analysis.

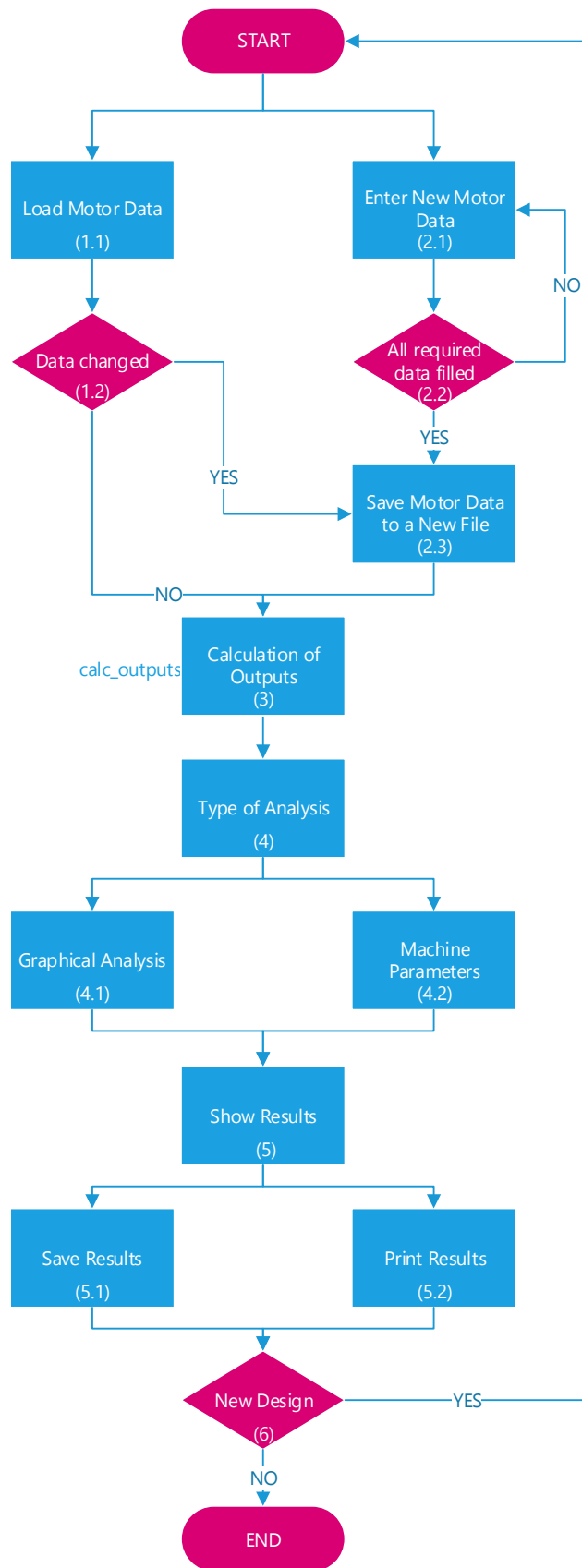


Figure 3.1 : Main Flow Chart of the Software

- *Box 1.1*

In Box 1.1, user chooses to load a previously analyzed motor. First, user chooses "Open" from "File" menu and then locates where the analyzed motor file is.

- *Box 1.2*

In Box 1.2, program checks whether any changes are made. If one or more parameter have been changed, then user must save this new analysis to a file (Box 2.3). If parameters are kept same, then user can analyze the motor (Box 3).

- *Box 2.1*

In Box 2.1, user chooses to make a new motor analysis. User chooses "New" from "File" menu and an empty form opens. In this form, user have to fill all required information for analysis of the new motor.

- *Box 2.2*

In Box 2.2, program checks whether all required data are filled or not. If all data is filled, then user have to save this new analysis to a file before starting analysis. If there is one or more missing data, program asks user to fill the missing parts.

- *Box 2.3*

In Box 2.3, program ask user to save the analysis and user locates where to save the analysis. Saved analysis can be later as described in Box 1.1.

- *Box 3*

In Box 3, the outputs of the program are calculated. This calculation process is given in the flowchart in Figure 3.2 more detailed. The list of outputs are given in Table 3.2.

- *Box 4*

In Box 4, user chooses what type of analysis are going to be made. This analysis are made with the results of the calculations which is going to be described in "calc_outputs" in Chapter 3.1.

- *Box 4.1*

In Box 4.1, graphical analysis are made. These graphs are torque-speed, output power-speed and current-speed graphs.

- *Box 4.2*

In Box 3.2, calculation of machine parameters are made. These machine parameters are resistance, inductance, volume etc.

- *Box 5*

In Box 4, the results of the analysis are going to be shown.

- *Box 5.1*

In Box 4.1, user can save results. If graphical analysis are made, results can be saved as image file or if machine parameters are calculated results can be saved to a file.

- *Box 5.2*

In Box 4.2, user can print the results by choosing a printer connected to computer or by choosing pdf writer.

- *Box 6*

In Box 5, after the results are shown user can close the program or start a new analysis. If user wants to start a new analysis, program goes to the first step of the flow chart.

3.1 Calculation of Outputs

The calculation of the outputs which is needed in Box 4.1 and 4.2, is described by a general flow chart given in Figure 3.2. The process of this flow chart is named as "calc_outputs". There are sub processes under this calculation of outputs process and these sub processes are going to be described below in details.

- *Box 1*

In Box 1, user enters the inputs to the analysis software and save these inputs to a file before starting analysis or opens a previous valid analysis. These inputs are checked in the software. All the inputs must be entered to the related text boxes, all the inputs must be numeric and all decimal numbers must be written with comma. The program does not save the inputs if the requirements stated above are not satisfied. The list of the inputs are given in Table 3.1. The B-H and core loss curves can be uploaded to the software in taking the inputs step.

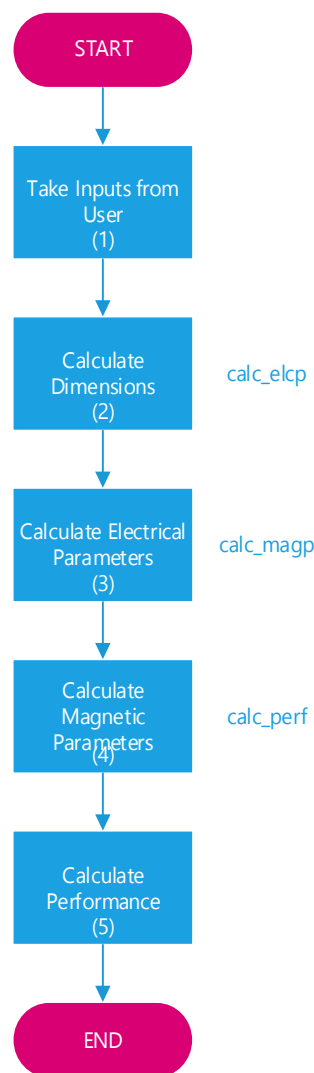


Figure 3.2 : Calculation of the Outputs

Table 3.1: Inputs of the Analysis Program.

| Tab | Name of the Parameter | Symbol | Unit |
|--------|------------------------------|-------------|--------|
| Main | Line Voltage | V_{line} | V |
| | Maximum Current | I_{max} | A |
| | Phase | $phase$ | - |
| | Pole Number | $pole$ | - |
| | Slot Number | N_{slot} | - |
| Stator | Axial Length | L_{sta} | mm |
| | Air Gap Length | g | mm |
| | Back-Core Depth | h_{bc} | mm |
| | Tooth Width | W_{th} | mm |
| | Coil Extension | L_{ext} | mm |
| | Turns per Coil | N_{turn} | - |
| | Coils per Phase | N_{coil} | - |
| | Stacking Factor | k_{stack} | - |
| | Fill Factor | k_{fill} | - |
| Rotor | Magnet Remanent Flux Density | B_r | T |
| | Diameter at Magnet Base | D_{mb} | mm |
| | Magnet Pitch/Pole Pitch | $alfa$ | Radian |
| | Magnet Height | h_{mag} | |
| | Rotor Leakage Factor | p_{rl} | - |
| Slot | Slot Opening Width | w_0 | mm |
| | Width of Bottom Part | w_1 | mm |
| | Width of Top Part | w_2 | mm |
| | Slot Opening Height | h_0 | mm |
| | Height of Bottom Part | h_1 | mm |
| | Height of Mid-Part | h_2 | mm |
| | Height of Top-Part | h_3 | mm |

- *Box 2*

In Box 2, calculation of dimensions are made. This process is named as "calc_dim".

- *Box 3*

In Box 3, calculation of electrical parameters are made. This process is named as "calc_elcp".

- *Box 4*

In Box 4, calculation of magnetic parameters are made. This process is named as "calc_magp".

- *Box 5*

In Box 5, calculation of performance of the motor are made. This process is named as "calc_perf".

3.1.2 Calculation of Dimensions

In this part, some of the machine dimensions are going to be calculated. The flow chart of the calculation process is given in Figure 3.3. First dimensions of stator and rotor laminations are going to be calculated. These dimensions are used in whole analysis process. Then areas of pole, air gap and stator tooth and back-core are going to be calculated. These areas are used in reluctance and flux density calculations. Finally, total mass of stator and rotor lamination is going to be calculated which is needed in core loss calculations.

- *Box 1*

In Box 1, stator inner and outer diameter and rotor diameter at magnet base and at q-axis are going to be calculated.

$$D_{si} = D_{mb} + 2 \times h_{mag} + 2 \times g \quad (3.1)$$

$$D_{so} = D_{si} + 2 \times h_{slot} + 2 \times h_{bc} \quad (3.2)$$

$$D_{ms} = D_{mb} + 2 \times h_{mag} \quad (3.3)$$

$$D_{mq} = D_{mb} + 2 \times h_{mag} - 2 \times 0.001 \quad (3.4)$$

D_{mb} is diameter of magnet base, h_{mag} is magnet height (in the middle of the magnet) and h_{slot} is total height of stator slot which are entered by the user.

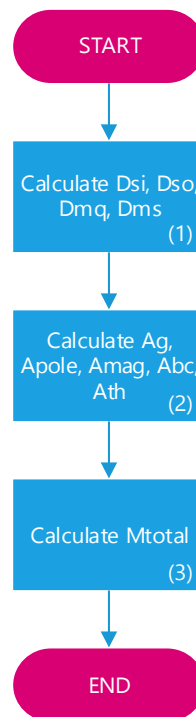


Figure 3.3 : Flow Chart of calc_dim

- *Box 2*

In Box 2, air gap, pole magnet, stator tooth and back core areas are calculated.

- Air gap area is described in section 2.1.1.1 and calculated from Equation 2.2.
- Pole area is explained in section 2.1.4 and Equation 2.21 is used to calculate the pole area.

- Magnet area is mentioned in section 2.1.2.1 and calculation of magnet area is done from Equation 2.10.
- Stator tooth and back-core areas are described in section 2.1.3, and calculated from Equations 2.16-17.
- *Box 3*

In Box 3, total mass of stator and rotor lamination are calculated.

- Mass of stator tooth is explained in section 2.2.4.2 and calculated from Equation 2.64.
- Mass of stator back-core is described in section 2.2.4.2 calculations are done from Equation 2.65.

3.1.2 Calculation of Electrical Parameters

In this section, electrical parameters of the motor is going to be calculated. These electrical parameters are phase resistance and d and q-axis inductances. The flow chart of this calculation process is given in Figure 3.4.

- *Box 1*

In Box 1, C_{pitch} (coil pitch) is calculated as given below.

$$C_{pitch} = \frac{S_{pitch}}{N_{slot}/pole} \quad (3.5)$$

Where S_{pitch} is slot pitch, N_{slot} is number of slots and $pole$ is number of poles which are entered to program by the user.

- *Box 2*

In Box 2, calculation of N_{coil} (number of coils) is given in Equation 3.6.

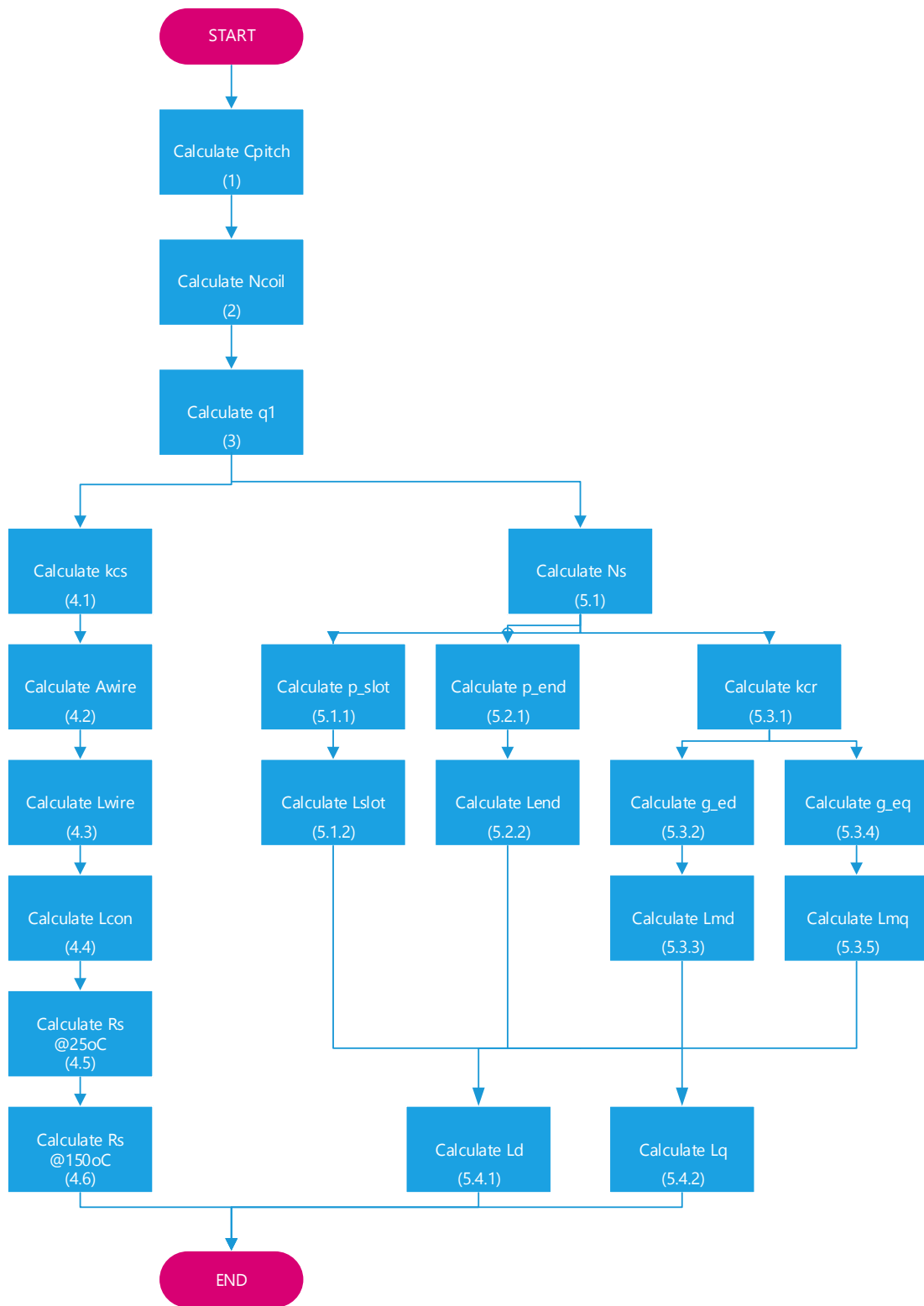


Figure 3.4 : Flow Chart of calc_elcp

$$N_{coil} = \frac{N_{slot}}{phase} \quad (3.6)$$

Where *phase* is number of phases determined by the user.

- *Box 3*

In Box 3, q_1 (slot per phase per pole) is figured out as given Equation 3.7.

$$q_1 = \frac{N_{slot}}{phase \times pole} \quad (3.7)$$

- *Box 4.1*

In Box 4.1, calculation of Carter's coefficient (k_{cs}) for stator is done. This coefficient is described in section 2.1.1.2 and Equation 2.4 is used to find the result. To find the Carter's coefficient; stator input diameter, number of slots, air gap length and slot opening width values are needed.

- *Box 4.2*

In Box 4.2, wire area (A_{wire}) is calculated. This calculation is explained in section 2.2.1.1 and calculated from Equation 2.34. For this calculation; diameter at magnet surface, angle span of the magnet, air gap length and stack length of the motor are used as the inputs.

- *Box 4.3*

In Box 4.3, conductor length in one coil (L_{wire}) is found. Description of this calculation is done in section 2.2.1.2 and the length is calculated from Equation 2.36. To find the conductor length, number of turns per coil, number of slots stack length, external length, slot pitch, stator inner diameter, slot height must be entered correctly.

- *Box 4.4*

In Box 4.4, conductor length for series connection of coils (L_{con}) is found out. This length is mentioned in section 2.2.1.2 and equation 2.37 is used. Calculation of this

length can be done if number of coils per phase, slot pitch, number of slots, stator outer diameter, slot height and external length are known.

- *Box 4.5*

In Box 4.5, phase resistance at room temperature (R_s) is calculated. For this calculation, outputs of the boxes mentioned above are used as inputs. The calculation of phase resistance is described in section 2.2.1 and calculated from Equation 2.32.

- *Box 4.6*

In Box 4.6, phase resistance at nominal conditions (R_{st}) is calculated. This value is used in equivalent circuit instead of the resistance value calculated in Box 4.5, because at steady state working condition conductor heats up. The resistance value is calculated at 150oC which is accepted as nominal temperature of motor. This calculation is described in section 2.2.1 and calculated from Equation 2.33.

- *Box 5.1*

In Box 5.1, effective number of turns (N_s) is calculated as given below

$$N_s = N_{coil} \times N_{turn} \times k_w \quad (3.8)$$

Where N_{coil} is number of coils per phase, N_{turn} is number of turns per coil and k_w is the winding factor.

- *Box 5.1.1*

In Box 5.1.1, slot leakage permeance coefficients (p_{slot}) are calculated. This calculation is described in section 2.2.2.1 and calculated from Equations 2.43-45. To calculate the specific slot permeances, slot dimensions should be entered to the program carefully.

- *Box 5.1.2*

In Box 5.1.2, slot leakage inductance (L_{slot}) is calculated from the coefficients found in Box 5.1.1. This calculation is explained under section 2.2.2.1 and Equation 2.48 is

used to find the result. For the calculation of slot leakage, effective number of turns, number of slots, stack length, coil pitch and specific slot leakage permeances are needed.

- *Box 5.2.1*

In Box 5.2.1, calculation of end winding leakage permeance (p_{end}) coefficient is done. This permeance is calculated as described in section 2.2.2.2 and from the Equation 2.51. Number of slots, phase number, pole number and end winding dimensions are needed to be known to calculate the permeance.

- *Box 5.2.2*

In Box 5.2.2, end winding leakage inductance (L_{end}) is calculated from the coefficient found in Box 5.2.1. Description of this calculation is done in section 2.2.2.2 and calculation is done from Equation 2.52. To find the end winding inductance, effective number of turns and slot per pole per phase values are calculated first. Then these values are used with end winding leakage permeance and end winding dimensions for calculating the inductance.

- *Box 5.3.1*

In Box 5.3.1, rotor's Carter Coefficient (k_{cr}) is found. This coefficient calculation is similar with the one calculated for stator, how the coefficient is found is explained in section 2.2.2.3 and equation 2.55 is used. Inputs of this equation are width of magnet, number of poles, diameter of magnet base, diameter of q-axis of rotor and diameter of magnet surface.

- *Box 5.3.2*

In Box 5.3.2, equivalent d-axis air gap length (g_{ed}) is calculated. Explanation of this calculation is done in section 2.2.2.3 and result is found from Equation 2.54. Air gap length, stator Carter's coefficient, magnet height and magnet permeability is used as the inputs of the Equation 2.54.

- *Box 5.3.3*

In Box 5.3.3, d-axis magnetizing inductance (L_{md}) is found. This inductance is calculated from the d-axis equivalent air gap length which is found in Box 5.3.3. Calculation of the inductance is explained in section 2.2.2.3 and Equation 2.57 is derived to find the result. Pole area, d-axis equivalent air gap length and effective number of turns are used in this box which are previously calculated.

- *Box 5.3.4*

In Box 5.3.4, calculation of equivalent q-axis air gap length (g_{eq}) is done with Equation 2.56. This calculation is described in section 2.2.2.3. Stator inner diameter, diameter of rotor in q-axis and Carter's coefficients (both for stator and rotor) are needed to find the length.

- *Box 5.3.5*

In Box 5.3.5, q-axis magnetizing inductance (L_{mq}) is calculated. This inductance is calculated from the d-axis equivalent air gap length which is found in Box 5.3.4. Description of this calculation is done in section 2.2.2.3 and Equation 2.58 is used to find the results. Inputs of this equation is same with Box 5.3.3 except for d-axis equivalent air gap length, instead of this, q-axis equivalent air gap length is used.

- *Box 5.4.1*

In Box 5.4.1, total d-axis inductance (L_d) is calculated from the sum of the inductances found in Boxes 5.1.2, 5.2.2 and 5.3.3. This calculation is explained in section 2.2.2 with Equation 2.38.

- *Box 5.4.2*

In Box 5.4.2, total q-axis inductance (L_q) is found from the sum of the inductances found in Boxes 5.1.2, 5.2.2 and 5.3.5. Description of this calculation is done in section 2.2.2 by using the Equation 2.39.

3.1.3 Calculation of Magnetic Parameters

In this section, magnetic parameters are going to be calculated such as reluctances and flux densities. This calculations process is described with the help of a flow chart given in Figure 3.5.

- *Box 1.1*

In Box 1.1, calculation of magnet internal leakage reluctance (R_{m0}) is done which is described in section 2.1.2 .The Equation 2.7 is derived to find the result of which inputs are magnet width, stack length, space air permeability, and magnet relative permeability and magnet heights of different regions.

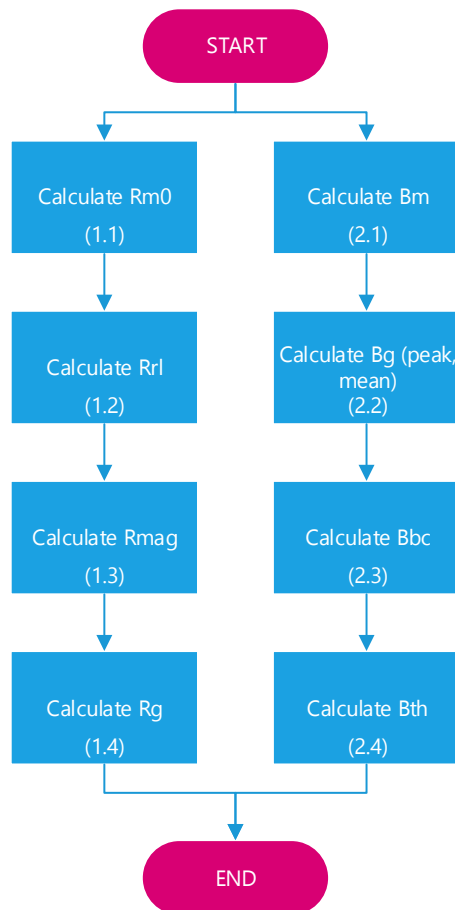


Figure 3.5 : Flow Chart of calc_magp

- *Box 1.2*

In Box 1.2, rotor leakage reluctance (R_{rl}) is calculated. The description of this calculation is done in section 2.1.2 and Equation 2.8 is used for calculation. This reluctance is assumed to be couple of times of magnet internal reluctance. User is defining the coefficient between rotor leakage reluctance and magnet internal leakage reluctance.

- *Box 1.3*

In Box 1.3, total magnet leakage reluctance (R_{mag}) is found. This calculation is explained in section 2.1.2 and calculated from Equation 2.9. For finding the overall magnet reluctance, magnet internal leakage reluctance (Box 1.1) and rotor leakage reluctance (Box 1.2) have to be calculated.

- *Box 1.4*

In Box 1.4, calculation of air gap reluctance (R_g) is done with the Equation 2.1. This calculation is described in 2.1.1. First air gap area and equivalent air gap length is calculated to find the air gap reluctance.

- *Box 2.1*

In Box 2.1, magnet operating flux density (B_m) is found. Explanation of this calculation is done in section 2.1.4. For calculation, Equation 2.25 is used with the inputs: air gap reluctance, rotor leakage reluctance and magnet reluctance.

- *Box 2.2*

In Box 2.2, air gap flux density (B_g), mean air gap flux density ($\overline{B_g}$) and peak flux density ($\widehat{B_g}$) are calculated as described in section 2.1.4 and results are found from Equations 2.19, 2.22 and 2.23. In the calculation of air gap flux density, magnet area, air gap area, magnet reluctance and air gap reluctance are used as inputs. For mean air gap flux density, the ratio of air gap area to pole are needed and for peak air gap flux density magnet height, air gap length and magnet permeability are required for calculation.

- *Box 2.3*

In Box 2.3, stator back-core flux density (B_{bc}) is found as the result of Equation 2.29. This calculation is described in section 2.1.4. To calculate the back-core flux density air gap area, back core area and air gap flux density is needed.

- *Box 2.4*

In Box 2.4, stator tooth flux density (B_{th}) is calculated. This calculation is described in section 2.1.4 and calculated from Equation 2.26. Stator inner diameter, number of slots and tooth width vales has to be entered correctly to find the tooth flux density.

3.1.4 Calculation of Performance

This section is the most important part of the program after calculating the parameters. All the performance analysis are done under this section which is the first thing that a designer is looking for. A program without showing the performance results has nothing special than a calculator. After the calculations are finished, the graphics can be seen on the display of the program and user can read the values of the point by clicking on the graph. The specialties of the analysis program are explained in detail below.

- *Box 1*

In Box 1, the speed matrix is defined. The maximum speed is entered by the user. As described in Chapter 2.3, calculations are needed to be solved for every speed. To shorten the analysis time, calculations are done for every 100th rpm. So number of equations to be solved increased from $w_{max} \times I_{max} \times 20$ to $w_{max} \times I_{max}/5$.

- *Box 2*

In Box 2, electrical frequency, f_e which corresponds to that relevant rotor speed is calculated in Equation 2.70. Since speed is defined as matrix, f_e is a matrix which has same column number with speed matrix.

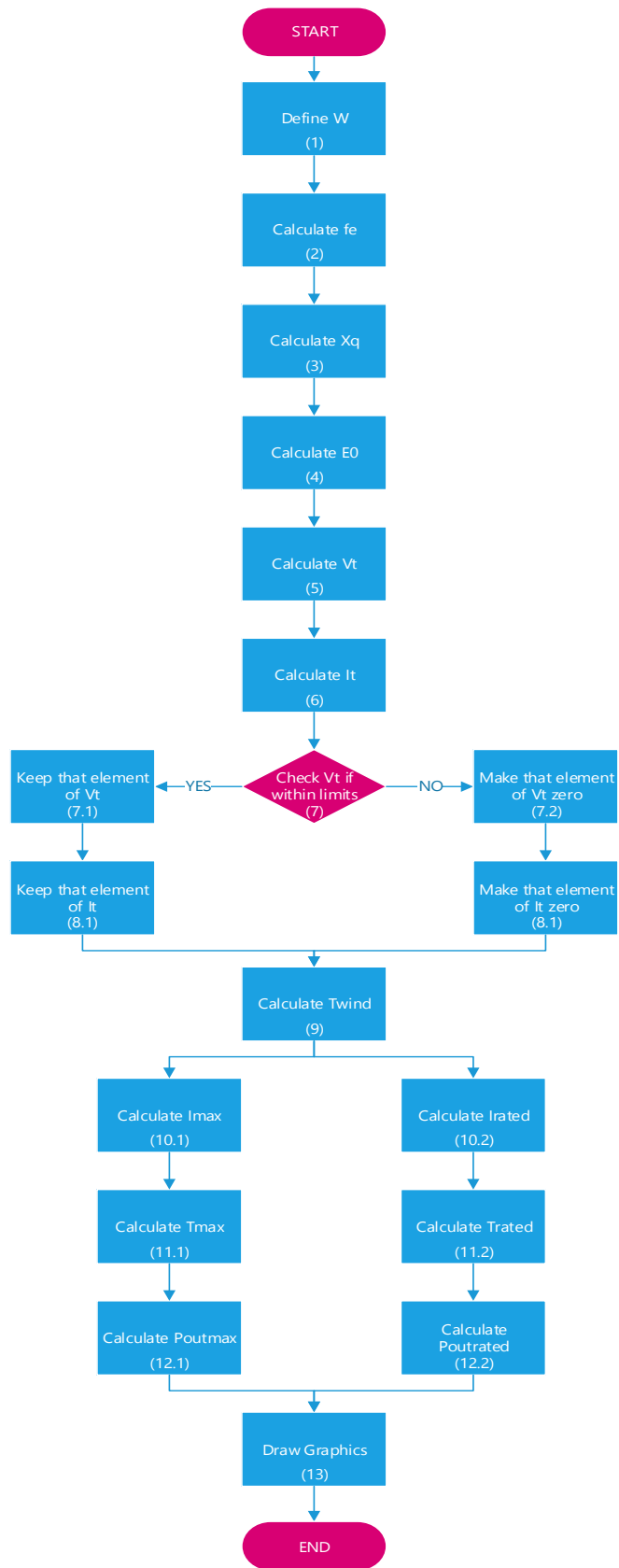


Figure 3.6 : Flow Chart of Performance Calculations

- *Box 3*

In Box 3, q-axis reactance X_q is calculated from Equation 2.71 which is multiplication of q-axis inductance L_q which is calculated in Equation 2.39 and electrical frequency f_e calculated above. Like speed and electrical frequency, q-axis reactance is a matrix with same dimensions.

- *Box 4*

In Box 4, induced emf E_0 for every speed needs to be calculated to find the terminal voltage V_t . As can be seen from Equation 2.72, induced emf is found via emf constant k_{emf} . Since this is a multiplication of a matrix and a constant, emf matrix has same dimensions with speed matrix.

- *Box 5*

In Box 5, terminal voltage V_t is calculated for the given speed range (0 to maximum) and for the current range (0 to maximum). As mentioned before, for this calculation matrix operations are used. Terminal voltage matrix has $(I_{max} \times 20) \times (w_{max}/100)$ dimensions which is shown in Equation 2.73. This matrix is going to be eliminated in Box 7.

- *Box 6*

In Box 6, current matrix I_t is defined such that current will be constant for every speed in each row and in each row current is increased 0.05 A to find out the maximum and rated current more precisely as given in Equation 2.74.

- *Box 7*

In Box 7, calculated terminal voltage matrix V_t in Box 5 is filtered whether if the elements are positive and less than the line voltage. For example if line voltage is 21V, the matrix elements must be less or equal to 8.57V.

- *Box 7.1*

In Box 7.1, if the controlled voltage matrix element is within limits then it is kept without any change.

- *Box 7.2*

In Box 7.2, if the controlled voltage matrix element is not within limits then the value of the element is changed to zero.

- *Box 8.1*

In Box 8.1, if the controlled voltage matrix element is within limits then relevant current matrix element is kept without any change too.

- *Box 8.2*

In Box 8.2, if the controlled voltage matrix element is not within limits then relevant current matrix element's value is changed to zero as made in Box 7.2.

- *Box 9*

In Box 9, friction and windage torque T_{wind} is calculated. This torque is very small and can be omitted for the cases where loss constants are not known. This matrix has $1 \times (w_{max}/100)$ dimensions.

- *Box10.1*

In Box 10.1, the maximum element of each column of I_t is assigned to a new matrix I_{max} . Here it should be noted that I_t matrix has $(I_{max} \times 20) \times (w_{max}/100)$ elements while I_{max} has $1 \times (w_{max}/100)$ elements as shown in Equation 2.75.

- *Box 10.2*

In Box 10.2, input current matrix I_t elements are checked and the elements greater than the current value at reference speed are made zero. After this elimination maximum of each column are assigned to a new matrix I_{rated} like the process done in Box 10.1. I_{rated} has same dimensions with I_{max} .

- *Box 11.1*

In Box 11.1, maximum developed torque T_{max} is calculated from Equation 2.76. Torque constant k_{torque} is known and maximum input current is multiplied by this constant and friction and windage torque is subtracted since it is on opposite direction.

- *Box 11.2*

In Box 11.2, rated torque T_{rated} , is calculated from rated current I_{rated} . Same equation in Box 11.1 is used for this calculation.

- *Box 12.1*

In Box 12.1, maximum output power $P_{out_{max}}$ is easily calculated from Equation 2.78.

- *Box 12.2*

In Box 12.1, rated output power $P_{out_{rated}}$ is found similarly to maximum output power.

- *Box 13*

In Box 13, torque, input current and output power versus speed graphics are drawn. The parameters required to draw these graphs are calculated above. Every i^{th} parameter of the torque, current and power matrices corresponds to the i^{th} parameter of the speed matrix. So for all elements of speed matrix there is an element in relevant matrix and graphics are drawn according to these points. The procedure that is followed to draw graphs are explained in detailed in Chapter 4.

3.2 Showing Outputs

Outputs are shown in the final tab of the program named “Outputs”. Outputs are classified into three groups: which are

- Dimensions
- Electrical parameters
- Magnetic parameters.

Details of these classes are given in Table 3.2. These outputs can be saved to an html file with inputs and also these analysis outputs can be printed out. Sample analysis outputs report is given in Appendix B and C.

Table 3.2: Outputs of the Analysis Program

| Output Tab | Description | Symbol | Unit |
|-------------------------------|------------------------------------|-----------------|-----------------|
| Dimensions | Stator inner diameter | D_{si} | mm |
| | Stator outer diameter | D_{so} | mm |
| | Magnet surface diameter | D_{ms} | mm |
| | Magnet base diameter | D_{mb} | mm |
| | Rotor q-axis diameter | D_{mq} | mm |
| | Air gap length | g | mm |
| | Magnet width | W_{mag} | mm |
| | Magnet height | h_{mag} | mm |
| | Magnet area | A_{mag} | mm ² |
| | Pole area | A_{pole} | mm ² |
| | Air gap area | A_{gap} | mm ² |
| | Stator back-core area | A_{bc} | mm ² |
| Stator tooth area | A_{th} | mm ² | |
| Electrical Parameters | Wire diameter | D_{wire} | mm |
| | Phase resistance | R_s | Ω |
| | d-axis inductance | L_d | mH |
| | q-axis inductance | L_q | mH |
| | Torque constant | k_{torq} | Nm/Arms |
| | EMF constant | k_{emf} | Vpk/rad/s |
| Magnetic Parameters | Magnet internal leakage reluctance | R_{m0} | AT/Wb |
| | Rotor leakage reluctance | R_{rl} | AT/Wb |
| | Magnet reluctance | R_m | AT/Wb |
| | Air gap reluctance | R_g | AT/Wb |
| | Magnet operating flux density | B_m | T |
| | Air gap flux density | B_g | T |
| | Stator tooth flux density | B_{th} | T |
| Stator back-core flux density | B_{bc} | T | |

Moreover, user is able to see the lamination of the analyzed motor with a scale for both quarter lamination and full lamination drawings. User can access this new form page from “Lamination” in Menu Bar. Lamination drawing can be send to a CAD program, can be saved as an image file or can be printed out. Sample lamination drawings are given in Appendix B and C.

User, also have the chance to see the graphical performance analysis results. There are two ways to do graphical analysis. First way is to enter all the required data in the main program and after calculating outputs, user chooses “Analysis from Dimensions” from “Analysis” in Menu Bar. Second way is to enter the required machine parameters like inductance, resistance, voltage and current values and run the analysis. “Analysis from Machine Parameters” is chosen from “Analysis” in Menu Bar.

After the analysis are done, user can see the torque, input current and output power characteristics of the analyzed motor and also user can save and print these graphics. User can also read values from graphics by clicking on the graph, these part is explained in detail in Section 4.5.

3.3 Conclusion

In this chapter, main body diagram of the analysis program is given with a flow chart at first. Then each step is described more detailed with the help of new flow charts. Every box used in the flow charts are described and how the calculations are carried out in the program are referred to Chapter 2. The inputs and outputs of the analysis program are given in tables with the symbols used in the equations followed in the analysis program. Each step is explained with the help of the equations given in Chapter 2. Also these flow charts are used in the implementation of the analysis program which are discussed in detail in Chapter 4.

CHAPTER 4

IMPLEMENTATION OF THE PMAC ANALYSIS SOFTWARE

4.1 Introduction

In previous chapters, basic calculations required to analyze a PMAC motor and the flow charts explaining the sequence of these calculations are described. An interface is required for getting the inputs from the user and making these calculations in a software. This software is developed in Microsoft Visual Studio with the programming language C#.

In this chapter, how the software is implemented is explained. Details of how the interface is created, types of toolboxes used, how calculations are done and how graphs and laminations are drawn are declared.

General concept of the developed program is to input the main information like line voltage, maximum current and number of poles and basic dimensions like diameter of rotor from the user and give outputs like machine parameters (phase resistance, inductance), graphical performance (torque-speed characteristic) and scaled lamination. Also software gives user the chance to save or print the outputs and open a previous analysis.

In the following sections, the developed software will be explained in detail with the help of the flowcharts described in previous chapter, the features of the interface will be explained for every tab in the software.

4.2 Technical Features

PMAC Motor Analysis Software is a windows application software developed for analyzing surface-mount permanent magnet AC motors. Features of the software are listed below.

- Performance analysis of permanent magnet AC motor according to user defined motor such as geometry and materials used data
 - Torque versus Speed
 - Current versus Speed
 - Output power versus Speed
- Machine parameters calculation from geometry
- Detailed analysis information such as flux density and reluctance values in various sections of the magnetic circuit
- Drawing lamination of the motor
- Analyzing the performance of the motor from parameters
- Print option for the calculation results and lamination

PMAC Analysis Software has a user friendly user interface besides satisfying these features. This interface is created with object oriented programming language called C#, with Microsoft Visual Studio (v2012) program. With the help of this program, required windows forms, text boxes, labels, buttons, tab pages and etc. are used to create the interface. C# is preferred because it is intended to be a simple, modern, general-purpose, object-oriented programming language.

The program has a setup file which installs the software with the required folders and examples. While the software is being installed, the setup file creates a shortcut at desktop, a folder in C:\Program Files named PMCAD with sample input file to run the analysis from machine dimensions, motor parameters file to run the analysis from machine parameters, BH Data folder with sample B-H curve data, Core Loss folder with sample core loss curve data and also creates a Results folder in PMCAD folder to save the analysis reports. It should be noted that to run the software, Microsoft .NET Framework (version 3.5 or higher) should be installed on the computer.

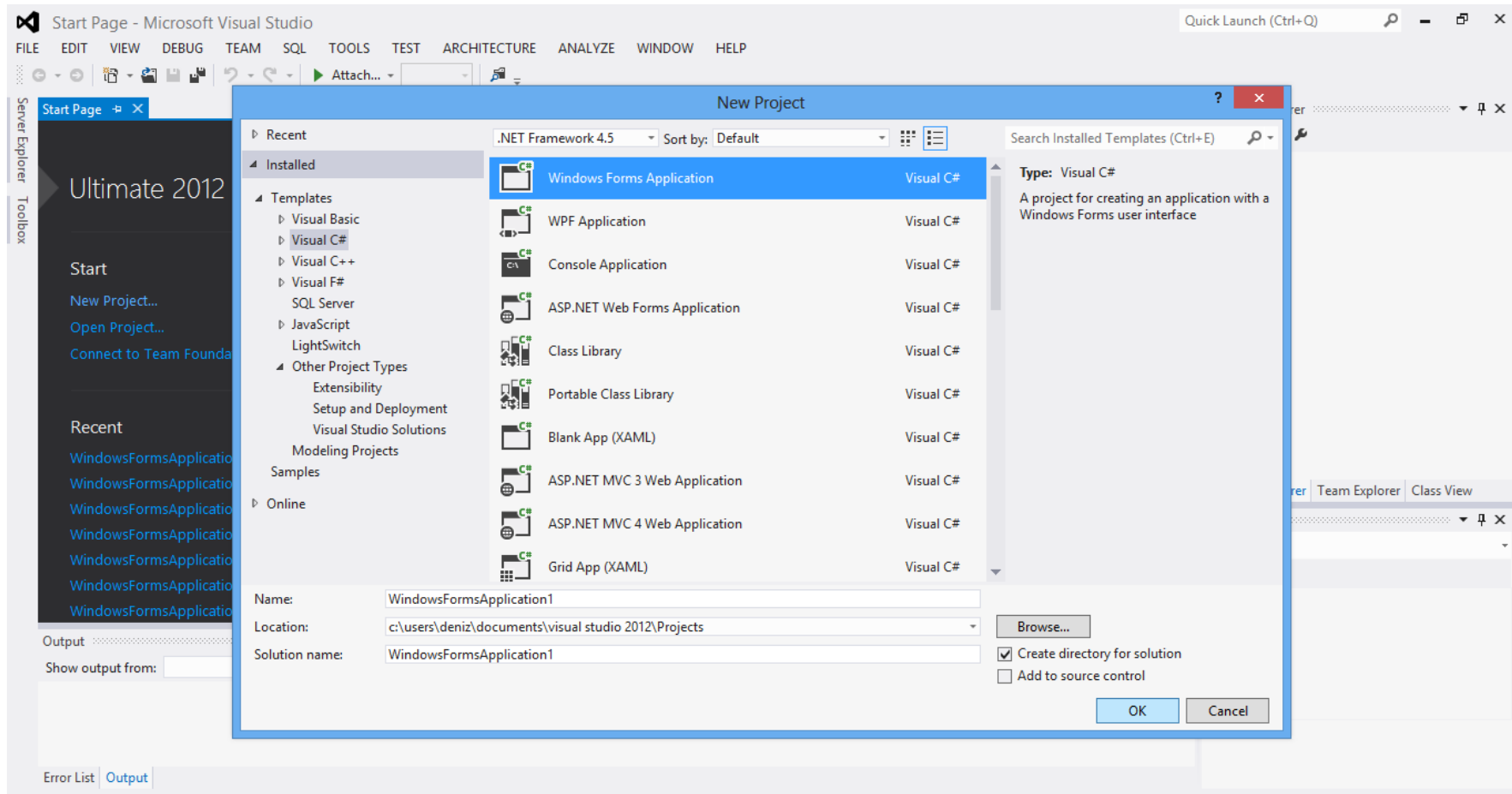


Figure 4.1 : The Screen Shot of Microsoft Visual Studio

4.3 Creating a Form in Visual Studio

Once the program is opened, New is selected from File menu and Project is selected from New menu. Visual C# is selected under Templates seen on the left hand side of the window which is given in Figure 4.1. Then Windows Form Application is selected. Program automatically creates the WindowsFormApplication1 project and Form1 windows form.

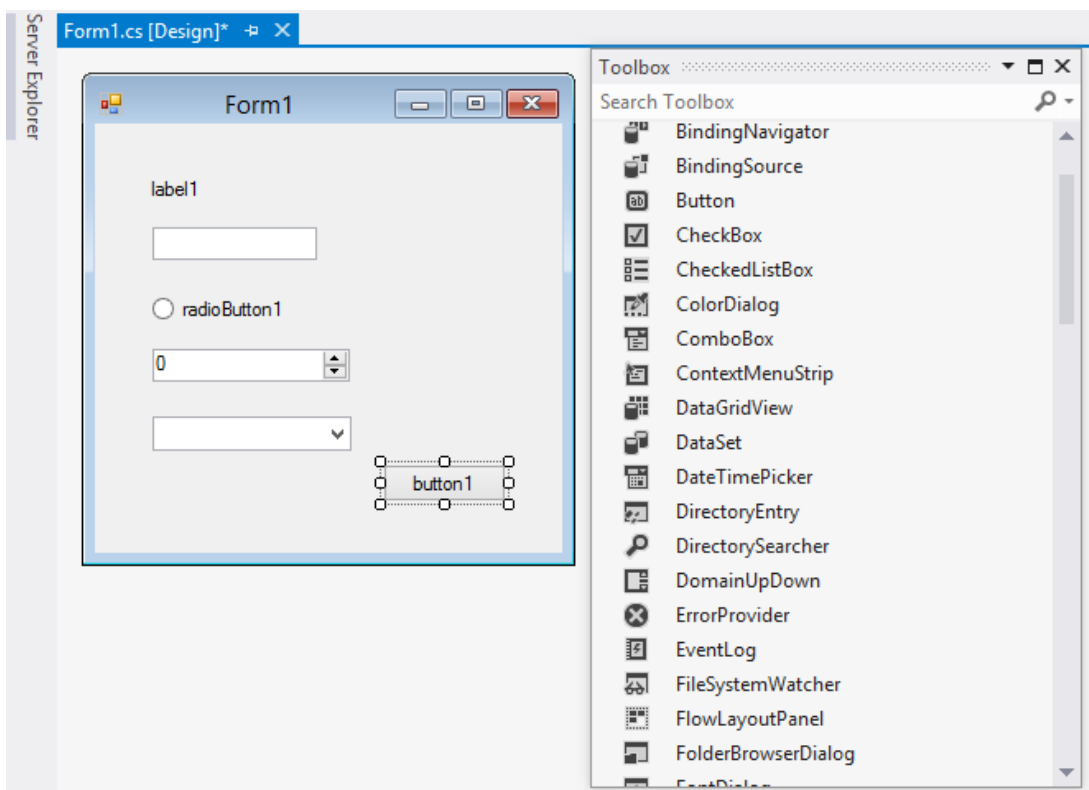


Figure 4.2 : Sample Form and Toolbox Window

In Figure 4.2, a sample form is given and toolboxes are placed with drag and drop method. The toolboxes in the Form1 from top to bottom are Label, TextBox, RadioButon, NumericUpDown, ComboBox and Button. These are the most commonly used toolboxes in the software. In addition to them TabControl, Panel and PictureBox toolboxes are used. For menu structure, OpenFileDialog,

SaveFileDialog, and PrintDialog toolboxes are used and the menu is created by MenuStrip. The used toolboxes are given in Table 4.1.

Table 4. 1: List of the Toolboxes Used in the Software

| Toolbox | Description |
|----------------|--|
| Panel | Panels are placed in forms, Their visibility can be changed by codes and toolboxes can be placed in panels. |
| TabControl | Tab control is used to classify inputs and outputs. By using tabs, interface becomes easier to use. |
| PictureBox | Image files are placed and graphics are drawn in picture boxes. |
| Label | Labels are used for giving description and units. |
| RadioButton | Radio buttons are used to make selections like slot type and magnet type. |
| ComboBox | Combo boxes are used where the selection is made from a known collection of inputs. |
| NumericUpDown | Numeric up and down is used for numerical inputs which increase and decrease arbitrarily. |
| TextBox | Text boxes are used to get inputs from the user. |
| Button | Buttons are used to save the inputs in the text boxes to the memory. |
| Timer | Timer function is used in the drawing function. |
| OpenFileDialog | Open file dialogs opens the standard file open interface used in every program. The folders that where the file is going to be opened is selected. |
| SaveFileDialog | Save file dialogs opens the standard save open interface. The folder where the file is going to be saved is selected and file name is entered. |
| PrintDialog | Print dialogs opens the standard print file interface where user can access printing options. |
| MenuStrip | Menu strip is used to create the menu bar. |

In the software there are buttons in each tab. When user clicks on the button, all the textboxes, combo boxes, radio buttons, numeric up and downs are checked whether the inputs are entered and if all of them entered, the inputs are checked whether they are in correct format or not. The correct format for an input should consist of only numeric values, if a floating number is needed to be entered comma must be used between numbers. The program warns the user with a message box to enter all the required data and enter the values in the correct format. All textboxes input must be numeric and floating numbers must be entered with comma so that the program accepts it correct. User can pass to the next tab if all the inputs are correct. This procedure is repeated for every tab that user enters the inputs.

After all the required inputs are entered and saved each input to a parameter with the same symbol used in the equations, the program runs the calculation process with the help of the flowcharts described in Chapter 3.

When the calculation process is over, the results are written to the labels in outputs tab, so that the user cannot change the value of the result by clicking on it like being able to do in inputs. The outputs are classified into three tabs; dimensions, electrical parameters and magnetic parameters. At the end of the outputs tab, there is a button named save results which saves the outputs and inputs to a table in a html file and when this html file automatically opens just after the save process. User can click on the print button in the opened html page. This report automatically saved into Results folder with file DesignReport-day.month.year-hour.minute.html

After the calculation of outputs, user can see the graphical performance analysis and lamination drawing which are described in detail in the following section.

4.4 Analysis Menu

Analysis is the most important part of the program. In this menu, user can see the performance characteristics of the motor which is analyzed by the data that user entered. The list of inputs is given in Table 3.1. Each input is kept in the memory of each form of the program with the same symbols used in the equations. The main

program form page is different than the form page of Analysis. At the beginning of the analysis form, the inputs are taken from main form and loaded to the new form which is created for graphical analysis. In the analysis form, picture boxes are used to draw graphics, labels are used for x and y axis labels and detailed slot and magnet dimensions, buttons are used to save graphics.

These characteristics are shown graphically on a new form. User is able to see torque versus speed, input current versus speed and output power versus speed characteristics on different graphs in this form. Also user can print these graphics or save to an image file. The calculation of performance outputs is described in previous chapters. How the graphs are drawn is explained in the following section in detail.

Graphical analysis can be done in two different ways. First one is to do analysis from geometrical dimensions entered by the user. By these dimensions, machine parameters required to run the analysis are found and performance calculations are done. The analysis from geometry window is shown in Figure 4.3. To run analysis from geometry, user have to fill all the required data into the main form and calculate the outputs. After this step required parameters are transferred to new form which does the calculations of terminal voltage, input current, torque and output power and draws the graphs for rated and maximum operation conditions.

The algorithm followed to draw the graphics is shown in Figure 3.6. In analysis program, there are three graphics which are drawn on different picture boxes. Picture boxes are added to the form from toolboxes menu and dimensions can be adjusted as desired. When one of the graphs is chosen by clicking one of the buttons placed on the top of the form, corresponding picture box made visible and other two picture boxes made invisible. User also can read the values from graph by clicking on the graph in if-else loops.

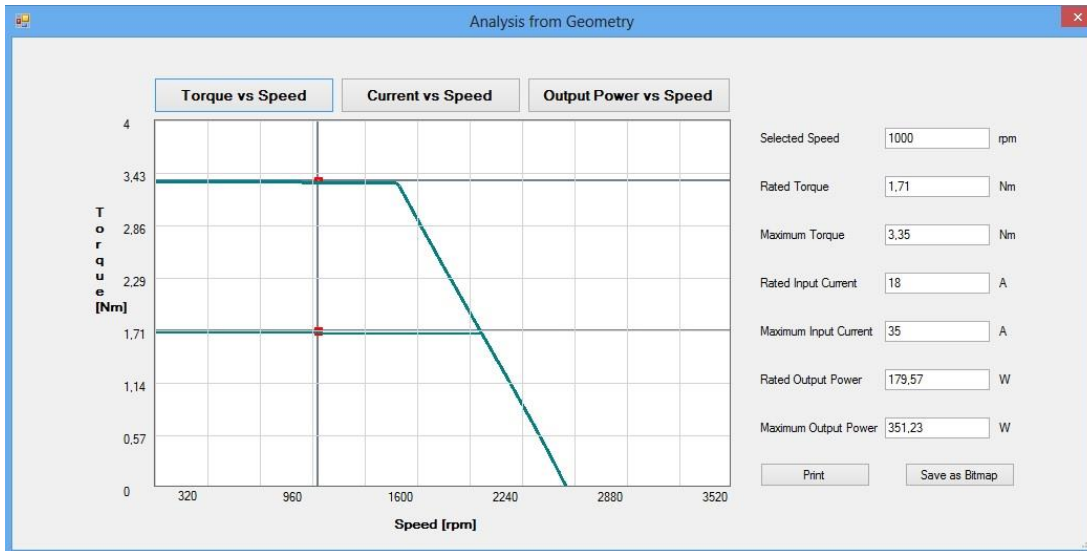


Figure 4.3 : Torque vs Speed Graph

The second way is getting required parameters from the user directly and doing the graphical analysis. These required machine parameters are phase resistance, d and q axis inductances, torque and emf constants, line voltage and maximum input current which is limited due to inverter ratings. The analysis from machine parameters window is given in Figure 4.4. The parameters entered in text boxes are saved to memory with the names used in the torque calculation when “Analyze” button is clicked. Then torque calculation function is called and the graphs are drawn according to the outputs of this function which is described in detail in the following section.

4.4.1 Torque-Speed Graph

As mentioned above, three graphical analysis are done in the analysis program for both analysis from geometry and analysis from machine parameters.

To draw the torque versus speed graph, first maximum torque is calculated for every element of speed matrix. Speed matrix are created such that the values are starting from 0 and increasing 100 rpm in every step until maximum speed like given in Equation 2.70, so the calculation time is decreased in the drawing process.

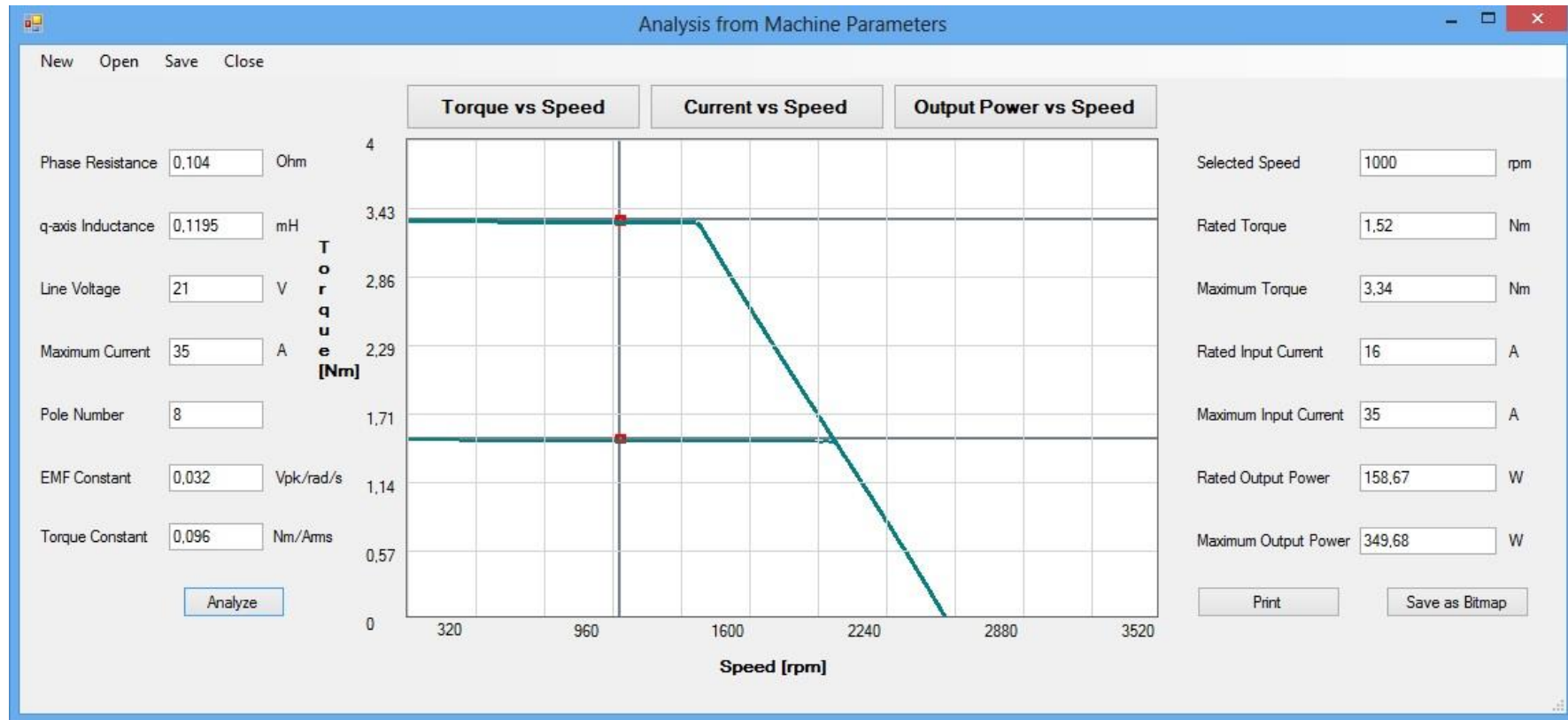


Figure 4.4 : Torque-Speed Graph from Machine Parameters

Every calculation results is saved to the elements of maximum torque matrix. Then while drawing graphics these matrix elements turns into coordinates of operation points such that x-coordinate of point i comes from the i^{th} element of speed matrix and y-coordinate of point i comes from the i^{th} element of maximum torque matrix

The elements of torque matrix is in Nm and speed matrix in rpm. These values are multiplied by conversion constants to obtain values in pixels. Then coordinates of every point is known in terms of pixels on the picture box on which graph is drawn. Lines are drawn between points i and $i+1$, where i starts from the first element of speed matrix and ends at the last element of speed matrix by using DrawLine functions in Graphics library. So the complete maximum torque versus speed graph is drawn on the corresponding picture box which has dimensions 350x550 pixels. To draw the rated torque versus speed graph same method is used and rated torque versus speed graph is drawn on the same picture box with maximum torque versus graph. To show the difference maximum torque line is drawn with a pen with 3 pixel width and rated line is drawn with a pen with 2 pixel width.

Labels of x and y axis are calculated from the maximum values of each graph value. For example, in torque versus speed curve, maximum torque value is used for x axis labeling. Assume a maximum torque value 3.4Nm. First the value is rounded such that there will be one significant digit; for 3.4Nm rounded value is 3. Secondly, this rounded value is compared with the original value. If the rounded value is bigger than the real value then the maximum value in x-axis will be the rounded value. But if the rounded value is smaller than the real value then the maximum value in x-axis becomes rounded value +1 which is 4 in this example. Then the graphs are scaled such that the maximum value of y-label is going to be equal to the height of the picture box which is 350 pixel and maximum of x-label is going to be equal to the width of picture box which is 550 pixel.

User can read the values on the graph by clicking on the graph so on picture box. For this purpose, MouseClick event of picture box is used which returns X and Y as the coordinates. The main parameter for this process is x-coordinate of mouse in pixels on the picture box which gives the speed value with the help of the conversion constant mentioned above. Then the y-coordinate value is calculated for that speed.

The calculated values are printed to the textboxes in the right hand side of the program. Also cursor lines are drawn parallel to the x and y axis where the cursor intersects the graph. Two cursor lines are drawn for calculated maximum and rated torque values which are parallel to x-axis and speed cursor line is drawn from the x-coordinate of the mouse which is parallel to the y-axis. These cursor lines are drawn with grey color and 3 pixel width. Also to show the intersections of these cursor lines where the maximum and rated torque are found, a red square is drawn around each intersection point, and each border of the square has 5 pixel length. For each click on the picture box, cursor lines are redrawn for the new speed value and user can read the outputs for this new speed value.

After the graphs are drawn, the calculated maximum and rated torque and speed value which is found from the mouse coordinates are written to the textboxes placed on the right hand side of the form. Also, input current and output power calculated for rated and maximum conditions are calculated and shown to the user in the textboxes.

When user clicks on other buttons, these values are kept in the textboxes for the last clicked speed value. Speed cursor line is redrawn for last speed value and new cursor lines are drawn for current or output power values.

4.4.2 Current-Speed Graph

Current versus speed graph is drawn similar to the torque versus speed graph. Input current values are calculated for each element of speed matrix and kept in the memory as elements of maximum current matrix given in Equation 2.76. Similarly, coordinates of each point in the graph are found from the elements of these matrixes where current values corresponds to y-coordinates and speed values corresponds to x-coordinates. Again lines are drawn between points and complete graph is obtained. Same procedure is followed for rated input current. The maximum and rated input current versus speed graphs are drawn on a different picture box with the same dimensions used in the torque versus speed graph.

Speed label (x-label) does not change for all graphs. Current label values are calculated according to the maximum value of current. For example, for the given

motor maximum current is 35A. These value have two digits and when the logic used in the torque labels is applied to the current label, the maximum value of current label is found as 40A. Then the conversion constant is calculated such as 40A is equal to the height of the picture box which is 350 pixel.

To read the values from graph, same procedure is followed. The cursor lines are drawn and calculated results are shown in the textboxes similarly.

4.4.3 Output Power-Speed Graph

Output power versus speed graph is drawn in the same way with torque graph which is described in detail above. The same procedure is followed to find the conversion constant, read the coordinates of mouse, and draw cursor lines and printing results to the textboxes.

Also last coordinates of last click of mouse is kept in memory for current versus speed and output power versus speed graphs and when user clicks on a different button to see other graphs, speed cursor line redrawn again and other two cursor lines which are parallel to x-axis are drawn for calculations done from the last coordinates.

4.5 Lamination Menu

Lamination menu opens a new form which contains a picture box for lamination drawing, a picture box to see which slot type is chosen and a picture box to see which magnet type is chosen. Also slot and magnet dimensions are shown in labels.

In the following section, the drawing of lamination for one quadrant of radial cross section of motor is described. Full lamination drawing is done similarly to this procedure.

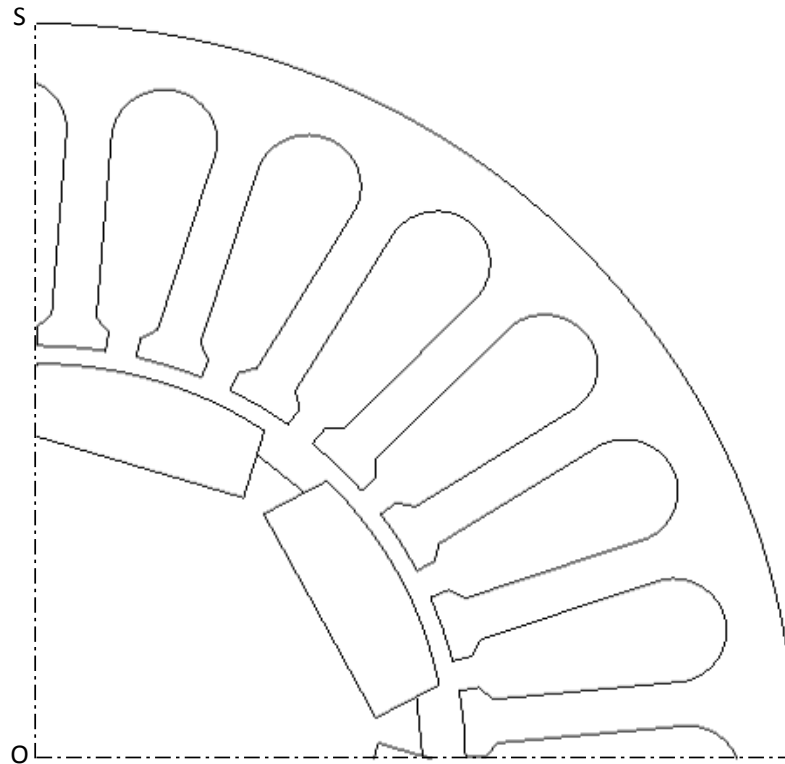


Figure 4.5 : Sample Lamination Drawing

The lamination is plotted with a scale such that height of the picture box in pixels is equal to the half of the stator outer diameter. Only one quadrant on radial is plotted, because the motor is symmetric. Coordinates of stator slots and rotor magnet is calculated according to the base point of motor lamination, but in the program the drawing is plotted according to point O (x-coordinate is 0 pixel and y-coordinate is 0 pixel), which are shown in Figure 4.5.

4.6.1 Creation of Repeating Stator Portion

The program gives user the chance to choose one of the three slots given in Figure 4.6. These slot drawings are repeating itself by stator slot number.

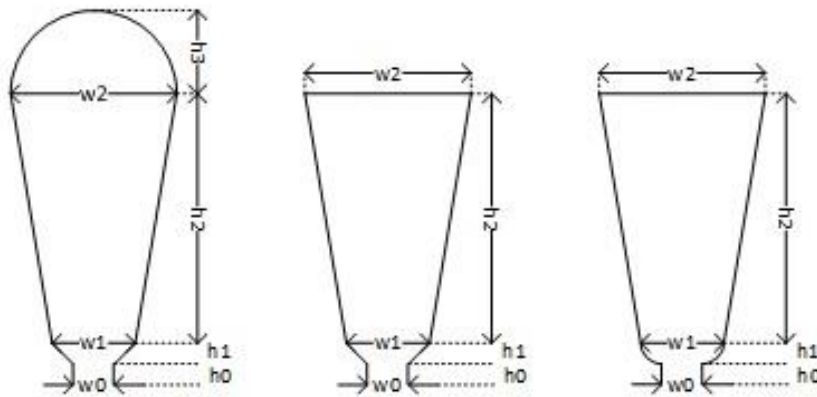


Figure 4.6 : Stator Slot Types

Sample stator slot pitch symmetry element is given in Figure 4.7. The slot dimensions are given in Figure 2.10. The drawing is plotted step by step between named points (A, B, C...) which is given in the sample stator slot drawing. The calculations of coordinates of these points are described below [6].

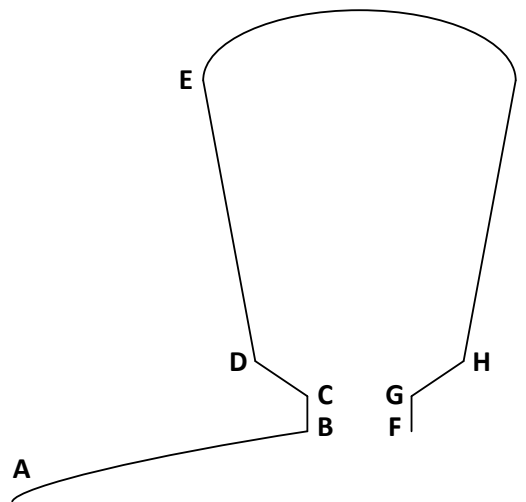


Figure 4.7 : Symmetrical Element of Stator Lamination

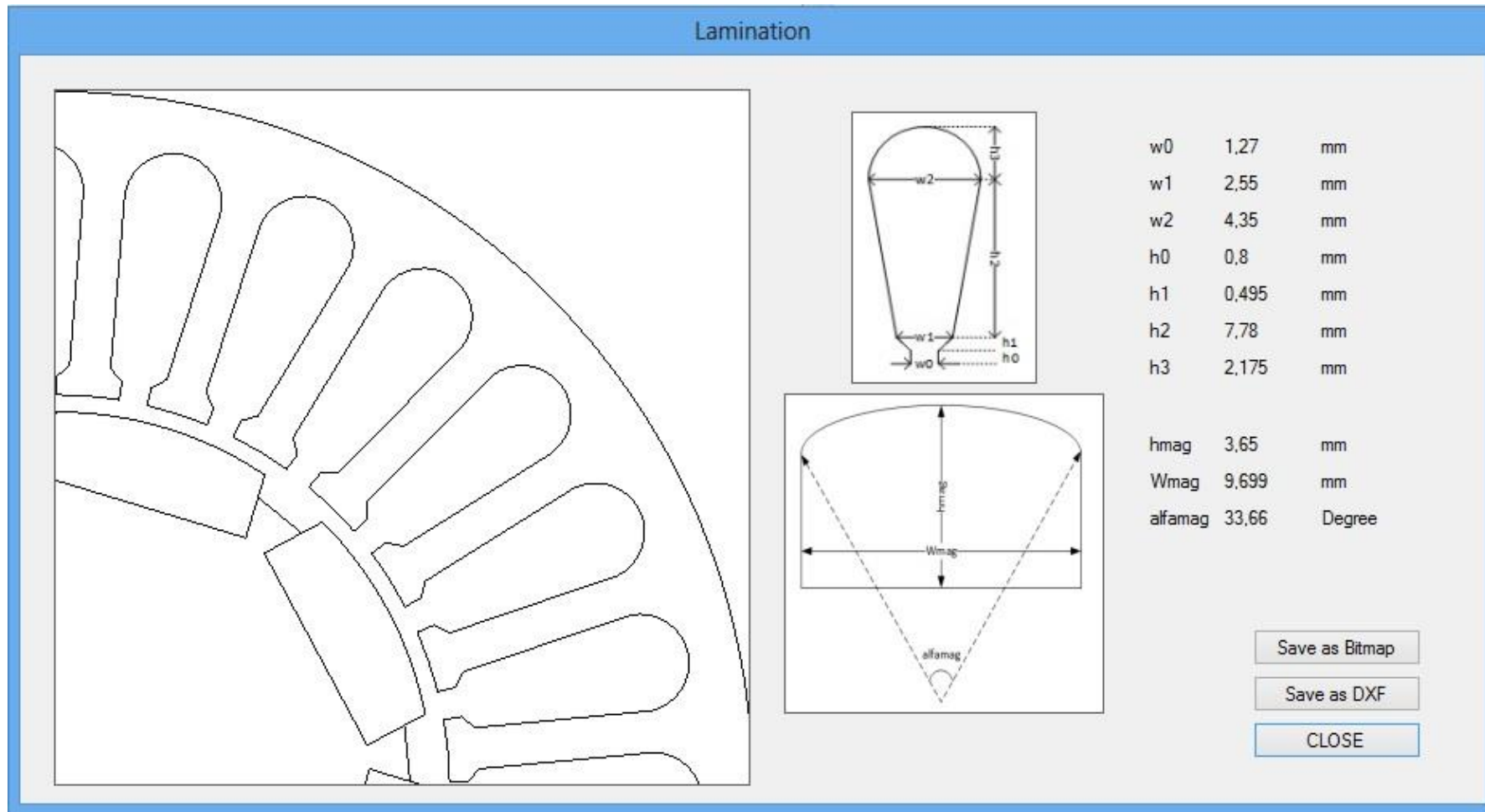


Figure 4.8 : Sample Lamination Drawing Form

First, outer diameter of stator is drawn with Draw Arc function which draws arc in a rectangular region between given angles and then the slots are drawn from the coordinates of the points shown in Figure 4.7. To calculate the coordinates of the points, stator tooth width angle should be calculated which is shown in Figure 4.9. The calculation of stator tooth pitch is given in Equations 4.1 and 4.2, where τ_{st} is stator tooth pitch, D_{si} is stator inner diameter, N_{slot} is number of slots, w_{th} is stator tooth width and w_0 is stator slot opening width.

$$\tau_{st} = \frac{\pi \times D_{si}}{N_{slot}} \quad (4.1)$$

$$w_{th} = \tau_{st} - w_0 \quad (4.2)$$

Stator tooth width angle, $alfa$ is calculated in radians found from Equation 4.3. The trigonometric functions used in the program takes inputs in radians, so all angles calculated in radians.

$$alfa = \frac{w_{th} \times 360^\circ}{\pi \times D_{si}} \quad (4.3)$$

Coordinates of points A and B are on the stator inner diameter. So the coordinates are just found with stator tooth width angle and stator inner diameter as given in Equations 4.4-7 where D_{so} is stator outer diameter. After coordinates of A and B points are calculated, an arc is drawn between these two points.

$$A_x = D_{si} \quad (4.4)$$

$$A_y = D_{so} - D_{si} \quad (4.5)$$

$$B_x = D_{si} \times \sin(alfa) \quad (4.6)$$

$$B_y = D_{so} - D_{si} \times \sin(alfa) \quad (4.7)$$

Since coordinates of point B is found above, it is enough to calculate the coordinates of point C, to draw the line between points B and C with Draw Line comment which draws line between two points of which coordinates are known in terms of pixels. It is known that the distance between points B and C is equal to the slot opening height h_0 , and coordinates of point C is calculated via this distance as given in Equations 4.8 and 4.9.

$$C_x = (D_{si} + h_0) \times \sin(\text{alfa}) \quad (4.8)$$

$$C_y = D_{so} - (D_{si} + h_0) \times \sin(\text{alfa}) \quad (4.9)$$

To draw the line between points C and D, some trigonometric calculations need to be done to find out the angles given in Figure 4.9. alfa is stator tooth width angle which is calculated above. delta1 is stator slot opening angle which is calculated from equation 4.10. In Figure 4.9, $\text{delta1}/2$ is shown.

$$\text{delta1} = \frac{w_0 \times 360^\circ}{\pi \times D_{si}} \quad (4.10)$$

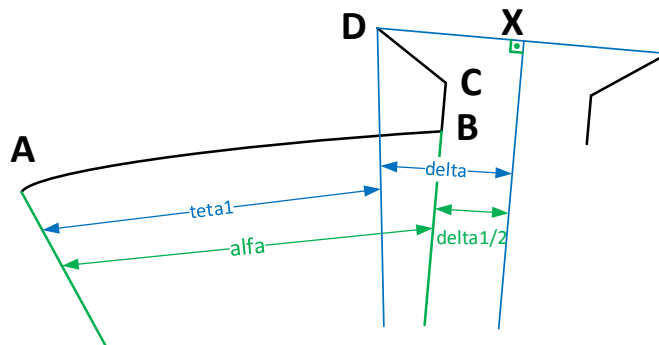


Figure 4.9 : Coordinates of Points C and D

To calculate teta1 , which is required to find the coordinates of point D, delta should be calculated geometrically from Equation 4.11.

$$\delta = \tan^{-1} \left(\frac{\frac{w_1}{2}}{D_{si} + h_0 + h_1} \right) \quad (4.11)$$

As can be seen from Figure 11, sum of α and $\delta/2$ is equal to sum of θ_1 and δ . The angle of the point D θ_1 , is found from this equality as given in Equation 4.12.

$$\theta_1 = \alpha + \delta/2 - \delta \quad (4.12)$$

After calculating θ_1 , coordinates of point D is found from Equations 4.13-14. Then, if slot type is 1 or 2, a line is drawn between points C and D. Otherwise, if slot type is 3 an arc is drawn between these two points with Draw Arc command. The distance between point D and center of motor is calculated as given in Equation 4.13 denoted by D_D .

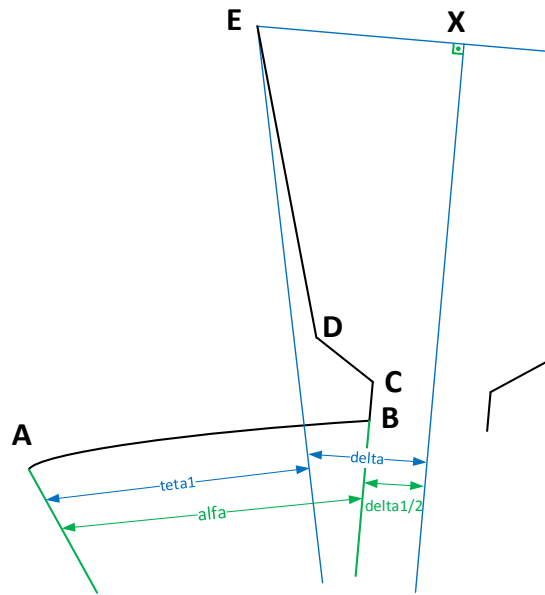


Figure 4.10 : Coordinates of Point E

After calculating θ_1 , coordinates of point D is found from Equations 4.14-15.

Then, if slot type is 1 or 2, a line is drawn between points C and D with Draw Line comment. Otherwise, if slot type is 3 an arc is drawn between these two points with Draw Arc comment. The distance between point D and center of motor is calculated as given in Equation 4.13 denoted by D_D .

$$D_D = \sqrt{\left(\frac{w_1}{2}\right)^2 + (D_{si} + h_0 + h_1)^2} \quad (4.13)$$

$$D_X = D_D \times \sin(teta1) \quad (4.14)$$

$$D_Y = D_{so} - D_D \times \sin(teta1) \quad (4.15)$$

Calculation of coordinates of point E is very similar to calculation of coordinates of point D, except for changes in angles $teta1$ and $delta$. These new angles are illustrated in Figure 4.10. New calculation of $delta$ is given in Equation 4.16.

$$delta = \tan^{-1}\left(\frac{\frac{w_2}{2}}{D_{si} + h_0 + h_1}\right) \quad (4.16)$$

Calculation of $teta1$ was given in Equation 4.12. Also the distance between center of motor and E point D_E is calculated by Equation 4.17. After $teta1$ and D_E are found, coordinates of point E can be calculated as shown in Equation 4.18-19.

$$D_E = \sqrt{\left(\frac{w_2}{2}\right)^2 + (D_{si} + h_0 + h_1)^2} \quad (4.17)$$

$$E_X = D_E \times \sin(teta1) \quad (4.18)$$

$$E_Y = D_{so} - D_E \times \sin(teta1) \quad (4.19)$$

Calculation of coordinates of point F and G are similar to B and C respectively. While angle for point B and C are $alfa$, angle of points F and G are $alfa + delta1$, where $alfa$ is stator tooth width angle and $delta1$ is stator slot opening angle. The coordinates of point F and G are calculated with Equations 4.20-23.

$$F_X = D_{si} \times \sin(alfa + delta1) \quad (4.20)$$

$$F_Y = D_{so} - D_{si} \times \sin(alfa + delta1) \quad (4.21)$$

$$G_X = (D_{si} + h_0) \times \sin(alfa + delta1) \quad (4.22)$$

$$G_Y = D_{so} - (D_{si} + h_0) \times \sin(alfa + delta1) \quad (4.23)$$

As left and right sides of stator slot is symmetric, coordinates of point H is calculated similar to point D. In Figure 4.11, change in the angle $teta1$ can be seen and calculation is represented in Equation 4.24. $delta$ is calculated as given in Equation 4.11.

$$teta1 = alfa + \frac{delta1}{2} + delta \quad (4.24)$$

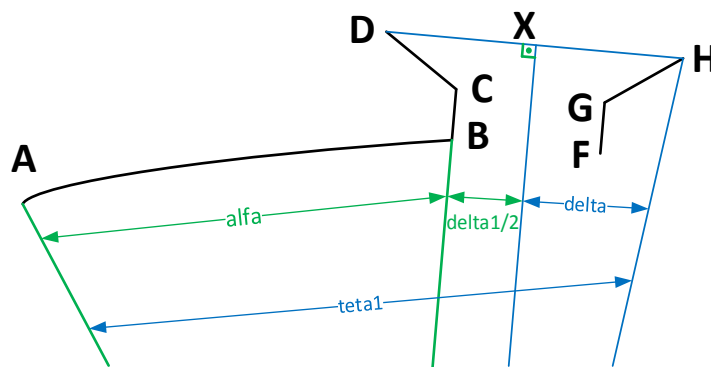


Figure 4.11 : Coordinates of Points G and H

$$I_X = D_I \times \sin(teta1) \quad (4.27)$$

$$I_Y = D_{so} - D_I \times \sin(teta1) \quad (4.28)$$

After the coordinates of point H and I are calculated, a line is drawn between these two points.

If slot type is 1, then an arc is drawn between points E and I of which center is point X. Else, (slot type is 2 or 3) a line is drawn between points E and I. Thus, a stator slot portion drawing is completed. To calculate the next symmetric stator slot portion, $2 \times \pi / N_s$ is added to *alfa* until the angle of the slot reaches $2 \times \pi$. So, stator lamination portion is completed.

4.6.2 Creation of Repeating Rotor Portion

Drawing the rotor portion is very similar to stator portion. As it is done in stator, rotor is divided into symmetric parts of which number is equal to number of poles. One rotor pole portion is given in Figure 4.13.

The angle span of the magnet surface is entered by the user which is assigned to *alfa_{mag}*. First, the arc between points A and B is drawn. The coordinates of points A and B are calculated as given in Equations 4.29-32.

$$A_X = D_{ms} \quad (4.29)$$

$$A_Y = D_{so} - D_{ms} \quad (4.30)$$

$$B_X = D_{ms} \times \sin(alfa_{mag}) \quad (4.31)$$

$$B_Y = D_{so} - D_{ms} \times \sin(alfa_{mag}) \quad (4.32)$$

$$\delta = \alpha_{mag} + \frac{\omega + \alpha_{mag}}{2} \quad (4.35)$$

After calculating required parameters, coordinates of point C can be found by using Equations 4.36-37. Then, a line is drawn between points B and C.

$$C_x = D_C \times \sin(\delta) \quad (4.36)$$

$$C_y = D_{so} - D_C \times \sin(\delta) \quad (4.37)$$

The coordinates of point D is calculated similar to point C. The distance between center of motor and point D, D_D is same with the distance of point C to center of motor, D_C . The angle that spans the magnet bottom, ω is known from Equation 4.34. The difference between angles of point D and C is equal to ω , the calculation of angle of point D is given in Equation 4.38.

$$\delta = \alpha_{mag} + \frac{\alpha_{mag} - \omega}{2} \quad (4.38)$$

Since the parameters of point D is known, coordinates can be calculated from Equations 4.39-40.

$$D_x = D_D \times \sin(\delta) \quad (4.39)$$

$$D_y = D_{so} - D_D \times \sin(\delta) \quad (4.40)$$

After coordinates of point D is calculated, lines are drawn between points D and A, and C and D. So, the magnet drawing is completed.

For the part between two magnets, coordinates of points E and F must be calculated. Before these calculations, the angle of magnet span at the diameter of rotor at quadratic axis, D_{mq} , α_{magq} is calculated in Equation 4.41 and the angle which spans this parts, γ is found from Equation 4.42, these angles can be seen from Figure 4.13.

$$alfa_{magq} = 2 \times \sin^{-1} \left(\frac{W_{mag}}{D_{mq}} \right) \quad (4.41)$$

$$gama = \frac{2 \times \pi}{pole} - alfa_{magq} \quad (4.42)$$

The coordinates of points E and F can be calculated easily after the angles are found. The angle of point E is *delta* of which equation is given below in Equation 4.43.Φ

$$delta = alfa_{mag} + \frac{alfa_{magq} - alfa_{mag}}{2} \quad (4.43)$$

The distance between center of motor and point E and point F is equal to D_{mq} . The coordinates of points E and F is calculated from equations 4.43-47.

$$E_X = D_{mq} \times \sin(delta) \quad (4.43)$$

$$E_Y = D_{so} - D_{mq} \times \sin(delta) \quad (4.44)$$

$$F_X = D_{mq} \times \sin(delta + gama) \quad (4.45)$$

$$F_Y = D_{so} - D_{mq} \times \sin(delta + gama) \quad (4.46)$$

For drawing the next symmetric rotor magnet portion, the angle is increased by $2 \times \pi / pole$. This part is repeated until angle reaches 2π .

After completing the drawing of stator and rotor lamination portions, lamination is shown in a picture box to the user which has 435x435 pixel dimensions and placed in the Lamination form . User can save the lamination drawing to an image file with bitmap extension or drawing can be saved in dwg extension which can be opened by a CAD program like AutoCAD. Also this drawing can be used in a 2D FEM analysis.

4.6 Conclusion

In Chapter 4, implementation of the software is explained. First how to create a Windows Form Application is described. The toolboxes used in the software are explained. The structure of the program is mentioned. All the tabs which are created according to the type of the inputs like stator and rotor tabs, are described with the help of the flow charts given in Chapter 3. Output tab has some sub-tabs which are again classified considering the type of the output like dimensions, electrical parameters or magnetic parameters. After calculating the outputs user save the analysis report, an example analysis report is given in Appendix B.

As mentioned before, outputs are not only numeric values found by calculations, user can see the lamination and graphical performance outputs too. How the lamination is drawn is explained in detail with the help of the geometric equations. The lamination can be saved or printed if required. Also the calculation of torque and output power is described in previous chapter, by using this information the torque, power and current values are calculated for whole speed range and graphs are drawn. These graphs can be saved and printed too.

CHAPTER 5

USER GUIDE FOR ANALYSIS SOFTWARE

In this chapter, the steps that user should follow to run the analysis are described in detail. The structure of the program is given in Chapter 3 and the implementation part is explained in Chapter 4. First user runs the program from the exe file which is created by the Microsoft Visual Studio. User should run the program in a computer with Windows operating system.

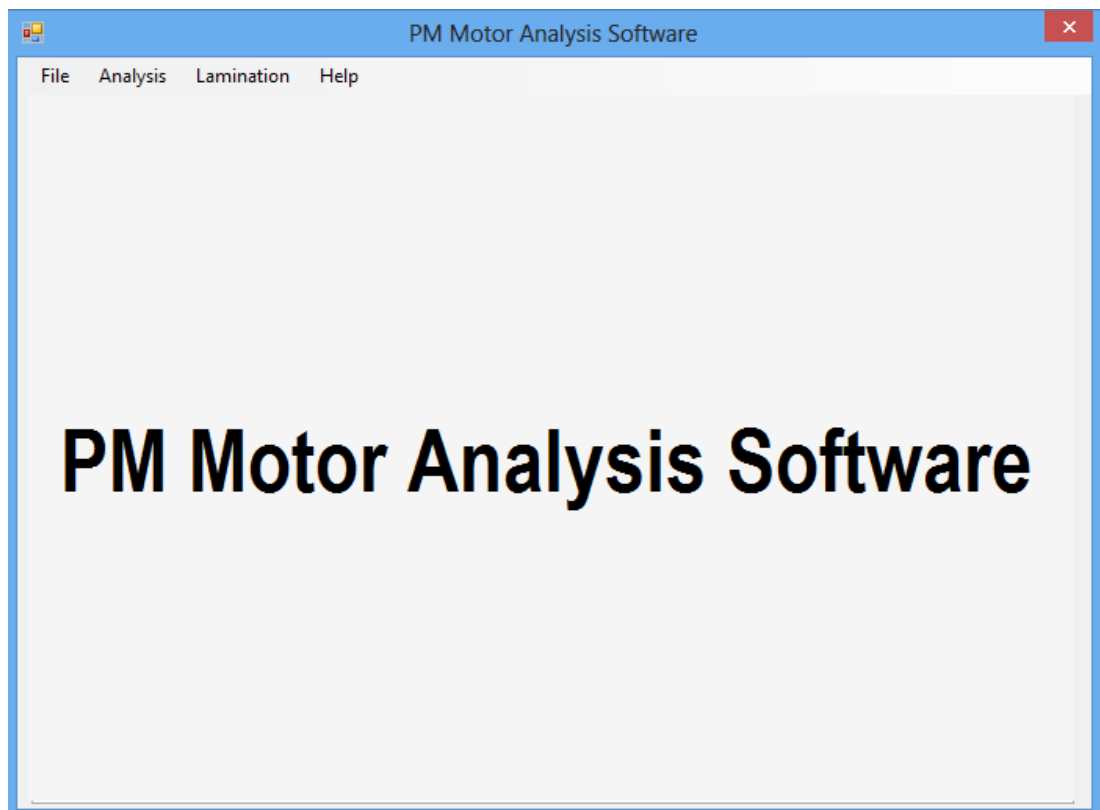


Figure 5.1 : Menu Structure of Program

Once the program is run, the form given in Figure 5.1 is opened. The next step is to choose whether a new analysis is going to be made or a previously saved analysis is going to be opened from file menu of which structure is explained below.

5.1 File Menu

File menu is used for opening a new analysis or a previously analyzed motor, also saving the new analysis and printing the analysis data, closing the analysis or closing the program.

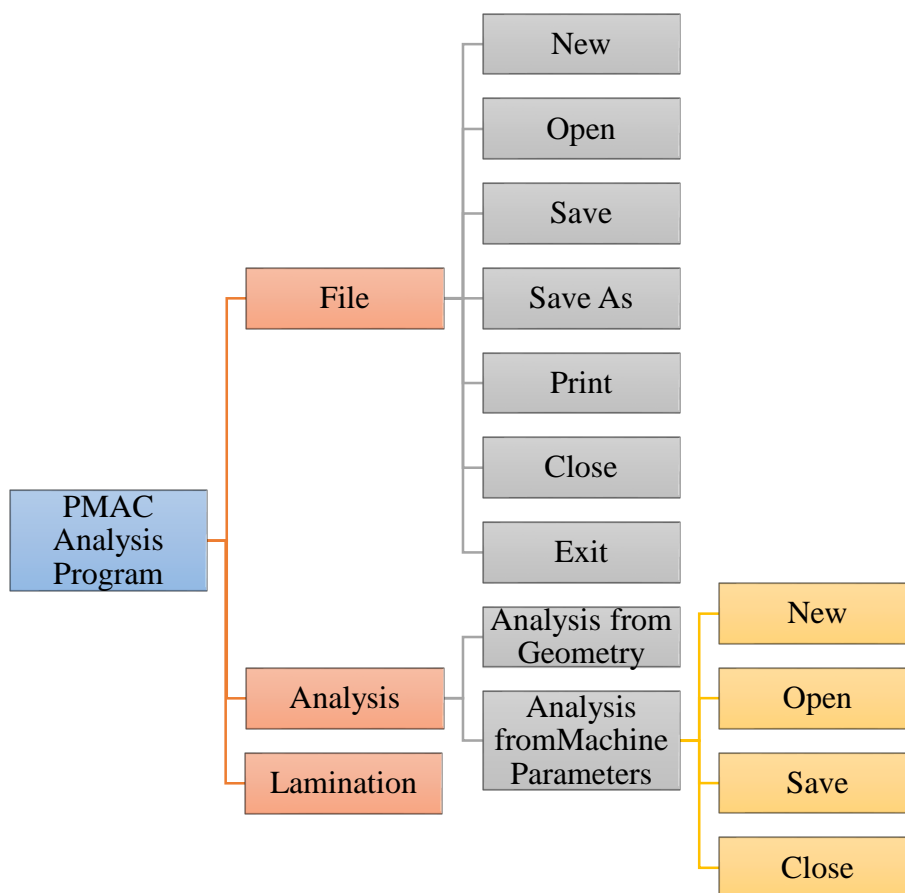
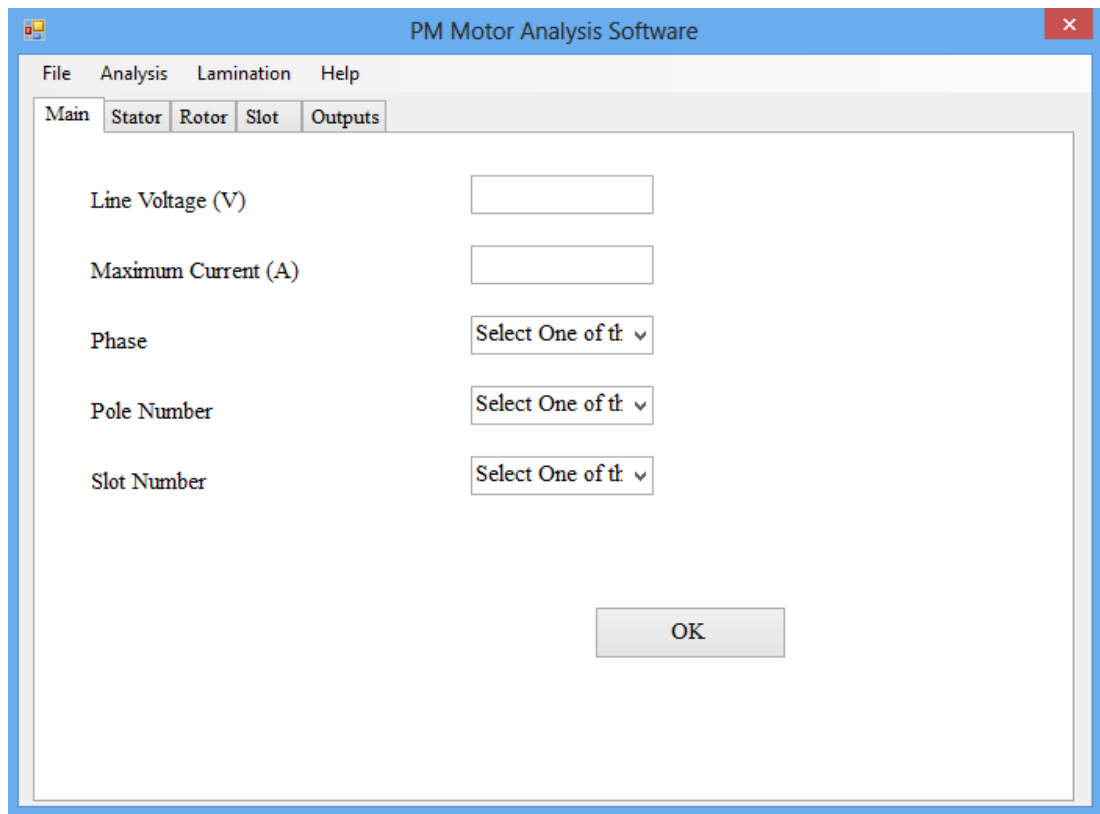


Figure 5.2 : Main Screen of the Program

5.1.1 New

This menu opens a new analysis sheet which is empty. This empty form is given in Figure 5.3. Main dimensions of motor, winding data, voltage-current limitations, number of poles and etc. are entered to this new form to start an analysis.



The image shows a screenshot of a software window titled "PM Motor Analysis Software". The window has a menu bar with "File", "Analysis", "Lamination", and "Help". Below the menu bar is a tabbed interface with tabs for "Main", "Stator", "Rotor", "Slot", and "Outputs". The "Main" tab is selected. The main area contains five input fields: "Line Voltage (V)" with a text box, "Maximum Current (A)" with a text box, "Phase" with a dropdown menu showing "Select One of th...", "Pole Number" with a dropdown menu showing "Select One of th...", and "Slot Number" with a dropdown menu showing "Select One of th...". At the bottom center of the form is an "OK" button.

Figure 5.3 : First Tab of the New Analysis Form

To get the required data from end user, text boxes are used which are controlled after OK button is pressed. If the entered value is not numeric a message box is shown and user is warned to enter numeric values. Also if numeric values are entered with dot, user is warned to enter numeric values with comma via message box. These textboxes are cleaned out until user enters valid values.

The list of the inputs is given in Table 3.1 and user should pay attention to the units given in that table. The units are also shown next to the text boxes of corresponding

input. In Figure 5.3, screen shot of main tab is given and units of voltage and current are given in parentheses.

In a new form user can enter the data by using keyboard shortcuts such that all textboxes can be filled respectively by pressing shift button. After all textboxes in a tab page are filled, user can pass to the next tab page by clicking OK button.

5.1.2 Open

This menu opens a previously saved analysis. User selects the file which is wanted to be opened. The required data is read from the selected file and written to textboxes. If user want to make changes in analysis data, it is required to click on the relevant textbox and refill the data in appropriate form. After clicking OK button on the tab page new variable is read from changed textbox. User can also use keyboard shortcuts as previously described.

| Parameter | Value |
|---------------------|-------|
| Line Voltage (V) | 21 |
| Maximum Current (A) | 35 |
| Phase | 3 |
| Pole Number | 8 |
| Slot Number | 27 |

Figure 5.4 : First Tab of Opened Analysis Form

5.1.3 Save

This menu saves the analysis data to a file of which name is entered by user. All data must be filled and data must be valid, otherwise user is warned via message box to fill all or the textboxes. After saving the data, user can open that file anytime needed. For ease of remembering file names should contain day, output power of motor and input current limit, i.e. 500W-20A-03.12.13.mtr. The files are saved with .mtr extension and in this file inputs of the text boxes are saved respectively.

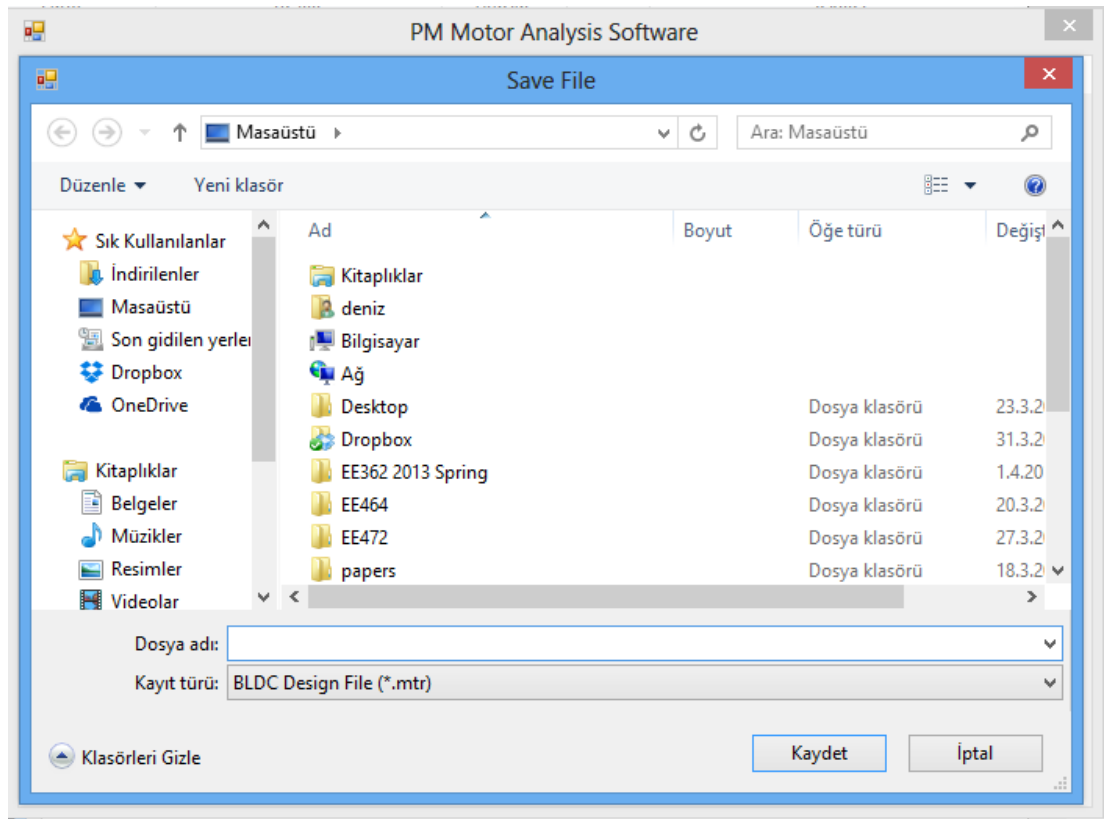


Figure 5.5 : Save File Dialog

5.1.4 Print

This menu print the analysis data entered by the user. All textboxes must be filled to print the data. User can print analysis data via a printer or a pdf created installed to that computer. The printing window for analysis data is given in Figure 5.6.

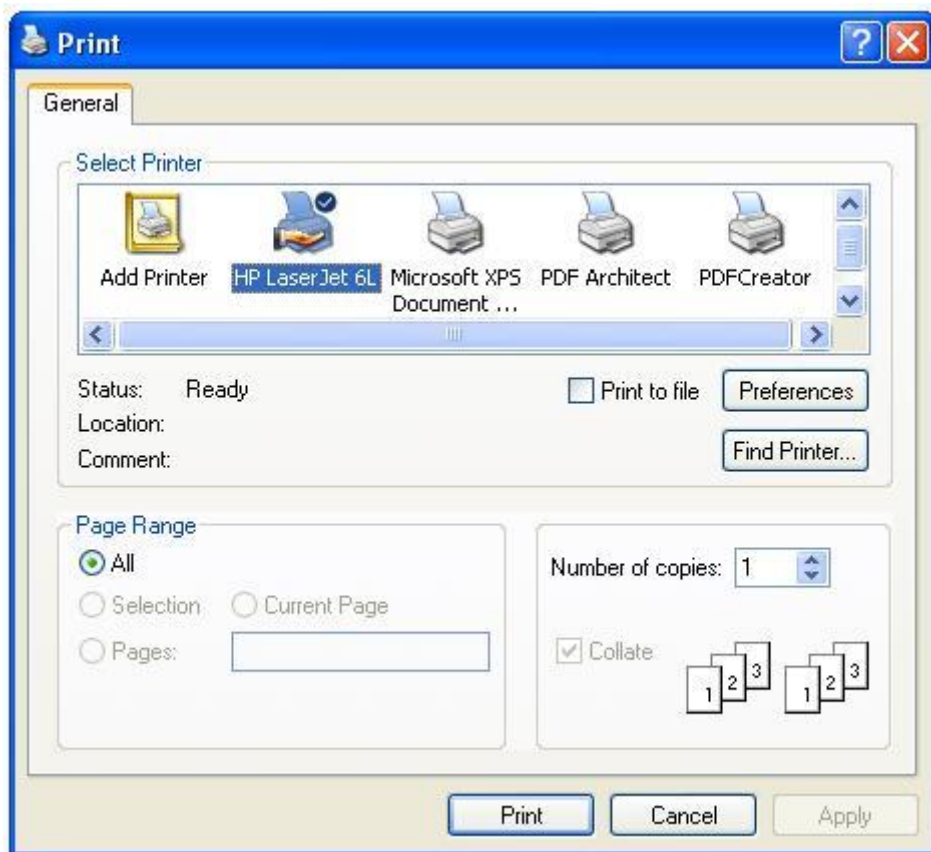


Figure 5.6 : Print File Dialog

5.2 Analysis Menu

The importance of the analysis menu is explained in detail in Chapter 4. The parameters may be calculated by hand in a longer time but the performance analysis cannot be done. Also for a designer, performance outputs is very important because it gives the idea whether requirements are satisfied or not. It is very important for an

analysis to satisfy the desired torque value for a given speed. This torque value is determined from the load that the motor will drive.

The program gives user the chance to do graphical analysis directly program machine dimensions or from machine parameters like resistance, inductance, emf and torque constants. In the first method, user enters all the inputs in correct format mentioned before and after the inputs are entered the program calculates the machine parameters both electrical and magnetic and shows in outputs tab of the program. Then user clicks on Analysis from the menu bar and analysis form is opened in a new window which is given in Figure 5.7. The outputs are transferred to this new form and graphics are drawn from these outputs.

In the second method, graphics are drawn directly from the parameters which may be obtained via tests on an existing machine. These parameters are phase resistance, d and q axis inductances, emf and torque constants, line voltage and maximum input current which is determined from the ratings of the inverter that drives the motor. The analysis from machine parameters window is given in Figure 5.8, this form is different from the form given in Figure 5.7 due to the text boxes that are used to get inputs from the user.

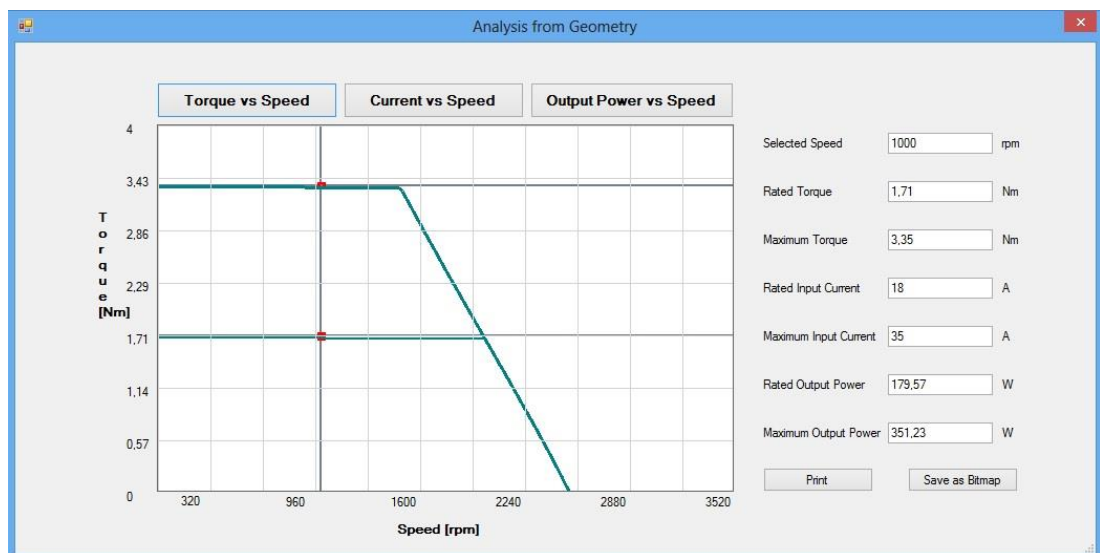


Figure 5.7 : Torque vs Speed Graph

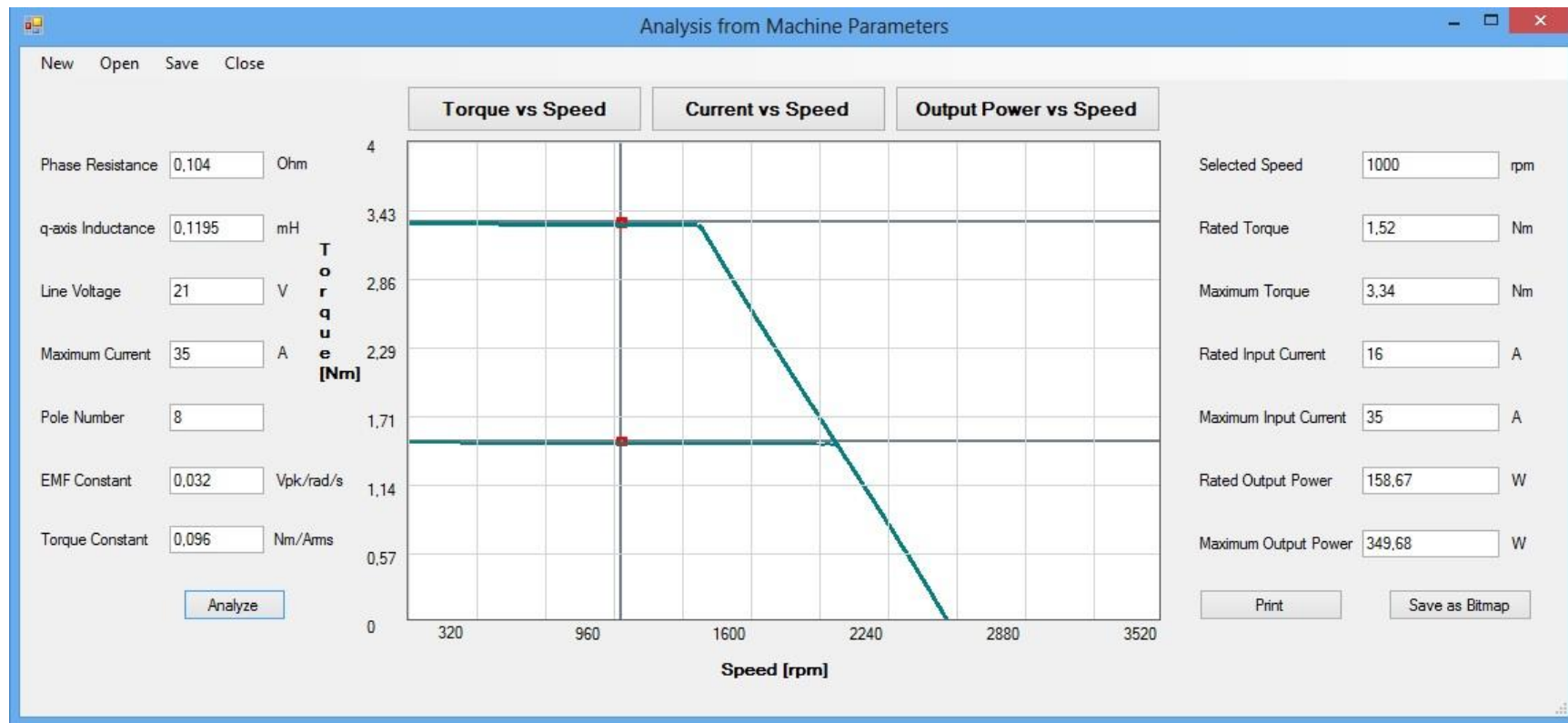


Figure 5.8 : Torque-Speed Graph from Machine Parameter

In analysis program, there are three graphics which are drawn on different picture boxes. When one of the graphs is chosen by clicking one of the buttons placed on the top-mid of the form, corresponding picture box made visible and other two picture boxes made invisible. User also can read the values from graph by clicking on the graph. Mouse coordinates are taken from the program. From x-coordinate speed value is calculated. After calculating the speed, the equations explained in Chapter 2.3 are used and related torque, input current and output power values are calculated and results are given in the text boxes which are placed on the right side of the form.

As mentioned above, three graphical analysis are done in the analysis program for both analysis from geometry and analysis from machine parameters.

5.2.1 Torque vs Speed Graphic

When the analysis form is opened, torque vs speed graph is seen as the default graph on the screen as given in Figure 5.7. The thicker line shows the maximum (pull-out) torque where thinner one shown the rated torque. As explained in Chapter 2.3, torque is calculated under vector control conditions. The most important graph for the designer is torque versus speed graph. Constant torque and constant power regions can be seen on the graph clearly. The values on the graph can be read from the textboxes on the right side of the form. Not only the torque values of selected speed but also current and power values are seen. The values on the axis labels are calculated for the analysis specifically.

5.2.2 Input Current vs Speed Graphic

When user clicks on Current vs Speed button, graphic changes to current versus speed graph as given in Figure 5.9. If user have clicked on the torque versus speed graph, selected speed is kept in memory and cursor lines are drawn for that speed on the new graph. Also other calculated parameters like output power and torque related to that speed are kept in memory too which are displayed in the textboxes on the right side of the program window.

If user selects a new speed and changes the graph that will intersect on the maximum and rated current values for the selected speed, new cursor lines are drawn on the new graph for the new selected speed. Like torque-speed graphic, thicker line represents the maximum and thinner line represents the rated operating condition performance.

Since current and torque are linearly dependent, characteristics against speed are same. Constant torque and constant power regions again can be seen on the graphic.

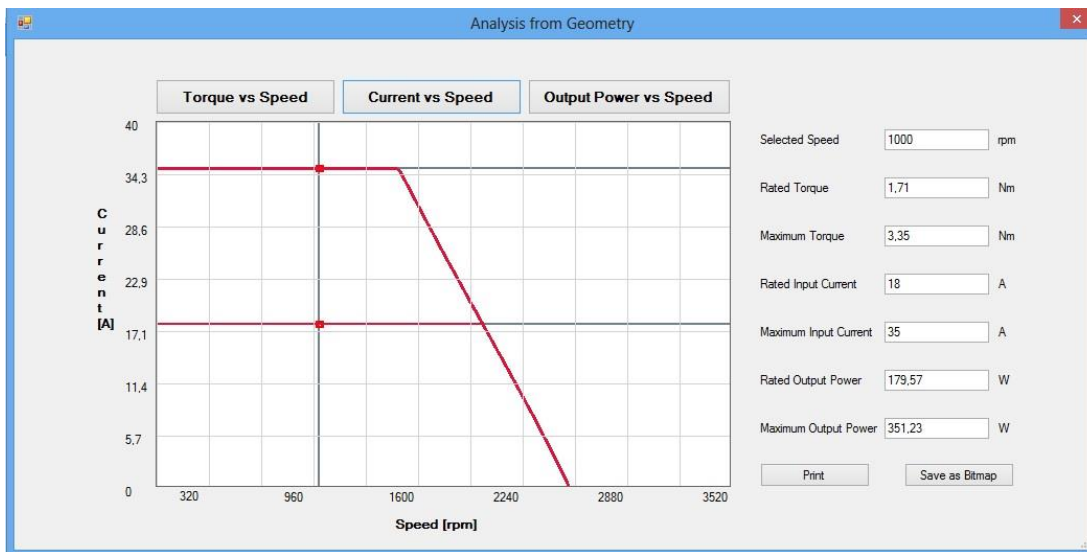


Figure 5.9 : Input Current vs Speed Graph

5.2.3 Output Power vs Speed Graphic

Output power versus speed graph is also can be seen by the user by clicking on Output Power vs Speed button which is shown in Figure 5.10. As mentioned above, if user have selected a speed before from other graphs cursor lines are drawn for that speed and calculated parameters are called from memory. Output power is calculated from the multiplication of torque and speed. Thicker line is drawn from the results of maximum torque times speed where thinner line is drawn from the results of rated torque and speed.

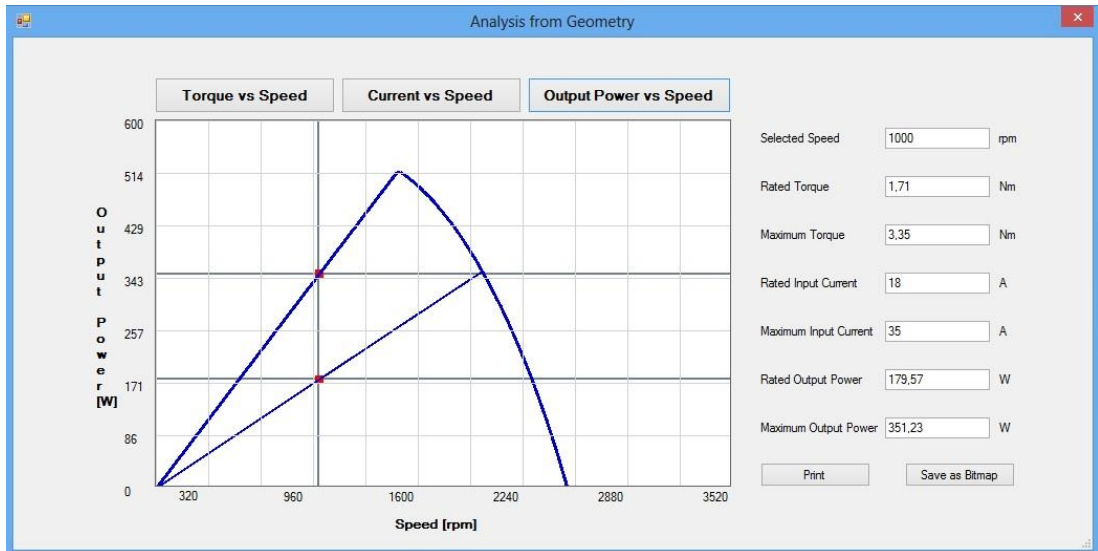


Figure 5.10 : Output Power vs Speed Graph

These three graphs have same specialties in both analysis from geometry and analysis from machine parameters. The only difference in these two analysis is machine parameters are located on the left side of the form in analysis from machine parameters.

5.3 Lamination Menu

Lamination drawing is another important part of the program. If there is any dimension entered wrong, lamination drawing will help to see this problem. Also lamination drawing is very important for the designer to continue analysis like computer aided electromagnetic analysis. For this reason, lamination part is added to the analysis program. Lamination is drawn by the program and user can save the drawing to an image file, print or save the drawing such that the drawing can be opened and edited in a Computer Aided Design (CAD) program.

The steps followed to get a lamination drawing is described in Chapter 4. And a sample lamination drawing is given in Figure 5.11.

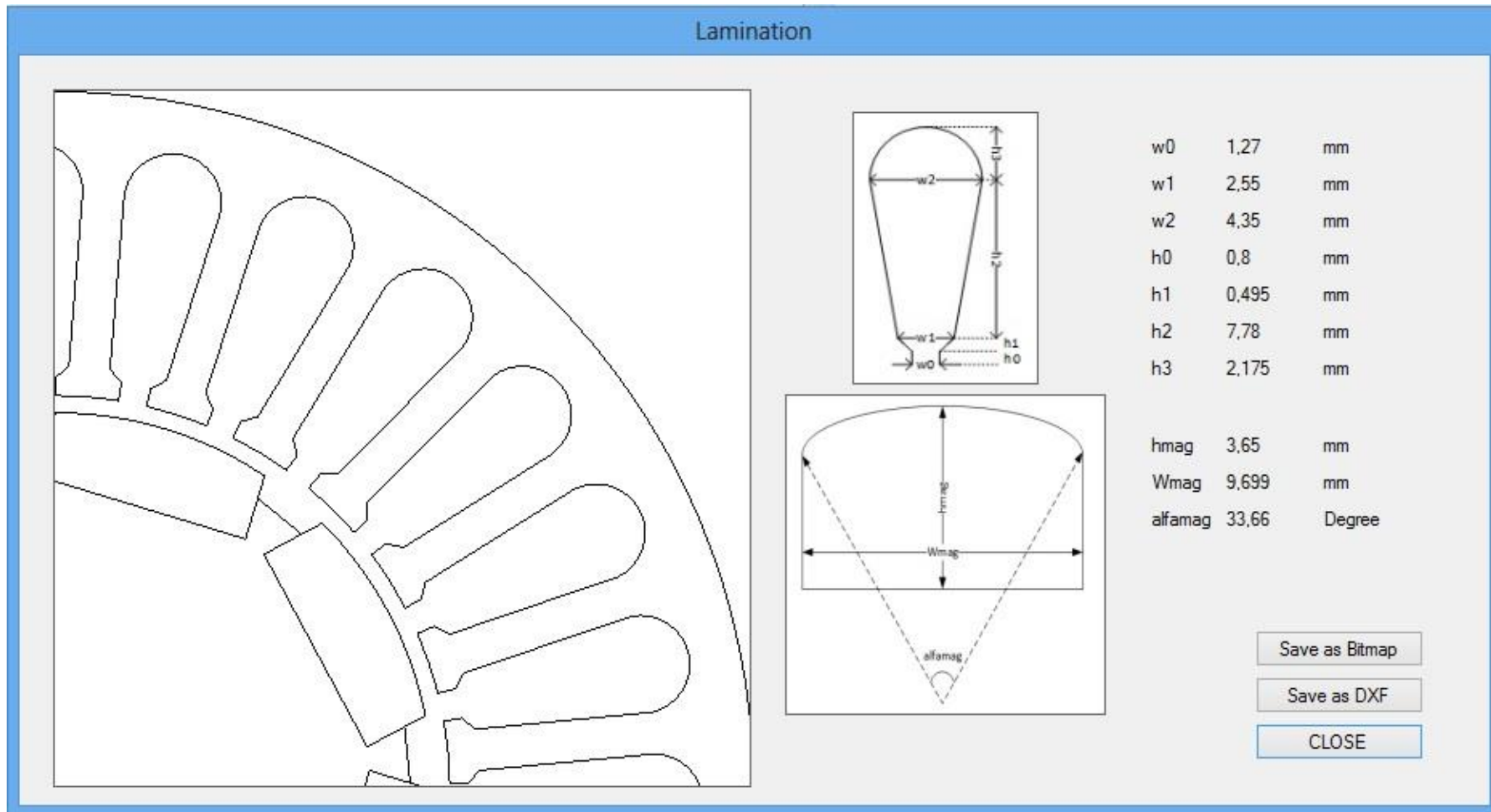


Figure 5.11 : Sample Lamination Drawing Form

After completing stator and rotor lamination portions, lamination is shown in a picture box to the user. User can save the lamination drawing to an image file with bitmap extension or drawing can be saved in dwg extension which can be opened by a CAD program.

5.4 Conclusion

The capabilities of the software is described in summery. The analysis starts with the inputs that user enters in the software and after outputs are calculated. If desired lamination drawing can be seen from lamination menu and graphical performance analysis can be seen from analysis menu. Results are saved to the analysis report in html format and results can be printed if needed.

CHAPTER 6

RESULTS

In this chapter verification of the analysis program is going to be made with two different permanent magnet motors. Program outputs are going to be compared with test results and manufacturer data. The input data and outputs of the program are going to be given in tables and important outputs like resistance, inductance, torque and emf constants are going to be given in tables and compared with test data and error between values are going to be calculated.

First, a 350W (rated) motor is going to be analyzed and results are going to be compared with results of previous model and since this is a tested motor results are going to be compared with motor's test results. Torque versus speed and output power speed characteristics and equivalent electrical circuit parameters are given in the data sheet.

Then, a 37kW PM motor is going to be analyzed and results are going to be compared with results of the test of motor which is given by the manufacturer. From the test torque, current and output power values for different speeds are known. For the same values of torque and speed, calculated current and output power are going to be compared with test results.

Table 6.1: List of Inputs of Motor A

| Tab | Name of the Parameter | Symbol | Value | Unit |
|--------|------------------------------|-------------|-------|--------|
| Main | Line Voltage | V_{line} | 21 | V |
| | Maximum Current | I_{max} | 35 | A |
| | Phase | $phase$ | 3 | - |
| | Pole Number | $pole$ | 8 | - |
| | Slot Number | N_{slot} | 27 | - |
| Stator | Axial Length | L_{sta} | 38 | mm |
| | Air Gap Length | g | 0,75 | mm |
| | Back-Core Depth | h_{bc} | 2,25 | mm |
| | Tooth Width | W_{th} | 1,82 | mm |
| | Coil Extension | L_{ext} | 15 | mm |
| | Turns per Coil | N_{turn} | 4 | - |
| | Coils per Phase | N_{coil} | 9 | - |
| | Stacking Factor | k_{stack} | 0,985 | - |
| | Fill Factor | k_{fill} | 0,339 | - |
| Rotor | Magnet Remanent Flux Density | B_r | 1,05 | T |
| | Diameter at Magnet Base | D_{mb} | 26,2 | mm |
| | Magnet Pitch/Pole Pitch | $alfa$ | 0,748 | Radian |
| | Magnet Height | h_{mag} | 3,65 | |
| | Rotor Leakage Factor | p_{rl} | 0,1 | - |
| Slot | Slot Opening Width | w_0 | 1,27 | mm |
| | Width of Bottom Part | w_1 | 2,55 | mm |
| | Width of Top Part | w_2 | 4,35 | mm |
| | Slot Opening Height | h_0 | 0,8 | mm |
| | Height of Bottom Part | h_1 | 0,495 | mm |
| | Height of Mid-Part | h_2 | 7,78 | mm |
| | Height of Top-Part | h_3 | 2,175 | mm |

6.1 Motor A

First motor is a brushless dc motor. This motor is studied and tested before [5]. In this thesis, previously developed model is improved, a graphical user interface is designed, and new features are added to this interface like choosing different slot types of winding type like single or double layer.

The inputs of the motor are given in Table 6.1. Coil extension is assumed as 15 mm. Stacking factor of steel is taken as 0,985. Slot fill factor is 0,339 from manufacturer data sheet. Magnet remanent flux density is taken as 1,05 T from magnet specifications. Rotor leakage factor is taken as 0,1 which is of the order 0,05-0,2 [1]. Slot type is taken as Slot -1 and magnet type is taken as Magnet -1.

The drawings of stator and rotor steels are known and from these drawings number of poles and stator slot and the dimensions required are filled. The presentation of dimensions are given in Figure 2.1 and slot dimensions are given in Figure 2.8.

Line voltage and maximum current are determined by the manufacturer. The motor is driven via inverter which is running under vector control conditions as presented in Figure 2.10. Maximum input current is determined from inverter ratings also the input voltage is taken from inverter ratings.

After entering the inputs in the correct format to the analysis program, the results are calculated. The analysis report created by the program can be seen in Appendix B.

6.1.1 Comparison of Results

Since the dimensions are taken from the lamination drawings dimensions like stator inner diameter and outer diameter same with the previous model. There is no need to compare the geometrical dimensions of motor.

Electrical parameters are the most important values for the analysis because it directly affects the performance of the motor. The calculation of electrical parameters are explained in Chapter 2.2. The results are given in Table 6.2.

As can be seen from Table 6.2, phase resistance values are nearly same and slightly smaller than measurement. In software phase resistance is calculated from Equation 2.33, in this equation phase resistance is found from conductor length in one coil L_{wire} from Equation 2.37 and conductor used for series connection of coils L_{con} from Equation 2.38. In MATLAB model, L_{wire} is calculated as the conductor length in one turn different from the software and L_{con} is the conductor used for series connection of coils same with software. Phase resistance value is calculated different than the Equation 2.33, since the conductor lengths are calculated different. Also, in MATLAB model external length which effects the all calculations steps of conductor length is taken as 10mm but in software it is taken as 15mm. That is why this small difference comes from.

Table 6. 2: Electrical Parameters of Motor A

| Description | Symbol | Software | MATLAB Model | Measurement | Unit |
|-------------------|------------|----------|--------------|-------------|------------|
| Phase Resistance | R_s | 0,0657 | 0,0658 | 0,068 | Ω |
| D-axis Inductance | L_d | 0,099 | 0,0946 | 0,110 | mH |
| Q-axis Inductance | L_q | 0,125 | 0,1387 | 0,130 | mH |
| EMF Constant | k_{emf} | 0,072 | 0,0710 | 0,071 | Vrms/rad/s |
| Torque Constant | k_{torq} | 0,088 | 0,0869 | 0,086 | Nm/Arms |

Inductances are sum of slot, end winding and magnetizing inductances as can be seen from Equations 2.39-40 for d and q axis respectively. Slot leakage inductance is calculated from slot geometry [4] since there no change in slot dimensions slot leakage inductances are same.

Magnetizing inductance is calculated from equivalent air gap lengths which are found from machine geometry [2] as given in Equation 2.58-59. That is why inductance values are not matching 100%. D and q axis inductance values are

different than previous model, because magnetizing inductance values have changed due to the modifications in equivalent air gap length calculation from Equations 2.55 and 57. Calculation of d-axis equivalent air gap length is done with using the minimum height of magnet h_{mag1} but to have better result the equation is modified with mean magnet height and Carter's coefficient is calculated from the maximum air gap length which is found from the minimum magnet height where Carter's coefficient is calculated from the air gap length at the q-axis of the motor. These changes result in a smaller equivalent air gap length in d-axis and this made the d-axis magnetizing inductance greater. In calculation of q-axis equivalent air gap length, Carter's coefficient of motor is not considered. With the multiplication of result with Carter's coefficient of rotor result in a greater air gap length in q-axis so a smaller magnetizing inductance in q-axis.

End winding inductance is found from an empirical equation which is given in Equation 2.53 [2]. In MATLAB model [5] a different equation is used for calculating end winding inductance but results of both equations are similar.

Values of torque and emf constants are slightly higher than the measurement. These constants are dependent of mean air gap flux density as seen from Equation 2.60-61. The value of air gap flux density has increased in the analysis program in spite of the change in the calculation of air gap area. The flux densities of motor for different areas are given in Table 6.3. Since air gap flux density has increased, mean value of air gap flux density has increased which result in an increase in torque and emf constants.

Air gap flux density calculation is given in Equation 2.15. To find the value of the air gap flux density, air gap area and reluctance and magnet area and reluctance must be known. Calculation of air gap area which is given in Equation 2.2, have changed due to effect of fringing and since air gap area has changed the reluctance also changed as can be seen from Equation 2.4. Calculation of magnet reluctance have also modified to have better approximation to real value. Instead of calculating reluctance via mean magnet height magnet is divided into 5 regions with equal widths as described in Chapter 2.1.2. Despite the changes described above, air gap flux density results have increased.

Table 6.3: Magnetic Parameters of Motor A

| Description | Symbol | Software | MATLAB Model |
|-------------------------------|------------------|----------|--------------|
| Air Gap Flux Density | B_g | 0,734 T | 0,711 T |
| Peak Air Gap Flux Density | \widehat{B}_g | 0,864 T | 0,864 T |
| Mean Air Gap Flux Density | \overline{B}_g | 0,611 T | 0,592 T |
| Magnet Operating Flux Density | B_m | 0,866 T | 0,871 T |
| Stator Back Core Flux Density | B_{bc} | 1,827 T | 1,770 T |
| Stator Tooth Flux Density | B_{th} | 1,891 T | 1,891 T |

Air gap flux density waveform is given in Figure 2.7 and mean and peak value of air gap flux density is shown. Magnet operating flux density have changed because of the change in the air gap reluctance, the effect of air gap reluctance is given in Equation 2.21. Also change in the air gap area and air gap reluctance have affected the stator back-core flux density of which calculation is shown in Equation 2.30. Peak value of air gap flux density and stator tooth flux densities are same because these values dependent on geometry.

Table 6. 4: Comparison of Results and Manufacturer Data

| Description | Symbol | Error between Software and Measurement | Error between MATLAB Model and Measurement |
|-------------------|------------|--|--|
| Phase Resistance | R_s | 3,3% | 3,2% |
| D-axis Inductance | L_d | 10% | 14% |
| Q-axis Inductance | L_q | 3,8% | 6,7% |
| EMF Constant | k_{emf} | 1,5% | 0 |
| Torque Constant | k_{torq} | 2,3% | 1,05% |

In Table 6.4, the errors between measurement and software results and MATLAB model results are given. It can be said that after modifications described above;

- Error in calculating phase resistance is not changed,
- Error in calculating d-axis inductance is reduced,
- Error in calculating q-axis inductance is reduced,
- Error in calculating emf constant is increased
- Error in calculating torque constant is increased.

The results obtained from the software is put in to the model which is used to calculated torque. In this model, measured voltages are used for each speed and core loss resistance is considered in the calculations since the loss constants are known due to the tests [5]. Then MATLAB model results and measurement results are put in the same model and maximum torque and current results are compared.

The line current is calculated from the equivalent electrical circuit. Since the motor is assumed to be driven under vector control, current at d-axis is taken as 0 and all useful current is flowing through q-axis. Since voltages are same for each speed, there are three important terms that effects the amount of current so the torque.

The torque and current values are given in Table 6.5. The maximum current is the limited, this value does not change in calculations. In software matrices are used since there are two unknowns which are terminal voltage and line current. Line current matrix is created such that the maximum value is 35A and it is limited. But in this model, since terminal voltage is known current is directly calculated from the equivalent circuit, so that the maximum value is not limited to 35A.

Table 6.5: Performance Outputs of Motor A

| Description | Symbol | Software | MATLAB Model | Measurement |
|-----------------|-----------|----------|--------------|-------------|
| Maximum Torque | T_{max} | 3,12 Nm | 3,03 Nm | 2,95 Nm |
| Maximum Current | I_{max} | 35,7A | 35 A | 34,5 A |

The software results are higher because higher torque constant means higher torque. Since the current is dependent on the impedance of the motor, and lower phase resistance and lower q-axis inductance result in lower impedance, line current is calculated higher than the result found the results of the model from measurement.

Table 6.6: Comparison of Torque and Current Values

| Description | Symbol | Error between Software Results and Measurement | Error between MATLAB Model and Measurement |
|-----------------|-------------|--|--|
| Maximum Torque | T_{max} | 5,7 % | 2,7 % |
| Maximum Current | T_{rated} | 3,5 % | 1,4 % |

From the results given in Table 6.6, the results obtained from the MATLAB model may look closer to the measurement results. But MATLAB result does not represent the real results. As described above and given in Table 6.4, phase resistance values are nearly same and the difference comes from the q-axis inductance. In MATLAB model current value is calculated lower than software, because the q-axis inductance value is calculated higher than the measurement result. Under similar conditions (phase resistance, torque and emf constants) higher inductance results in higher impedance so a lower line current which makes the result closer to the measurement.

The errors between software results and measurement results is higher but the parameters used for these calculations are closer to the measurement results given in Table 6.4.

The torque, current and output power versus speed graphics and lamination drawing of motor A are given in Appendix B. Maximum torque and maximum current versus speed graphs obtained from the results discussed above are given in Figure 6.1-2.

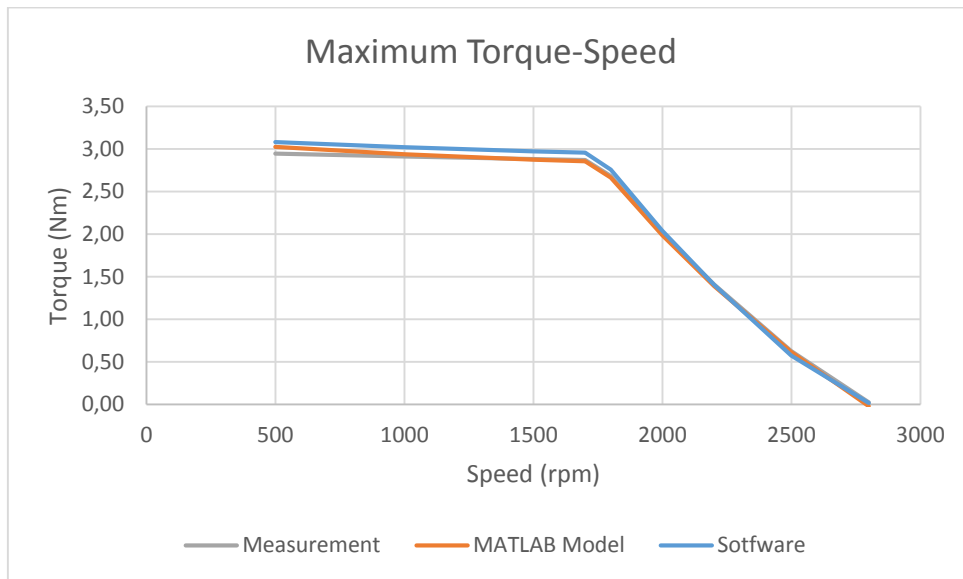


Figure 6.1 : Maximum Toque vs Speed Graph

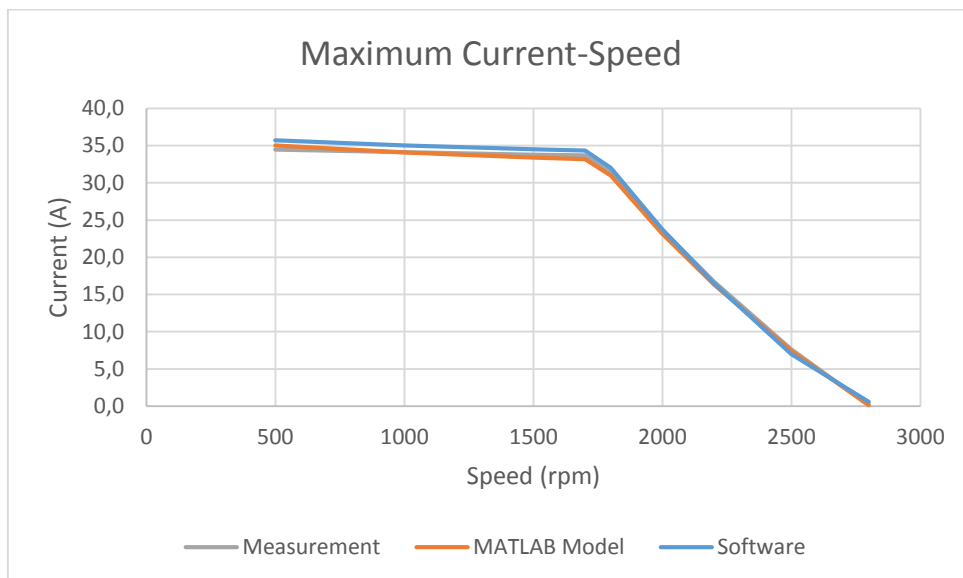


Figure 6.2 : Maximum Current vs Speed Graph

From Figures 6.1-2, maximum torque calculated from software is higher than the results found from MATLAB model and measurement and these graphs supports the results obtained from Table 6.5. The results are discussed in detail above.

6.2 Motor B

The second motor to be analyzed to verify the software is “Motor B”. This is a permanent magnet synchronous motor with 37kW output power and 40000rpm maximum speed. The motor is voltage source driven. The supply ratings are known 380 V, 50 Hz. The winding scheme of the motor is known, number of poles, coils per phase, wire diameter and number of turns per coil are found from the winding scheme. The lamination drawing and dimensions are given in Figure 6.3.

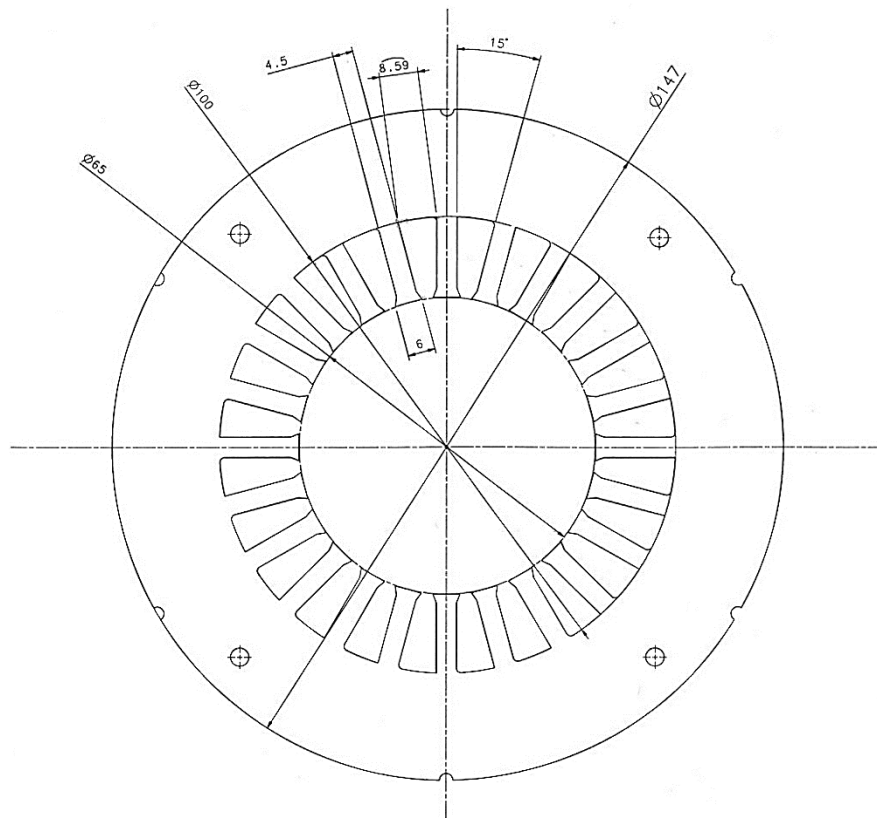


Figure 6.3 : Stator Lamination of Motor B

From Equation 6.1, back-core depth is calculated from stator outer diameter D_{so} and diameter at top of stator slot D_{ts} which are given in Table 6.7.

$$h_{bc} = \frac{D_{so} - D_{ts}}{2} = \frac{147 - 100}{2} = 23.5 \text{ mm} \quad (6.1)$$

Table 6.7: Dimensions of Stator Lamination

| Description | Symbol | Value | Unit |
|-----------------------------|------------|-------|------|
| Number of Slots | N_{slot} | 24 | - |
| Stator Outer Diameter | D_{so} | 147 | mm |
| Stator Inner Diameter | D_{si} | 65 | mm |
| Diameter at Stator Slot Top | D_{ts} | 100 | mm |
| Tooth Width | W_{th} | 4.5 | mm |
| Tooth Width at Slot Opening | W_{td} | 6 | mm |

From Figure 6.3, number of slots N_{slot} is counted as 24. By using number of slots and tooth width at tooth at slot opening, width of slot opening is calculated from Equation 6.2.

$$w_0 = \frac{\pi \times D_{si}}{N_{slot}} - W_{td} = \frac{\pi \times 65}{24} - 6 = 2.5 \text{ mm} \quad (6.2)$$

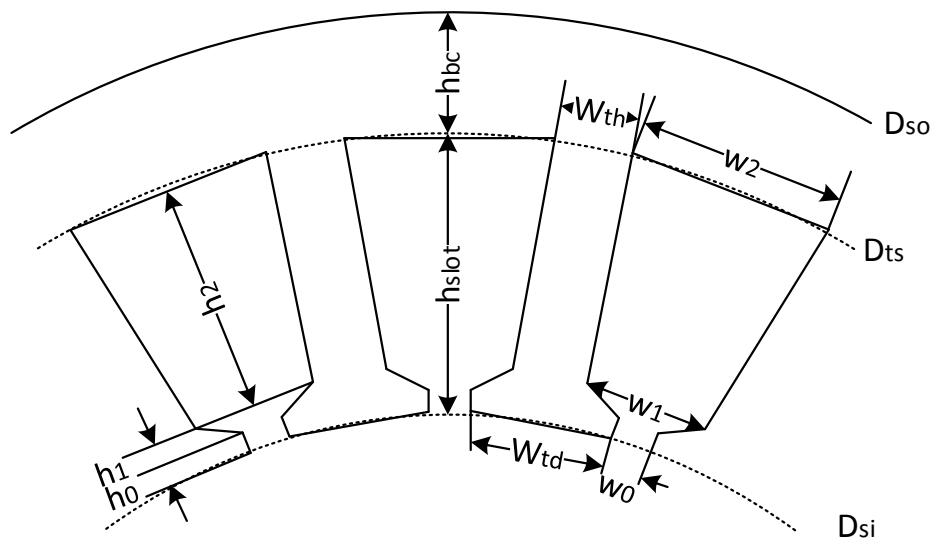


Figure 6.4 : Stator Lamination Dimensions

Slot height is also calculated from the given dimensions as shown in Equation 6.3 below.

$$h_{slot} = \frac{D_{ts} - D_{si}}{2} = \frac{100 - 65}{2} = 17.5 \text{ mm} \quad (6.3)$$

Width of top of slot w_2 is found from the given dimensions D_{ts} , W_{th} and number of slots, N_{slot} .

$$w_2 = \frac{\pi \times D_{ts}}{N_{slot}} - W_{th} = \frac{\pi \times 100}{24} - 4.5 = 7.09 \text{ mm} \quad (6.4)$$

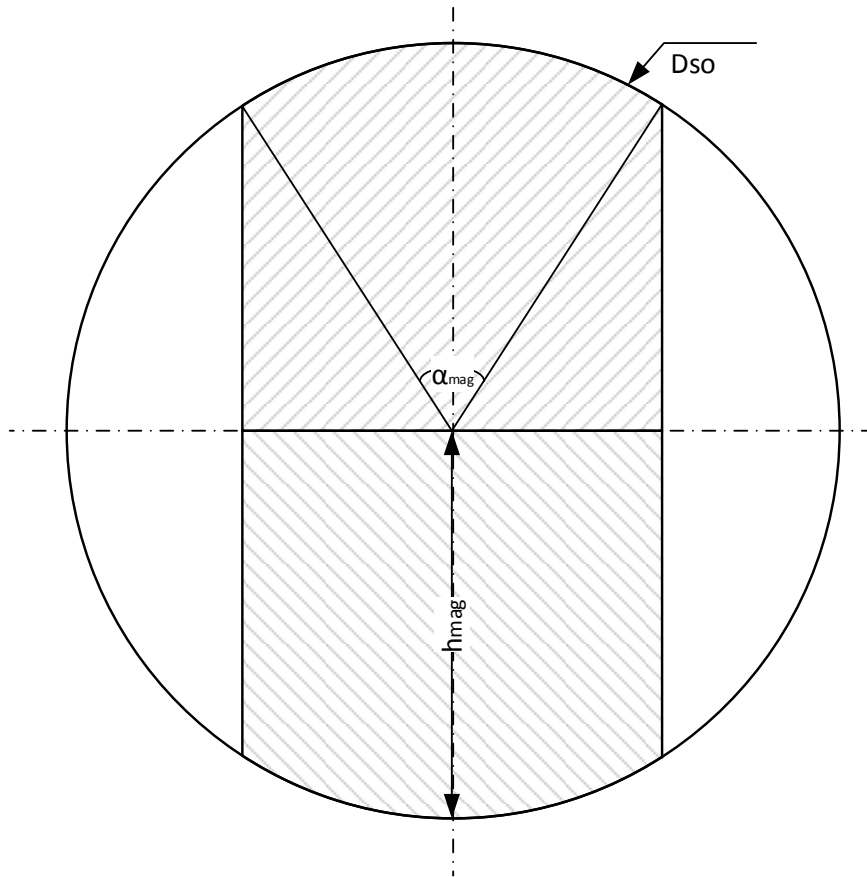


Figure 6.5 : Rotor Drawing

Slot opening height h_0 is assumed to be 1 mm. In motor B, 3rd type of slot given in Figure 4.6 is used and other dimensions w_1 , h_1 , h_2 are measured from the drawing such that the measured slot height corresponds to 17.5 mm and values are found 3.5 mm, 2 mm and 14.5 mm respectively. Stator slot dimensions can be seen Figure 6.4.

In Figure 6.5, cross section of rotor is given. The outer diameter of rotor which is equal to the diameter at magnet surface D_{ms} is measured as 54 mm. Magnets are illustrated with shaded area. Number of poles which is 2. Magnet height in the middle is taken as 27 mm so the diameter at magnet base D_{mb} is zero as shown in Figure 6.5. The angle of magnet is taken as $134,64^\circ$, same with the magnet used in motor A, to have an air gap flux density which is closed to a sinusoidal waveform. Selected magnet type is SmCo of which magnetic residual flux density B_r is 0.8T and coercive force H_c is 557 kA/m.

In the drawings air gap length is given as 2 mm but outer surface of rotor is covered with titanium which has 3 mm thickness. Titanium is non-magnetic like the air gap, because of this thickness of titanium is added to the air gap length and air gap length becomes 5.5 mm. The value given in Table 6.8 includes the titanium thickness.

Stack length of the motor is given as 80 mm. The number of turns per coil of stator is given as 5 and number of coils per phase is given as 4. The number of conductors in one turn N_{con} is given as 47 and diameter of each conductor is 0.55mm. From these conductor information slot fill factor can be calculated as given in Equation 6.3.

$$k_{fill} = \frac{A_{slot}}{A_{wire}} = \frac{h_2 \times (w_2 + w_1) + h_1 \times (w_1 + w_0)}{2 \times N_{con} \times \pi \times \left(\frac{D_{con}}{2}\right)^2} = 0.593 \quad (6.5)$$

Rotor leakage factor, stacking factor and coil extension are taken as 0.1, 0,985 and 15 mm respectively which are same with Motor A. So all the inputs of motor B that software requires is presented in Table 6.8.

Table 6. 8: List of Inputs of Motor B

| Tab | Name of the Parameter | Symbol | Value | Unit |
|--------|------------------------------|-------------|-------|------|
| Main | Line Voltage | V_{line} | 380 | V |
| | Maximum Current | I_{max} | 100 | A |
| | Phase | $phase$ | 3 | - |
| | Pole Number | $pole$ | 2 | - |
| | Slot Number | N_{slot} | 24 | - |
| Stator | Axial Length | L_{sta} | 80 | mm |
| | Air Gap Length | g | 5,5 | mm |
| | Back-Core Depth | h_{bc} | 23,5 | mm |
| | Tooth Width | W_{th} | 4,5 | mm |
| | Coil Extension | L_{ext} | 15 | mm |
| | Turns per Coil | N_{turn} | 5 | - |
| | Coils per Phase | N_{coil} | 4 | - |
| | Stacking Factor | k_{stack} | 0,985 | - |
| | Fill Factor | k_{fill} | 0,593 | - |
| Rotor | Magnet Remanent Flux Density | B_r | 0,8 | T |
| | Diameter at Magnet Base | D_{mb} | 0 | mm |
| | Magnet Pitch/Pole Pitch | $alfa$ | 0,748 | - |
| | Magnet Height | h_{mag} | 27 | |
| | Rotor Leakage Factor | p_{rl} | 0,1 | - |
| Slot | Slot Opening Width | w_0 | 2,5 | mm |
| | Width of Bottom Part | w_1 | 3,5 | mm |
| | Width of Top Part | w_2 | 7,09 | mm |
| | Slot Opening Height | h_0 | 1 | mm |
| | Height of Bottom Part | h_1 | 2 | mm |
| | Height of Top-Part | h_3 | 14,5 | mm |

6.2.1 Calculation of Parameters and Terminal Voltage

From the inputs given in Table 6.8, electrical and magnetic parameters are calculated. These calculations are explained in detail in Chapter 2.

First the parameters in electrical equivalent circuit of the motor which is given in Figure 6.6 is calculated. In this circuit, E_0 is induced emf calculated from emf constant and rotor speed, R_a is armature resistance calculated from stator geometry, X_a is armature reactance which is calculated from machine geometry and rotor speed.

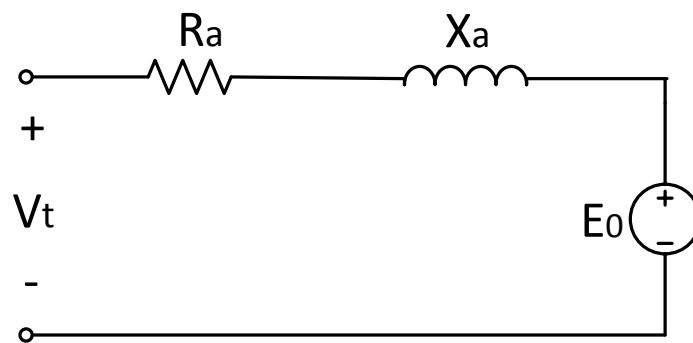


Figure 6.6 : Equivalent Electrical Circuit of Motor B

Phase resistance is calculated from Equation 2.33. Number of coils per phase, number of turns per coil, stack length, external length, slot pitch, number of slots, stator inner and outer diameter and slot height are used to calculate the phase resistance and the result is found as 0,0457 Ω .

It is assumed that the motor is driven under vector control and current in d-axis is zero. Then the reactance value that must be included in the impedance of the motor is q-axis reactance. Reactance is found from Equation 2.72 and as given in this equation q-axis inductance should be calculated. The calculation of reactance is given in Equation 6.6 below.

$$X_a = 2 \times \pi \times f \times L_a \quad (6.6)$$

Q-axis inductance is calculated from sum of slot leakage inductance, end winding leakage inductance and magnetizing inductance. Slot leakage inductance is calculated from Equation 2.41-42 from slot dimensions and found 0,08897 mH. End winding inductance is calculated from 2.53 as 0,01261 mH. Magnetizing inductance of q-axis is calculated as 0,5624 mH from Equation 2.69. Total q-axis leakage inductance is found as 0,664 mH from sum of the components described above. After finding the inductance, reactance value is calculated for different speeds and given in Table 6.9.

The back-emf is multiplication of speed and emf constant. Emf constant is calculated from Equation 2.60 and this equation includes number of poles, pole area and air gap flux density which is given in the following paragraph. Emf constant is calculated as 0,079 Vpk/rad/s. From emf constant back emf voltage is calculated for different speeds and given in Table 6.9.

For calculation of line current, it is assumed that the given electromechanical torque is developed by the motor for the given speed. So current can be calculated with the help of torque constant, k_t found from 2.61 as 0,0955 Nm/Arms.

After calculating the components of the circuit given in Figure 6.6, terminal voltage is calculated from Equation 6.7.

$$V_t = E_0 + R_a \times I_a + j \times X_a \times I_a \quad (6.7)$$

The values of terminal voltage for different speed values are given in Table 6.9 for line to line. The voltage calculated for 36000 rpm is 358V and expected voltage value for rated speed, 40000 rpm is close to 380V, supply voltage.

Also magnetic flux densities should be checked. Mean value of air gap flux density is 0,3284 T and peak value of air gap flux density is 0,6590 which is very low compared to motor A. But this motor is working at high speed values which results in higher frequencies so higher core loss. That is why air gap flux density is kept small. Back core flux density is 0,6531 T and tooth flux density is 1.1407 T which are also lower when compared to motor A. These flux densities are used in core loss calculation which is given in following section.

Table 6.9: Armature Reactance, Induced EMF and Terminal Voltage Values for Different Speeds

| Speed (rpm) | Speed (rad/s) | Frequency (Hz) | Inductance (H) | Reactance (Ω) | Induced EMF (V) | Terminal Voltage (V) |
|-------------|---------------|----------------|----------------|------------------------|-----------------|----------------------|
| 10000 | 1047,20 | 166,67 | 6,64E-04 | 0,70 | 34 | 61 |
| 12000 | 1256,64 | 200,00 | 6,64E-04 | 0,83 | 41 | 74 |
| 12500 | 1309,00 | 208,33 | 6,64E-04 | 0,87 | 43 | 77 |
| 15000 | 1570,80 | 250,00 | 6,64E-04 | 1,04 | 51 | 95 |
| 17500 | 1832,60 | 291,67 | 6,64E-04 | 1,22 | 60 | 115 |
| 20000 | 2094,40 | 333,33 | 6,64E-04 | 1,39 | 68 | 137 |
| 22500 | 2356,19 | 375,00 | 6,64E-04 | 1,56 | 77 | 162 |
| 25000 | 2617,99 | 416,67 | 6,64E-04 | 1,74 | 85 | 191 |
| 27500 | 2879,79 | 458,33 | 6,64E-04 | 1,91 | 94 | 224 |
| 30000 | 3141,59 | 500,00 | 6,64E-04 | 2,09 | 102 | 259 |
| 32500 | 3403,39 | 541,67 | 6,64E-04 | 2,26 | 111 | 298 |
| 36000 | 3769,91 | 600,00 | 6,64E-04 | 2,50 | 123 | 358 |

Note also that the drive for motor B is fed from 380 V mains and therefore, the required terminal voltage should be less than 380V at the highest speed. This requirement is also met by the choice of permanent magnet and its geometry.

6.2.2 Method of Calculation of Torque Curve

Test results of motor B is given in Table 6.10. For different speed values, current, electromagnetic torque and output power is measured for different speed values between 10000 rpm and 36000 rpm. As mentioned above, current is calculated from given torque values and the change of torque with respect to current is given in Figure 6.7 below.

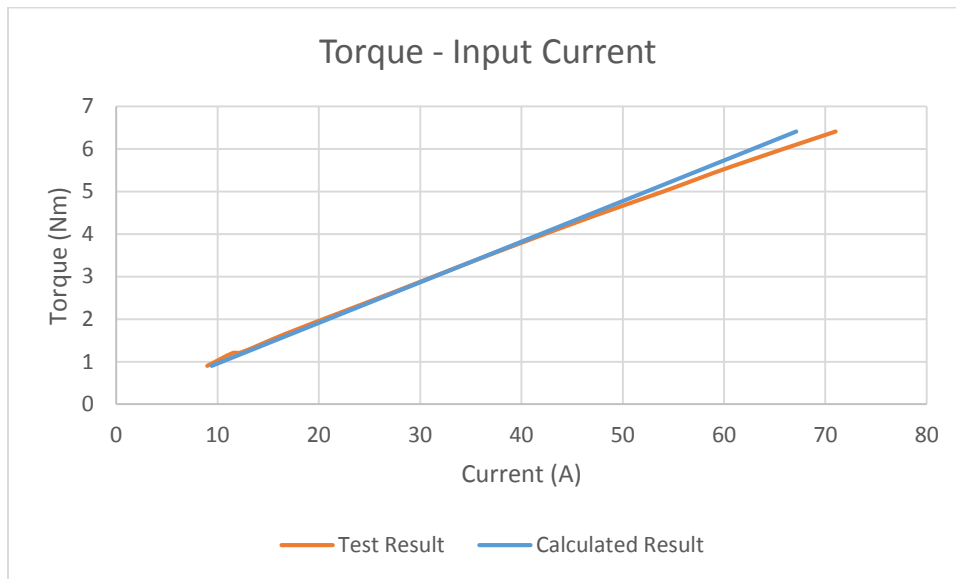


Figure 6.7 : Torque vs Input Current

The blue line is drawn from calculated current values and orange line is drawn from given test results. From this graph, it can be seen that the calculated currents and test currents are very close to each other. In other words, calculated torque constant is very close to the torque constant calculated from the given torque and current values.

From test results torque constant k_{torq} can easily be found from division of torque to speed in radians per second from Equation 2.61. It is seen that the torque constant is between 0,1 and 0,09 Nm/Arms. The average value of torque constant is calculated as 0,0961 Nm/Arms from measurements and the calculated value by the software is 0,0955 Nm/Arms from Equation 2.61. The difference between these values is 0,6% which means calculated value is very close to the real value .

6.2.3 Comparison of Test Results and Software Results

The motor B is tested at different speed values between 10000 and 36000 rpm. For each speed value, torque, input current and output power is recorded and given in Table 6.10 and also change of torque, current and output power versus speed is given in Figure 6.8 below.

Table 6.10: Test Results of Motor B

| Speed (rpm) | Input Current (A) Test | Torque (Nm) | Output Power (kW) | Input Current (A) Calculated |
|-------------|------------------------|-------------|-------------------|------------------------------|
| 10000 | 9 | 0,9 | 0,9 | 9,19 |
| 12000 | 11,5 | 1,2 | 1,5 | 12,26 |
| 12500 | 12,4 | 1,22 | 1,6 | 12,46 |
| 15000 | 16,7 | 1,65 | 2,6 | 16,85 |
| 17500 | 21,9 | 2,13 | 3,9 | 21,76 |
| 20000 | 27,7 | 2,66 | 5,6 | 27,17 |
| 22500 | 38,8 | 3,23 | 7,6 | 32,99 |
| 25000 | 40,3 | 3,82 | 10 | 39,02 |
| 27500 | 47,1 | 4,42 | 12,7 | 45,15 |
| 30000 | 54 | 5 | 15,7 | 51,07 |
| 32500 | 60,9 | 5,6 | 19 | 57,20 |
| 36000 | 71 | 6,41 | 24,2 | 65,47 |

To verify the results first it is assumed that the motor is developing the measured torque for corresponding measured speed. Then from the Table 6.9, torque constant k_{torq} is calculated and this constant is compared with the one calculated via software. Since the error between measured and calculated value is very small, it is assumed that the parameters of the motor are calculated close to the real values. Then it is known that the motor is voltage source driven. But the specifications of drive is not known, which means that the terminal voltage V_t is not known for each speed. The terminal voltage is calculated for each speed and it is expected that the terminal voltage at rated speed (40000 rpm) should be very close to 380 V (supply voltage). After satisfying this requirement, the output power is calculated and compared with the test results given in the table above.

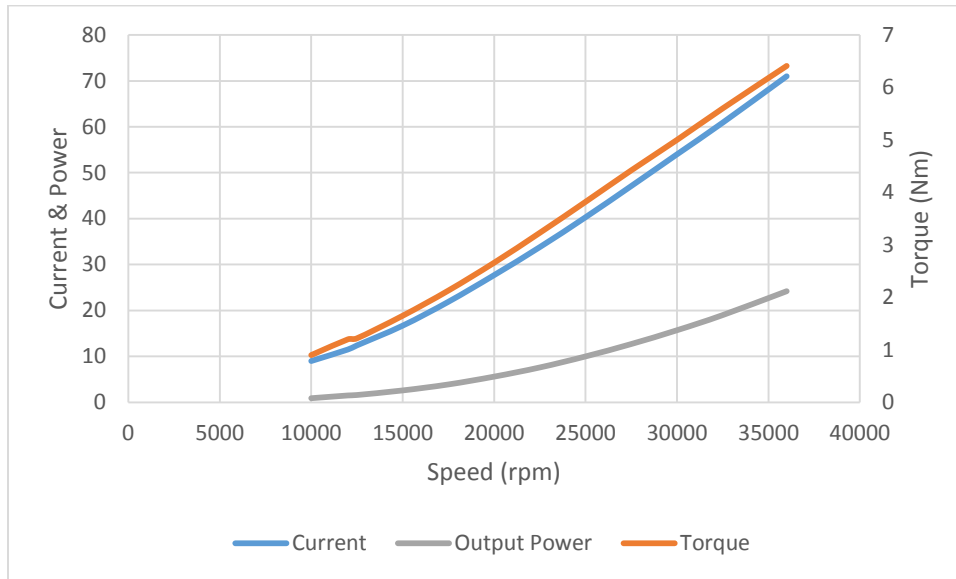


Figure 6.8 : Test Results of Motor B

It is known that the output power of a permanent magnet synchronous motor is equal to torque times speed or induced emf times armature current as shown in Equation 6.8-9.

$$P_{out} = T \times \omega \quad (6.8)$$

$$P_{out} = 3 \times \hat{E}_0 \times I_a \quad (6.9)$$

The output power is found from Equations 6.9 where \hat{E}_0 is the calculated back-emf voltage and I_a is calculated line current. and results are given in Table 6.11. Also test measurements are given in the same table for the same speeds.

Since the test results are measured in kW range, its precision is low. The results are very much close to the test measurements. The error between calculated and measured output power is %0,58.

Table 6. 11: Output Power Results

| Speed (rpm) | Pout_Test (kW) | Pout_3*Ea*Ia (W) |
|-------------|----------------|------------------|
| 10000 | 0,9 | 941,49 |
| 12000 | 1,5 | 1506,39 |
| 12500 | 1,6 | 1595,30 |
| 15000 | 2,6 | 2589,10 |
| 17500 | 3,9 | 3899,34 |
| 20000 | 5,6 | 5565,26 |
| 22500 | 7,6 | 7602,54 |
| 25000 | 10 | 9990,26 |
| 27500 | 12,7 | 12715,36 |
| 30000 | 15,7 | 15691,52 |
| 32500 | 19 | 19039,04 |
| 36000 | 24,2 | 24139,83 |

6.2.4 Calculation of Core Loss, Copper Loss and Efficiency

Copper loss can easily be calculated from the Equation 6.10 given below.

$$P_{cu} = 3 \times I_a^2 \times R_a \quad (6.10)$$

The core loss is calculated for stator tooth and back-core. The core loss in rotor lamination is neglected. For calculation of core loss Equation 6.11 is used [24]. This equation is valid for if $\alpha_{tt} \leq \pi - \beta_m$ where α_{tt} is effective tooth arc and $(1 - \beta_m)$ is pole width in radians calculated from stator geometry.

In the Equation 6.11, k_e is eddy current coefficient, k_h is hysteresis loss constant and k_{exc} is excess loss constant given by the manufacturer. Excess loss is the additional iron loss caused by the magnetic domain structure including eddy current concentration around moving domain wall due to continuous arrangements of the domain configurations. α and k_h are obtained by curve fitting the hysteresis loss data measured and calculated from the hysteresis loss area.

$$\begin{aligned}
P_{core} = & \left(k_h \times f_e \times B_{th}^\alpha + \frac{4}{\pi} \times f_e^2 \times B_{th}^2 \times \frac{k_e}{\alpha_{tt} + \sigma_t} + \left(\frac{4}{\pi} \times \frac{k_{exc}}{\alpha_{tt} + \sigma_t} \right)^{\frac{3}{4}} \right. \\
& \left. \times f_e^{\frac{3}{2}} \times B_{th}^{\frac{3}{2}} \right) \times M_{th} \\
& + \left(k_h \times f_e \times B_{bc}^\alpha + \frac{8}{\pi} \times f_e^2 \times B_{bc}^2 \times \frac{k_e}{\beta_m} + \left(\frac{8}{\pi} \times \frac{k_{exc}}{\beta_m} \right)^{\frac{3}{4}} \right. \\
& \left. \times f_e^{\frac{3}{2}} \times B_{bc}^{\frac{3}{2}} \right) \times M_{bc}
\end{aligned} \tag{6.11}$$

k_e is calculated from conductivity of material σ equal to $6,99 \cdot 10^6$ S/m, weight density of material γ_{fe} equal to 7650 kg/m³ and thickness of steel lamination d which is $0,15$ mm and the result is found as $3,43 \cdot 10^{-6}$ from Equation 6.12.

$$k_e = \frac{\sigma \times \pi^2 \times d^2}{6 \times \gamma_{fe}} \tag{6.12}$$

It is seen that the eddy current constant loss is proportional to square of lamination thickness.

In MATLAB model which is used for simulation of motor A, k_e is taken as $65,36 \cdot 10^{-6}$ for motor A and it is also known that the lamination thickness of motor A is $0,5$ mm. From the ratio of square of lamination thicknesses, k_e is calculated as $5,882 \cdot 10^{-6}$ for motor B and from the Equation 6.12, k_e is calculated as $3,426 \cdot 10^{-6}$. The effect of this difference in total core loss is very small, so k_e is used as $3,426 \cdot 10^{-6}$. The hysteresis and excess loss constants are not known for motor B and these values are taken as same with the constants used in MATLAB model which is taken as $65,36 \cdot 10^{-6}$ and $32,68 \cdot 10^{-6}$ respectively, for motor A.

α is constant for certain range of flux densities and in this calculation taken as 2. B_{th} and B_{bc} are peak values of stator tooth and back-core flux densities respectively, of which values are given in previous section. And W_{th} and W_{bc} are total volume of stator tooth and back-core are calculated from Equations 6.13-14.

$$W_{th} = N_{slot} \times h_{slot} \times W_{th} \times L \quad (6.13)$$

$$W_{bc} = \pi \times \left(D_{so} - 2 \times \frac{h_{bc}}{2} \right) \times h_{bc} \times L \quad (6.14)$$

In Equations 6.13-14, N_{slot} is number of slots, h_{slot} is slot height, h_{bc} back-core depth, D_{so} is stator outer diameter, W_{th} is stator tooth width and L is stack length. These values are calculated in previous section and given in Table 6.8. Total volume of stator tooth is calculated as $1,512 \cdot 10^{-4} \text{ m}^3$ and volume of back-core is found as $7,294 \cdot 10^{-4} \text{ m}^3$. The mass of stator tooth and back-core are calculated from multiplication of volume and density of steel which is 7650 kg/m^3 .

In Equation 6.11, σ_t is the skew angle of tooth and is zero for motor B, α_{tt} is effective tooth arc and $(1 - \beta_m)$ is pole width in radians found from Equations 6.15-16 where *alfa* is the ratio of magnet width top pole width. Effective tooth arc is 0,2618 rad and Pole width is 0,7917 rad.

$$\alpha_{tt} = 2 \times \pi \times \frac{\text{pole}}{2} / N_{slot} \quad (6.15)$$

$$\beta_m = \pi \times (1 - \text{alfa}) \quad (6.16)$$

After these calculations, copper loss and core loss are found for different speed values and given in Table 6.12. The change of copper and core loss with respect to speed is given in Figure 6.9.

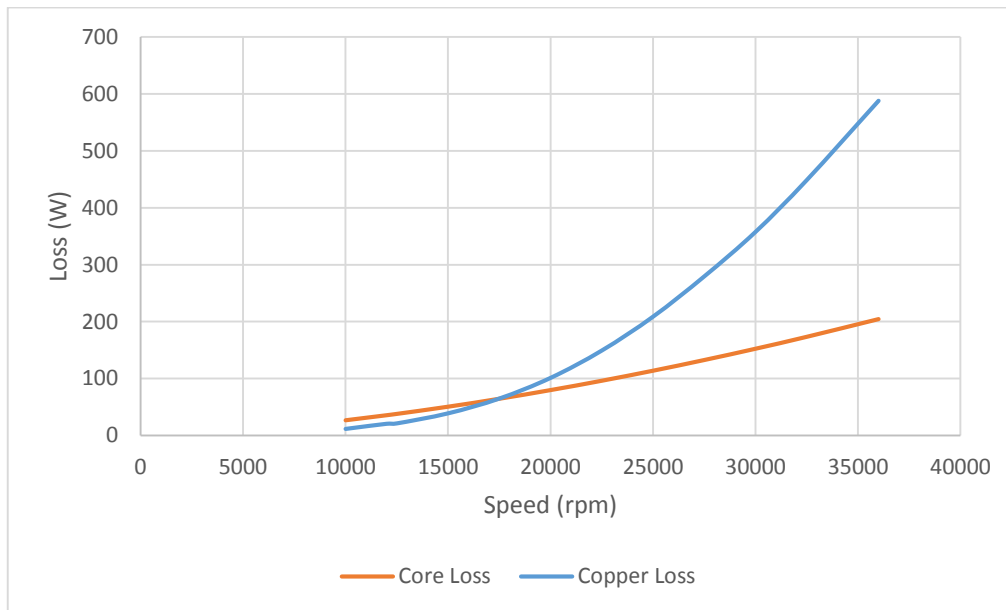


Figure 6.9 : Copper and Core Loss versus Speed

Table 6.12: List of Input and Output Power, Losses and Efficiency

| Speed (rpm) | P_Cu (W) | P_Core (W) | P_out (W) | P_in (W) | Efficiency |
|-------------|----------|------------|-----------|----------|------------|
| 10000 | 11,59 | 26,74 | 914,75 | 953,102 | 0,95976 |
| 12000 | 20,60 | 35,60 | 1470,79 | 1527,02 | 0,96317 |
| 12500 | 21,29 | 37,96 | 1557,35 | 1616,64 | 0,96333 |
| 15000 | 38,94 | 50,59 | 2538,51 | 2628,11 | 0,96591 |
| 17500 | 64,90 | 64,56 | 3834,78 | 3964,34 | 0,96732 |
| 20000 | 101,21 | 79,79 | 5485,46 | 5666,61 | 0,96803 |
| 22500 | 149,24 | 96,25 | 7506,29 | 7751,97 | 0,96831 |
| 25000 | 208,74 | 113,88 | 9876,39 | 10199,3 | 0,96834 |
| 27500 | 279,46 | 132,64 | 12582,72 | 12995,1 | 0,96826 |
| 30000 | 357,61 | 152,51 | 15539,01 | 16049,5 | 0,96819 |
| 32500 | 448,59 | 173,45 | 18865,59 | 19488,1 | 0,96806 |
| 36000 | 587,74 | 204,53 | 23935,30 | 24728,2 | 0,96794 |

The input power for motor B can be calculated from the Equation 6.17 below where V_t is line-to-line voltage, I_a is line current and $\cos \theta$ is the power factor of motor B calculated from the Figure 6.10. The values of input power for different speeds are given in Table 6.12.

$$P_{in} = \sqrt{3} \times V_t \times I_a \times \cos \theta \quad (6.17)$$

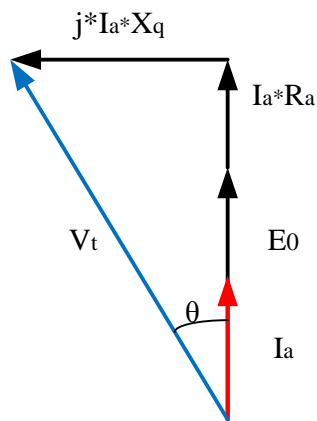


Figure 6.10 : Phasor Diagram of Motor B

Measured power is electromechanical output power and it includes core losses. When core loss is subtracted from measured power, mechanical output power is obtained. Since the input and the output powers are known, the efficiency of motor B for different speeds can be calculated. The calculation result is given in Table 6.12 and the change of efficiency with respect to speed is presented in Figure 6.11.

The input power can also be calculated from the sum of electromechanical power and copper loss which gives the same result with Equation 6.17.

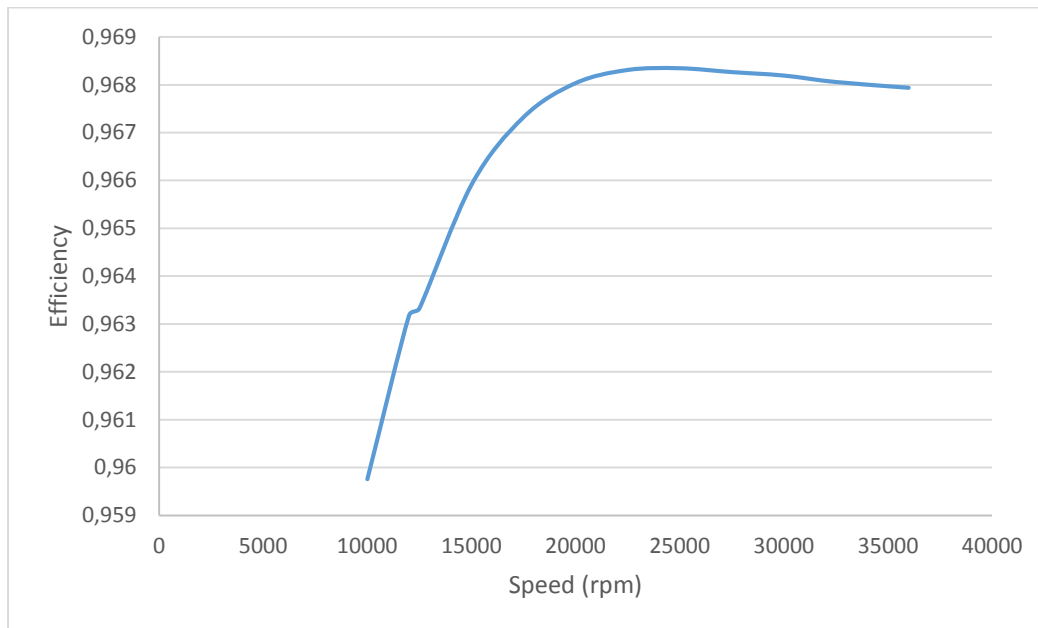


Figure 6.11 : Efficiency versus Speed

6.3 Conclusion

In Chapter 6, the developed software program is tested with two different analysis. The difference between them are the slot type, magnet type and winding type. These analysis differences is overcome with the alternative slot, magnet and winding types added to the interface, so that the user can select what type of analysis criteria is required.

The results are compared with the known characteristics of motor. For example, torque-speed curve and electrical parameters are known for motor A, where for motor B test results are known only. The comparisons are made with the help of tables given in the Chapter 6 and also errors between results are calculated and comments are made on errors.

CHAPTER 7

CONCLUSION AND FUTURE WORK

A MATLAB based model of permanent magnet AC motor have been developed by İ.Şahin in the Electrical and Electronics department [5]. The calculations are done under m files for each step (calculations of dimensions, electrical parameters, magnetic parameters, performance calculations) and also inputs are entered by m files (independent variables and assumptions and definitions). Every equation is solved in order and results can be seen in work space. Also torque-speed and current-speed graphs are plotted for rated and maximum conditions.

In this study, purpose is to rewrite these MATLAB procedures in Microsoft Visual Studio with programming language C# and develop a user interface for the analysis process. The features of the developed interface is listed below;

- Improve the PM motor model which is developed before,
- Implementation of a software to analyze performance from motor dimensions,
- Analyze motor performance directly from machine parameters (resistance, inductance etc.)
- Drawing the full and quarter lamination of analyzed motor,
- The capability of saving analysis, opening a saved analysis, printing analysis outputs within a report format, printing drawings (lamination and graphics)
- Check the accuracy of the software by comparing the results with manufactured motors.

As mentioned above, a previously developed model is improved in this thesis. In Chapter 2, new model is described in detail. The modifications are given in Appendix D. The calculation steps in the order with the software program are given in Chapter 3 to give a general idea for the calculation process. These flow charts are used in programming the software.

Implementation and technical details of the program is given in Chapter 4. Description of the software development in Microsoft Studio is given in detail. How the interface window is designed, how the inputs are taken from user and kept in memory, how calculations are done, how the lamination and graphics are drawn is mentioned.

A basic user guide for the developed software is given in Chapter 5. How to use the menu bar, how to enter data in a valid format and save the inputs, how to run the analysis and how to read values from performance graphics and how to obtain the lamination drawing is described.

The developed software is tested with a manufactured motor of which datasheet is given in Appendix A. The results are compared with the measured motor parameters. The resistance, inductance, torque constant and emf constant values are compared with the results obtained from tests [5]. From the comparisons the following outcomes are obtained:

- The analysis outputs which are used in performance calculations (phase resistance, d-axis inductance, q-axis inductance, EMF constant and torque constant) are compared with measurement results and with MATLAB model results. It is seen that the difference between results decreased except for EMF and torque constants. While the error in calculation of phase resistance, d-axis inductance, and EMF and torque constants are decreased, the error in calculation of q-axis inductance increased from 4.3% to 6%. (The numeric values are given in Table 5.4).
- The difference between phase resistances calculated by software and MATLAB model is 0,1%, which is a result of using an approximate external conductor length in calculations.

- The difference between d-axis inductance calculated by software and measurement is 10% which is lower than the difference between measurement and MATLAB model result. Also the difference between q-axis inductance calculated by software and measurement is 3,8% where the difference between MATLAB result and measurement of q-axis inductance is %6,7. The reason why the results improved is given in Appendix D.
- The difference in calculation of emf constant in software is 1,5% and torque constant is 2,3%. These differences come from the difference in calculation of air gap flux density. In calculation of air gap flux density, the effect of fringing flux is considered approximately and change in calculation of the magnet reluctance which is given in Appendix D.
- The results are checked in the motor model for the voltages that tests are done and maximum currents are calculated from the circuit parameters discussed above and the currents and calculated output torques are compared and the differences between results are described.
- Also the program outputs are tested with a second motor. The torque, current and output power versus speed values are known from test results. The resistance, inductance and torque and EMF constants are calculated from program. During these calculations motor is assumed to be developing the torque which is given in test results.
- The torque constant is easily calculated from the division of torque to armature current and the error between the results of this calculation and software calculation is 0,6%.
- Since the torque constant calculation of program is very close to the calculation result from test data, the emf constant is assumed as to be calculated correctly. The back EMF value is calculated from EMF constant and speed. The armature current is calculated from the torque given in test data and torque constant obtained from the software. The output power test data is compared with the output power calculated from back EMF and armature current and the error between results is calculated for every speed that test is done. The average value of the errors calculated for different speed is found as 0.5% which is very low.

- Also, since the drive method used in the test is not known, the only known criteria known for the voltage is supplied from three phase grid (380V, 50Hz). Terminal voltage is calculated from the Equation 6.6 and for rated speed (40000rpm) the voltage is found nearly 380V which is acceptable.
- From the loss constants of motor A, core loss is calculated. And copper loss is calculated from phase resistance and line current. Output power is found from the test results and efficiency of motor B is calculated.

In addition to the software developed in this thesis, the following parts can be studied in a future work;

- The analytical model of buried/interior PM motor can be added to the software as an option.
- The B-H curves and core-loss curves can be offered to user by user or user can be able to upload and save own curves as input.
- Magnet loss and friction and windage loss can be modelled.
- Core loss can be modelled and added to the calculation part of the software.
- Optimization menu can be added to the software to obtain same performance output with less magnet or an optimization program can be called from software and required data can be transferred to optimization program.

REFERERENCES

- [1] T.J.E. Miller, "Brushless Permanent-Magnet and Reluctance Motor Drives", Claredon Press, Oxford University Press, 1989.
- [2] J.F. Gieras, M. Wing, "Permanent Magnet Motor Technology - Design and Applications", 2nd Ed., Marcel Dekker Inc., New York, ISBN:0-8427-0739-7, 2002.
- [3] D. Hanselman, "Brushless Permanent Magnet Motor Design", 2nd Ed., The Writers' Collective, ISBN:1-932133-63-1, 2003.
- [4] T.A. Lipo, "Introduction to AC Machine Design", Vol.1, Wisconsin Power Electronics Research Center, University of Wisconsin, 1996.
- [5] İ. Şahin, "Measurement of Brushless DC Motor Characteristics and Parameters and Brushless DC Motor Design", MSc Thesis, METU, 2010.
- [6] M. İzgüden, "Design Software Development for Induction Motors", MSc Thesis, METU, 2011.
- [7] S. Küçük, "Serial and Parallel Robot Manipulators - Kinematics, Dynamics, Control and Optimization", InTech, ISBN 978-953-51-0437-7, 2012.
- [8] H.B. Ertan, M. Aftahi, "SPCAD a tool for computer aided design of single phase induction motors", *IMACS TC 1-93 Proc. Computational Aspects of Electromechanical Energy Converters*, pp.311-316, 1993.

- [9] L.B. Yalçın, “A Software for Analysis and Design Optimization of Switched Reluctance Motor”, MSc Thesis, METU, 2004.
- [10] A. Consoli, A. Raciti, “Analysis of permanent magnet synchronous motors”, *Industry Applications Society Conference*, vol. 1, pp: 63-68, 1989.
- [11] A. Consoli, G. Renna, “Interior type permanent magnet synchronous motor analysis by equivalent circuits”, *IEEE Transactions on Energy Conversion*, vol. 4, pp: 681-689, 1989.
- [12] C. Zhang, K.J. Tseng, “Analysis and Comparison of Axial Flux PM Synchronous Motor and Induction Motor”, *IPEC*, pp: 572-577, 2010.
- [13] H.C. Jong, H.K. Jung, “Design and Parametric Analysis of Axial Flux PM Motors with Minimized Cogging Torque”, *IEEE Transactions on Magnetics*, pp: 2855-2858, 2009.
- [14] A. Cavagnino, M. Lazzeri, “A Comparison Between the Axial Flux and the Radial Flux Structures for PM Synchronous Motors”, *IEEE Transactions on Industry Applications*, pp: 1517-1524, 2001.
- [15] M. Aydın, T.A. Lipo, “Design and 3D electromagnetic field analysis of non-slotted and slotted TORUS type axial flux surface mounted permanent magnet disc machines”, *Electric Machines and Drives Conference*, pp: 645-651, 2001.
- [16] W.L. Soong, M. Aydın, “Design and Experimental Verification of a 50 kW Interior Permanent Magnet Synchronous Machine”, *Industry Applications Conference*, vol. 4, pp: 1941-1948, 2006.

- [17] C.C. Hwang, S.M. Chang, "Estimation of parameters of interior permanent magnet synchronous motors", *Journal of Magnetism and Magnetic Materials*, vol. 239, pp: 600-603, 2002.
- [18] Y. C. Jang, J.K. Kyoung, "Experimental Works and Analysis for Influence of Stator Slot Number on Performance of Interior PM Motor", *Electromagnetic Field Computation (CEFC)*, 2010.
- [19] Lipo T.A., Aydin M., "Performance Comparison of Dual-Rotor Radial-Flux and Axial-Flux Permanent-Magnet BLDC Machines", *Electric Machines and Drives Conference*, vol. 3, pp: 1948-1954, 2003.
- [20] Z. Wu, D. Depernet, "Electrical Motor Design for Hybrid Heavy-Duty Electrical Powertrain", *Vehicle Power and Propulsion Conference*, pp: 486-493, 2009.
- [21] G.R. Slemon, "On the Design of High-Performance Surface-Mounted PM Motors", *Industry Applications Society Annual Meeting Conference Record*, vol. 1, pp: 279-285, 1992.
- [22] N. Bianchi , S. Bolognani, "Design techniques for reducing the cogging torque in surface-mounted PM motors", *IEEE Transections on Industry Applications*, vol.38, pp: 1259-1265, 2002.
- [23] J. Wang, Y. Xibo, "Design Optimization of a Surface-Mounted Permanent-Magnet Motor with Concentrated Windings for Electric Vehicle Applications", *IEEE Transections on Vehicular Technology*, vol. 62, pp: 1053-1064, 2013.
- [24] F. Deng, "An Improved Iron Loss Estimation for Permanent Magnet Brushless Machines", *IEEE Transections on Energy Conversion*, vol. 14, pp: 1391-1395, 1999.

- [25] Microchip AN885 Application Note “Brushless DC (BLDC) Motor Fundamentals”, 2003.
- [26] Wikipedia, The First Electric Motor, “http://en.wikipedia.org/wiki/Electric_motor#The_first_electric_motors”, Last visited on Feb 10, 2014.
- [27] Wikipedia, Brushless DC electric motor, “http://en.wikipedia.org/wiki/Brushless_DC_electric_motor”, Last visited on Feb 10, 2014.
- [28] ANSYS, “<http://www.ansys.com/Products/Simulation+Technology/Electronics/Electromechanical/ANSYS+RMxpvt>”, Last visited Feb 17, 2014.
- [29] Magsoft Corporation, “<http://magsoft-flux.com/products/speed>”, Last visited Feb 17, 2014.

APPENDIX A

MANUFACTURER DATA FOR MOTOR A

D323-L15_S4_21V_35Arms

These are calculated curves.
The actual motor performance might vary up to 5%

| | | | | | |
|------------------------|---|--------------------------|------------------------|-------------------|-------------------|
| input: | stack length | L | 15 | *0,1 inch | |
| | maximum Current | I_{max} [Arms] | 35 | Arms | |
| | connection of coils | D / S | s | | |
| | number of turns | # | 4 | | |
| | copper fill factor | Kcu | 33,9% | | |
| | saturation at max. current | Satt | 11% | | |
| | bus voltage | Udc | 21 | V | |
| | rated speed | Nn | 6300 | rpm | |
| | kt-variation factor | km | 1 | | |
| | ambiente temperature | Tu | 25 | °C | |
| | thermal resistance | Rth | 0,975 | K/W | |
| | stall data continuous data with: Duty Cycle = 100 % dT = 100 K | continuous stall torque | ⊙ Mo [Nm] | 1,64 | Nm |
| | | continuous stall current | ⊙ Io [Arms] | 19,03 | Arms |
| peak stall torque | | Mmax [Nm] | 2,9 | Nm | |
| peak stall current | | I _{max} [Arms] | 35,0 | Arms | |
| nominal values | rated torque | ⊙ Mn [Nm] | 1,47 | Nm | |
| | rated current | ⊙ In [Arms] | 17,0 | Arms | |
| | rated power | ⊙ Pn [W] | 0 | W | |
| | rated speed | ⊙ Nn [rpm] | 5200 | rpm | |
| other data | theoretical no load speed | ⊙ Ntheo [rpm] | 2820 | rpm | |
| | maximum speed | ⊙ Nmax [rpm] | 48360 | rpm | |
| | torque constant | kt [Nm/Arms] | 0,086 | Nm/Arms | |
| | EMK-constant | ke [Vpk/rad/s] | 0,071 | Vpk/rad/s | |
| | terminal to terminal resistance | ⊙ Rtt [Ohm] | 0,136 | Ohm | |
| | terminal to terminal inductance | ⊙ Ltt [mH] | 0,237 | mH | |
| | inductance Ld | ⊙ Ld [mH] | 0,125 | mH | |
| | inductance Lq | ⊙ Lq [mH] | 0,133 | mH | |
| | thermal resistance | ⊙ Rth [°C/W] | 0,975 | °C / W | |
| | electr. time constant | ⊙ T [ms] | 1,743 | ms | |
| | inertia w/o brake | J [kgcm ²] | 0,4 | kgcm ² | |
| | mass w/o brake | m [kg] | 2,0 | kg | |
| | brake | inertia with small brake | J [kgcm ²] | 0,5 | kgcm ² |
| inertia with big brake | | J [kgcm ²] | 0,6 | kgcm ² | |
| mass with small brake | | m [kg] | 2,2 | kg | |
| mass with big brake | | m [kg] | 2,3 | kg | |

⊙ With motor mounted on a steel plate 300 x 300 x 12 mm and 100 K dT between windings and still air ambient

⊙ nominal speed at maximum continuous output power

⊙ speed, where EMF is equal to bus voltage 21 V

⊙ speed, where EMF is 20 volts

⊙ measured at 25°C

MOOG-GmbH: EM: GAA

30J

Figure A.1: Electrical and Mechanical Specifications

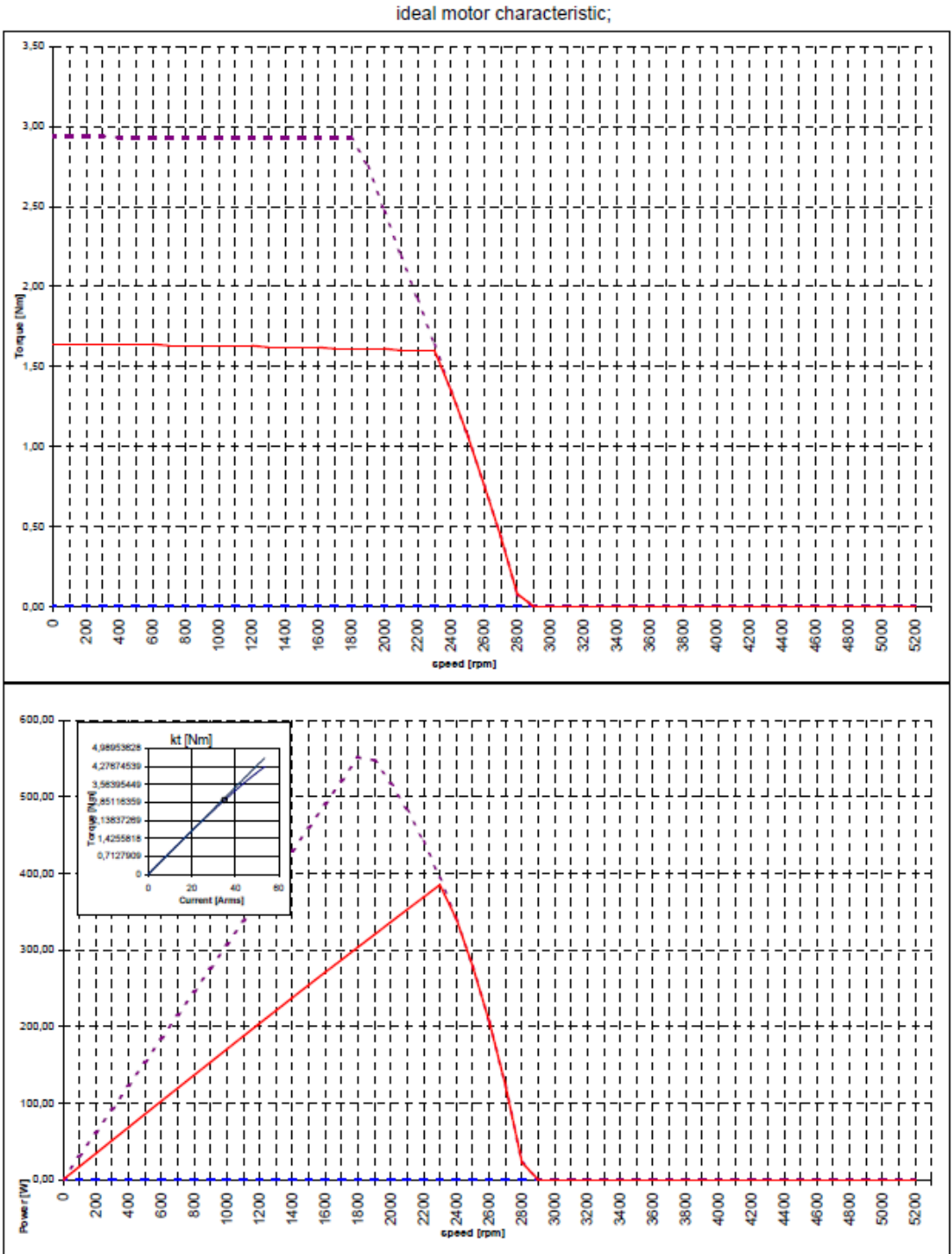


Figure A. 2: Torque Speed(top) and Output Power-Speed (bottom) Characteristics

APPENDIX B

ANALYSIS REPORT OF MOTOR A

Table B.1: Analysis Report of Motor A

ANALYSIS REPORT

| | | | |
|----------------------|--------|-------|----|
| Main Inputs | | | |
| Line Voltage | Vline | 21 | V |
| Maximum Current | Imax | 35 | A |
| Phase | phase | 3 | |
| Pole Number | pole | 8 | |
| Slot Number | Nslot | 27 | |
| Stator Inputs | | | |
| Axial Length | Lsta | 38 | mm |
| Air Gap | g | 0,75 | mm |
| Back-Core Depth | hbc | 2,25 | mm |
| Tooth Width | Wth | 1,82 | mm |
| Coil Extension | Lext | 15 | mm |
| Turns per Coil | Nturn | 4 | |
| Coils per Phase | Ncoil | 9 | |
| Stacking Factor | Kstack | 0,985 | |
| Fill Factor | Kfill | 0,339 | |

Table B.1: Analysis Report of Motor A (continued)

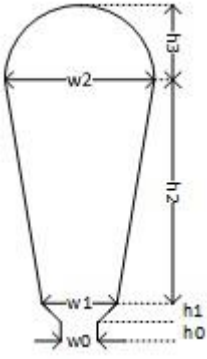
| Rotor Inputs | | | |
|--|-----------|---------|-----------------|
| Magnet Remanent Flux Density | Br | 1,05 | T |
| Diameter at Magnet Base | Dmb | 26,2 | mm |
| Magnet Pitch/Pole Pitch | alfa | 0,748 | |
| Magnet Height | hmag | 3,65 | mm |
| Rotor Leakage Factor | prl | 0,1 | |
| Slot Inputs | | | |
| *Please see the figure in program for slot dimensions! | | | |
|  | w0 | 1,27 | mm |
| | w1 | 2,55 | mm |
| | w2 | 4,35 | mm |
| | h0 | 0,8 | mm |
| | h1 | 0,495 | mm |
| | h2 | 7,78 | mm |
| | h3 | 2,175 | mm |
| | hslot | 11,25 | mm |
| | Aslot | 34,272 | mm ² |
| | Slot type | 1 | |
| OUTPUTS | | | |
| Dimensions | | | |
| Air Gap | g | 0,75 | mm |
| Magnet Width | Wmag | 9,7 | mm |
| Magnet Height (Region-1) | hmag1 | 3,19 | mm |
| Magnet Height (Region-2) | hmag2 | 3,53 | mm |
| Magnet Height (Region-3) | hmag3 | 3,65 | mm |
| Magnet Area | Amag | 368,576 | mm ² |
| Pole Area | Apole | 511,098 | mm ² |
| Air Gap Area | Ag | 425,576 | mm ² |

Table B.1: Analysis Report of Motor A (continued)

| | | | |
|------------------------------------|-------|-----------|-----------------|
| Back-Core Area | Abc | 85,5 | mm ² |
| Tooth Area | Ath | 69,16 | mm ² |
| Stator Inner Diameter | Dsi | 35 | mm |
| Stator Outer Diameter | Dso | 65 | mm |
| Magnet Surface Diameter | Dms | 33,5 | mm |
| Magnet Base Diameter | Dmb | 26,2 | mm |
| Rotor Q-axis Diameter | Dmq | 31,5 | mm |
| Electrical Parameters | | | |
| Wire Diameter | Dwire | 1,4 | mm |
| Phase Resistance | Rs | 0,066 | Ohm |
| D-axis Inductance | Ld | 0,099 | mH |
| Q-axis Inductance | Lq | 0,125 | mH |
| Torq Constant | kemf | 0,0292 | V/rad/s |
| EMF Constant | ktorq | 0,0870 | Nm/Arms |
| Magnetic Parameters | | | |
| Magnet Internal Leakage Reluctance | Rmag0 | 7009,045 | AT/Wb |
| Rotor Leakage Reluctance | Rrl | 70090,452 | AT/Wb |
| Magnet Total Leakage Reluctance | Rmag | 6371,859 | AT/Wb |
| Air Gap Reluctance | Rgap | 1522,529 | AT/Wb |
| Magnet Operating Flux Density | Bm | 0,866 | T |
| Air Gap Flux Density | Bg | 0,734 | T |
| Back-Core Flux Density | Bbc | 1,827 | T |
| Tooth Flux Density | Bth | 1,891 | T |

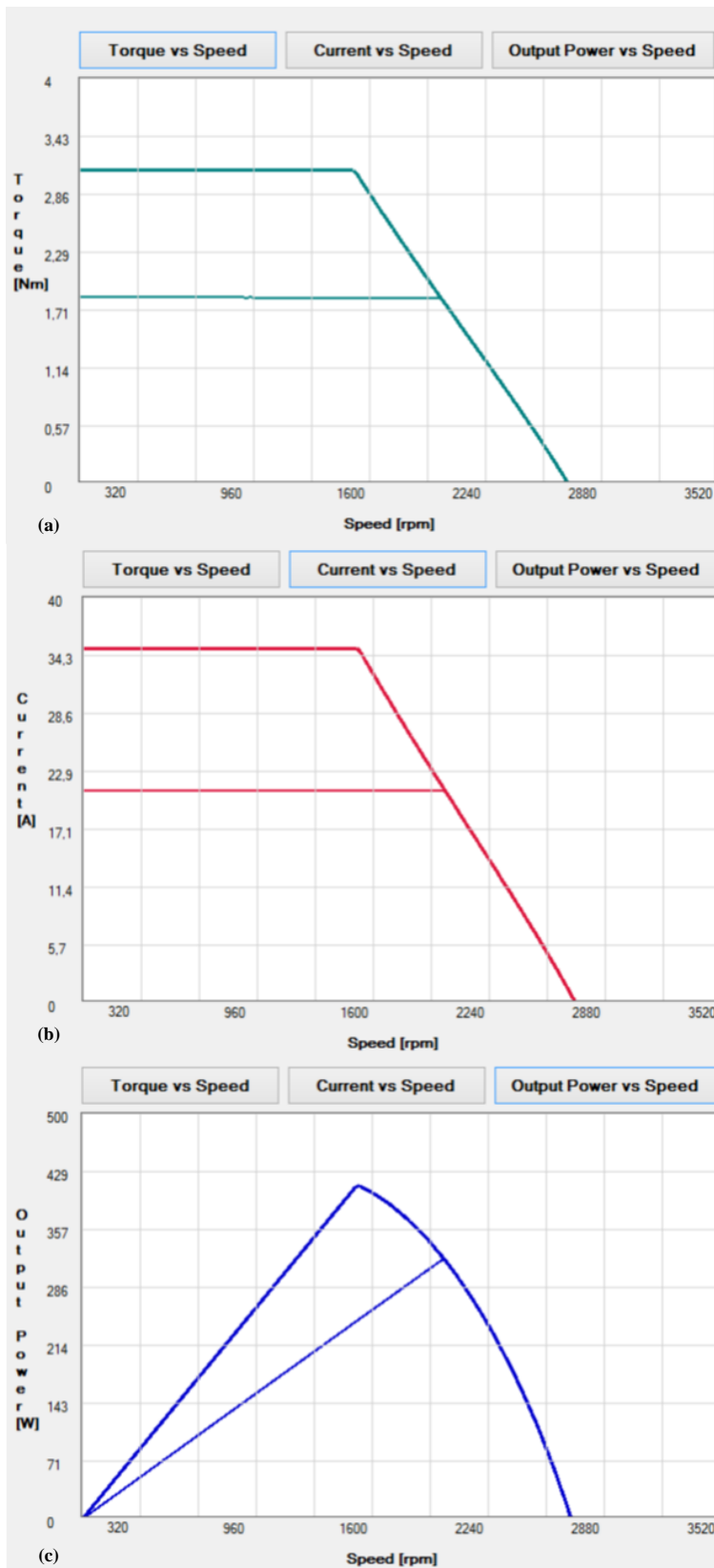


Figure B.2: Torque-Speed (a), Input Current-Speed (b), Output Power-Speed (c) Graphics

APPENDIX C

ANALYSIS REPORT OF MOTOR B

Table C.1: Analysis Report of Motor B

ANALYSIS REPORT

| | | | |
|----------------------|--------|-------|----|
| Main Inputs | | | |
| Line Voltage | Vline | 380 | V |
| Maximum Current | Imax | 100 | A |
| Phase | phase | 3 | |
| Pole Number | pole | 2 | |
| Slot Number | Nslot | 24 | |
| Stator Inputs | | | |
| Axial Length | Lsta | 80 | mm |
| Air Gap | g | 5,5 | mm |
| Back-Core Depth | hbc | 23,5 | mm |
| Tooth Width | Wth | 4,5 | mm |
| Coil Extension | Lext | 15 | mm |
| Turns per Coil | Nturn | 5 | |
| Coils per Phase | Ncoil | 4 | |
| Stacking Factor | Kstack | 0,985 | |
| Fill Factor | Kfill | 0,539 | |
| Rotor Inputs | | | |

Table C.1: Analysis Report of Motor B (continued)

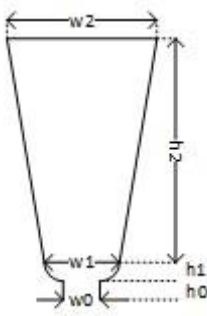
| | | | |
|--|-------|-------|-----|
| Magnet Remanent Flux Density | Br | 0,76 | T |
| Diameter at Magnet Base | Dmb | 0 | mm |
| Magnet Pitch/Pole Pitch | alfa | 0,748 | |
| Magnet Height | hmag | 27 | mm |
| Rotor Leakage Factor | prl | 0,1 | |
| Slot Inputs | | | |
| *Please see the figure in program for slot dimensions! | | | |
|  | w0 | 1,27 | mm |
| | w1 | 2,55 | mm |
| | w2 | 4,35 | mm |
| | h0 | 1 | mm |
| | h1 | 2 | mm |
| | h2 | 14,5 | mm |
| | h3 | 0 | mm |
| | hslot | 17,5 | mm |
| | Aslot | 97 | mm2 |
| Slot type | 1 | | |
| OUTPUTS | | | |
| Dimensions | | | |
| Air Gap | g | 5,5 | mm |
| Magnet Width | Wmag | 49,8 | mm |
| Magnet Height (Region-1) | hmag1 | 15,9 | mm |
| Magnet Height (Region-2) | hmag2 | 24,1 | mm |
| Magnet Height (Region-3) | hmag3 | 27 | mm |
| Magnet Area | Amag | 4000 | mm2 |
| Pole Area | Apole | 7500 | mm2 |
| Air Gap Area | Ag | 4900 | mm2 |

Table C.1: Analysis Report of Motor B (continued)

| | | | |
|------------------------------------|-------|--------|-----------------|
| Back-Core Area | Abc | 1900 | mm ² |
| Tooth Area | Ath | 360 | mm ² |
| Stator Inner Diameter | Dsi | 65 | mm |
| Stator Outer Diameter | Dso | 147 | mm |
| Magnet Surface Diameter | Dms | 54 | mm |
| Magnet Base Diameter | Dmb | 0 | mm |
| Rotor Q-axis Diameter | Dmq | 54 | mm |
| Electrical Parameters | | | |
| Wire Diameter | Dwire | 27 | mm |
| Phase Resistance | Rs | 0,0457 | Ohm |
| D-axis Inductance | Ld | 0,202 | mH |
| Q-axis Inductance | Lq | 0,664 | mH |
| Torq Constant | kemf | 0,0318 | V/rad/s |
| EMF Constant | ktorq | 0,0955 | Nm/Arms |
| Magnetic Parameters | | | |
| Magnet Internal Leakage Reluctance | Rmag0 | 386,92 | AT/Wb |
| Rotor Leakage Reluctance | Rrl | 3869 | AT/Wb |
| Magnet Total Leakage Reluctance | Rmag | 351,5 | AT/Wb |
| Air Gap Reluctance | Rgap | 922,4 | AT/Wb |
| Magnet Operating Flux Density | Bm | 0,615 | T |
| Air Gap Flux Density | Bg | 0,492 | T |
| Back-Core Flux Density | Bbc | 0,637 | T |
| Tooth Flux Density | Bth | 1,080 | T |

APPENDIX D

MODIFICATIONS ON EQUATIONS

Table D.1: Comparison of Equations

| Description | | Equations |
|---|------------------------------|--|
| Carter's Coefficient | MATLAB | $k_{cs} = \frac{\pi \times D_{si}/N_{slot}}{\pi \times D_{si}/N_{slot} - \frac{w_0^2}{w_0 + 5 \times g_3}}$ <p>where g_3 is the maximum air gap length.</p> |
| | Şahin's Thesis (Eqn 4.15) | $k_{cs} = \frac{\pi \times D_{si}/N_{slot}}{\pi \times D_{si}/N_{slot} - \frac{w_0^2}{w_0 + 5 \times g}}$ |
| | This Thesis (Eqn 2.4) | $k_{cs} = \frac{\pi \times D_{si}/N_{slot}}{\pi \times D_{si}/N_{slot} - \frac{w_0^2}{w_0 + 5 \times g}}$ |
| In software, the equation in Şahin's thesis is used to have a more accurate equivalent air gap model. | | |
| Magnet Internal Reluctance | MATLAB | $R_{mag0} = \frac{1}{\mu_r \times \mu_0 \times A_{mag}} \times h_{mag,mean}$ $h_{mag,mean} = h_{mag1} + (h_{mag3} - h_{mag1}) \times 2/\pi$ |
| | Şahin's Thesis (Eqn 4.5) | $R_{mag0} = \frac{1}{\mu_r \times \mu_0 \times \frac{W_{mag}}{5} \times L} \times \left(\frac{2}{h_{mag1}} + \frac{2}{h_{mag2}} + \frac{1}{h_{mag3}} \right)^{-1}$ |

Table D.1: Comparison of Equations (continued)

| | | |
|--|-------------------------------|---|
| Magnet Internal Reluctance | This Thesis (Eqn 2.7) | $R_{mag0} = \frac{1}{\mu_r \times \mu_0 \times \frac{A_{mag}}{5}}$ $\times \left(\frac{2}{h_{mag1}} + \frac{2}{h_{mag2}} + \frac{1}{h_{mag3}} \right)^{-1}$ |
| In software, the equation in Şahin's thesis is used to calculate a magnet reluctance to have a closer results to the real value. | | |
| Magnet Reluctance | MATLAB | $R_{mag} = \left(\frac{1}{R_{mag0}} + \frac{1}{R_{rl}} \right)^{-1}$ |
| | Şahin's Thesis (Eqn 4.15) | $R_{mag} = R_{mag0}$ |
| | This Thesis (Eqn 2.4) | $R_{mag} = \left(\frac{1}{R_{mag0}} + \frac{1}{R_{rl}} \right)^{-1}$ |
| In software, the equation in MATLAB is used to have a more accurate magnet reluctance model. | | |
| Magnet Heights | MATLAB | $h_{mag1} = h_{mag} - 0.5$ $\times \left[D_{ms} - D_{ms} \times \cos \left(\frac{2}{4} \alpha_{mag} \right) \right]$ $h_{mag2} = h_{mag} - 0.5$ $\times \left[D_{ms} - D_{ms} \times \cos \left(\frac{1}{4} \alpha_{mag} \right) \right]$ |
| | Şahin's Thesis (Eqn 4.5-7) | $h_{mag1} = 0.5 \times \left[D_{ms} \times \cos \left(\frac{2}{5} \alpha_{mag} \right) - D_{mb} \right]$ $h_{mag2} = 0.5 \times \left[D_{ms} \times \cos \left(\frac{1}{5} \alpha_{mag} \right) - D_{mb} \right]$ |
| | This Thesis (Eqn 2.11-12) | $h_{mag1} = 0.5 \times \left[D_{ms} \times \cos \left(\frac{2}{5} \alpha_{mag} \right) - D_{mb} \right]$ $h_{mag2} = 0.5 \times \left[D_{ms} \times \cos \left(\frac{1}{5} \alpha_{mag} \right) - D_{mb} \right]$ |
| In software, the equation in Şahin's thesis is used to model magnet more accurate. | | |

Table D.1: Comparison of Equations (continued)

| | | |
|--|---------------------------|--|
| End Winding Inductance | MATLAB | $L_{ew} = 4 \times \mu_0 \times \frac{(N_{coil} \times N_{turn} \times k_w)^2}{pole} \times \lambda_{end} \times L_{1e}$ |
| | Şahin's Thesis (Eqn 4.48) | $L_{ew} = 4 \times \mu_0 \times \frac{(N_{coil} \times N_{turn} \times k_w)^2}{pole} \times \lambda_{end} \times L_{1e}$ |
| | This Thesis (Eqn 2.52) | $L_{ew} = 4 \times \mu_0 \times \frac{(N_{coil} \times N_{turn} \times k_w)^2}{pole} \times \lambda_{end} \times L_{1e}$ |
| In software, the equation in MATLAB is used since it is correct. | | |
| D-axis Equivalent Air Gap Length | MATLAB | $g'_d = g \times k_{cs} + \frac{h_{mag1}}{\mu_r}$ where h_{mag1} is minimum magnet height. |
| | Şahin's Thesis (Eqn 4.56) | $g'_d = g \times k_{cs} + \frac{h_{mag}}{\mu_r}$ where h_{mag} is maximum magnet height. |
| | This Thesis (Eqn 2.54) | $g'_d = g \times k_{cs} + \frac{h_{mag,mean}}{\mu_r}$ where $h_{mag,mean}$ is mean magnet height. |
| In software, mean magnet height is used which is between minimum and maximum heights. | | |
| Q-axis Equivalent Air Gap Length | MATLAB | $g'_q = \frac{(D_{si} - D_{mq})}{2} \times k_{cs}$ |
| | Şahin's Thesis (Eqn 4.57) | $g'_q = \frac{(D_{si} - D_{mq})}{2} \times k_{cs} \times k_{cr}$ |
| | This Thesis (Eqn 2.56) | $g'_q = \frac{(D_{si} - D_{mq})}{2} \times k_{cs} \times k_{cr}$ |
| In software, the equation in Şahin's thesis is used, to calculated q-axis equivalent air gap length Carter's coefficients of both stator and rotor should be considered. | | |